

## STATUS OF THESIS

Title of thesis The Effects of  $K_v/K_h$  on Gas Assisted Gravity Drainage Process

I THAM BOON KEAT

hereby allow my thesis to be placed at the Information Resource Center (IRC) of Universiti Teknologi PETRONAS (UTP) with the following conditions:

1. The thesis becomes the property of UTP
2. The IRC of UTP may make copies of the thesis for academic purposes only.
3. This thesis is classified as

Confidential

Non-confidential

If this thesis is confidential, please state the reason:

---

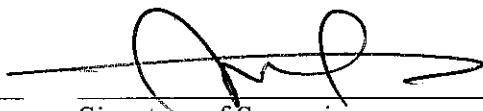
The contents of the thesis will remain confidential for \_\_\_\_\_ years.

Remarks on disclosure:

---

Endorsed by

  
Signature of Author  
THAM BOON KEAT  
100, Taman Utara Jejawi,  
02600 Arau,  
Perlis Indera Kayangan,  
Malaysia

  
Signature of Supervisor  
Assoc. Prof. Dr. Ismail Bin Mohd Saaid  
Department of Geoscience & Petroleum  
Engineering,  
Universiti Teknologi PETRONAS,  
Bandar Seri Iskandar, 31750  
Tronoh,  
Perak Darul Rizuan, Malaysia.

Date : 29/3/2013

Date : 29/3/13

UNIVERSITI TEKNOLOGI PETRONAS

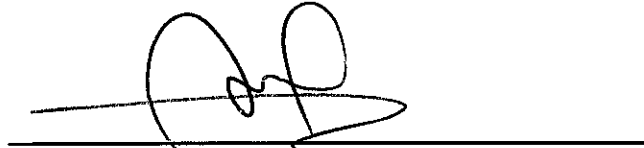
THE EFFECT OF  $K_v/K_H$  ON GAS ASSISTED GRAVITY DRAINAGE PROCESS

by

THAM BOON KEAT

The undersigned certify that they have read, and recommend to the Postgraduate Studies Programme for acceptance this thesis for the fulfilment of the requirements for the degree stated.

Signature:



Main Supervisor:

Assoc. Prof. Dr. Ismail Bin Mohd Saaid

Signature:



Head of Department:

Assoc. Prof. Dr. Ismail Bin Mohd Saaid

Date:

29/3/13

Assoc Prof Dr Ismail M Saaid  
Head, Petroleum Engineering Department  
Universiti Teknologi PETRONAS

THE EFFECT OF  $K_V/K_H$  ON GAS ASSISTED GRAVITY DRAINAGE PROCESS

by

THAM BOON KEAT

A Thesis

Submitted to the Postgraduate Studies Programme

as a Requirement for the Degree of

MASTER OF SCIENCE

PETROLEUM ENGINEERING BY RESEARCH

DEPARTMENT OF PETROLEUM ENGINEERING

UNIVERSITI TEKNOLOGI PETRONAS

BANDAR SERI ISKANDAR,

PERAK

JUNE 2012

DECLARATION OF THESIS

Title of thesis

The Effects of  $K_v/K_h$  on Gas Assisted Gravity Drainage Process

I THAM BOON KEAT  
hereby declare that the thesis is based on my original work except for quotations and citations which have been duly acknowledged. I also declare that it has not been previously or concurrently submitted for any other degree at UTP or other institutions.

Witnessed by



Signature of Author  
Tham Boon Keat  
100, Taman Utara Jejawi,  
02600 Arau,  
Perlis Indera Kayangan,  
Malaysia



Signature of Supervisor  
Assoc. Prof. Dr. Ismail Bin Mohd Saaid  
Department of Geoscience & Petroleum  
Engineering,  
Universiti Teknologi PETRONAS,  
Bandar Seri Iskandar, 31750  
Tronoh,  
Perak Darul Rizuan, Malaysia.

Date : 29/3/2013

Date : 29/3/13

To my beloved parents, sister and brother...

## ACKNOWLEDGEMENTS

I would like to express my sincere gratefulness and appreciation to my supervisor, Assoc. Prof. Dr. Ismail Bin Mohd Saaid for his tremendous encouragement and endless support during my study despite his tight schedule. He has been more like a friend and father, from whom I have learned to be a true professional reservoir engineer. I would also like to extend my gratitude to my former supervisor, Prof. Dr. Mehmet Raif Birol Demiral, for his guidance during the completion of this research. Not to forget Prof. Dr. Ahmad Kamal Idris from Department of Petroleum Engineering, Universiti Teknologi Malaysia (UTM) that has inspired me for this research topic.

My special thanks to all the lab technologists who provided constructive and scientific advice for my project setup. These include Mr. Mohd Riduan Bin. Ahmad and Mr. Shahrul Rizzal Md. Yusuf from Department of Geoscience and Petroleum Engineering, UTP, Mr. Azhar Zainal Abidin. from Department of Electrical and Electronic, UTP, Mr. Jani Bin Alang Ahmad and Mr. Shaiful Hisham Bin Samsudin, from Department of Mechanical Engineering, UTP, and Mr. Roslan from Department of Petroleum Engineering, UTM.

Furthermore, I would like to express my gratitude to UTP for providing me with the Short Term Internal Research Fund (STIRF Code No: 64/09.10) under my team leaders, Mr. Muhammad Sanif Bin Mauluat and Mr. Ellias Abllah from Department of Geoscience and Petroleum Engineering, UTP.

Finally, I wish to thank to my father, Tham Sin Chiong, my mother Ooi Hoon Ean, my sister, Tham Ker Chia and my brother, Tham Wooi Kiat for their love, support, and understanding and most importantly for their patience.

## ABSTRACT

Gas Assisted Gravity Drainage (GAGD) was proposed to overcome the gravity segregation effect which happened in Water Alternating Gas (WAG) process. Since most of the development strategy in Malaysia concentrated on WAG, introduction of GAGD might help in increasing the oil recovery. However, previous researches on GAGD process were done base on homogeneous porous media, there is yet any reported research done to investigate the effect of  $k_v/k_h$  on GAGD process.

The objectives of this research are first to history match the simulated results from ECLIPSE simulator with respect to the observed laboratory result for simulation model validation. After the ECLIPSE model is validated, the effect of  $k_v/k_h$  on gravity segregation in GAGD process is investigated by using the ECLIPSE model. Based on the ECLIPSE model, different development strategies on GAGD process were also proposed. This covers different well design and different selection of injection gas. Finally, Petrel pre-processor and ECLIPSE simulator were used to investigate the feasibility of implementing GAGD process in the field level based on Gulfaks field as the reference field.

This research was divided into two directions; the simulation investigations and the laboratory studies. To overcome the time cost and limitation of the laboratory model, the research concentrated mainly on ECLIPSE simulation while the laboratory results were used as a complementary to validate the simulation run.

Outcome of the research showed that the ECLIPSE models (laboratory level investigation and field level investigation) were validated. The different between the ECLIPSE simulator and laboratory studies were history matched and keep to within 1%. For field level of investigations, gas and oil production rate were matched over the actual production rate from Gulfaks field.

Results from simulation model and laboratory measurements have suggested that

GAGD process is more favour in the reservoir with more dominance in vertical permeability. However, this is provided that there is a very good well control.

For a laboratory scale of investigation, two vertical wells (injector and producer) will yield the highest recovery (63.89%ROIP) but the investigation does not take the implementation of inflow control valves into account. From ECLIPSE compositional simulation investigation, CO<sub>2</sub> was proposed to be the best injection gas with consideration of the minimum miscible pressure and cost efficiency.

Base on simulation using data from Gulfalks field, GAGD process (26.4%IOIP) has proven to be a better choice over WAG process (23.8%IOIP) and the recovery can further increase with the usage of inflow control valves (26.7%IOIP).

## ABSTRAK

GAGD dicadangkan untuk mengatasi kesan segregasi graviti yang terjadi dalam WAG. Memandangkan majoriti reserboir di Malaysia menumpu pada WAG, GAGD dijangka dapat meningkatkan kadar perolehan minyak. Penelitian ini dilakukan berdasarkan reserboir heterogen ( $k_v/k_h$ ), di mana belum dicuba oleh kajian GAGD yang telah diterbitkan.

Objektif pengajian ini adalah untuk mengesahkan keputusan simulasi daripada ECLIPSE simulator. Seterusnya, pengaruh  $k_v/k_h$  atas segregasi gravity akan dikaji dengan menggunakan ECLIPSE simulator. Kesan pelbagai parameter operasi dalam GAGD dan jenis gas untuk suntikan dalam pembangunan reserboir juga dikaji dalam kajian ini. Akhirnya, kebolehlaksanaan GAGD pada peringkat sebenar telah dikaji berdasarkan Gulfaks.

Kajian dibahagikan kepada dua bahagian, iaitu kajian daripada makmal dan kajian melalui simulasi dengan menggunakan simulator. Namun, kajian ditumpukan pada simulasi kerana kajian makmal yang terhad.

Keputusan kajian telah mengesahkan keputusan model ECIPSE. Perbezaan antara keputusan ECLIPSE dan keputusan makmal dihadkan dalam 1% manakala kadar pengeluaran minyak dan gas di peringkat sebenar telah dipadankan dengan keputusan ECLIPSE.

Kajian dari makmal menunjukkan GAGD lebih memihak kepada ketelapa melintang yang lebih dominan. Dengan syarat telaga dikawal dengan baik.

Kajian tahap makmal menunjukkan kombinasi injektor dan penerbit menegak berkebolehan mencapai 63.89%ROIP. Kajian ECLIPSE komposisi simulasi menunjukkan CO<sub>2</sub> adalah gas suntikan yang paling sesuai.

Kajian berdasarkan reserboir Gulfaks menunjukkan bahawa GAGD

(26.4%IOIP) adalah pilihan yang lebih baik berbanding dengan WAG (23.8%IOIP). Pengeluaran minyak boleh dipertingkatkan dengan penggunaan injap pengawalan pengaliran masuk.

In compliance with the terms of the Copyright Act 1987 and the IP Policy of the university, the copyright of this thesis has been reassigned by the author to the legal entity of the university,

Institute of Technology PETRONAS Sdn Bhd.

Due acknowledgement shall always be made of the use of any material contained in, or derived from, this thesis.

© Tham Boon Keat, 2013

Institute of Technology PETRONAS Sdn Bhd

All rights reserved.

## TABLE OF CONTENTS

STATUS OF THESIS.....	i
APPROVAL PAGE.....	ii
TITLE PAGE .....	iii
DECLARATION OF THESIS.....	iv
ACKNOWLEDGEMENT .....	vi
ABSTRACT .....	vii
ABSTRAK .....	ix
COPYRIGHT PAGE .....	xi
TABLE OF CONTENTS.....	i
LIST OF TABLES.....	i
LIST OF FIGURES .....	i
LIST OF ABBREVIATIONS .....	i
LIST OF SYMBOLS .....	i
LIST OF APPENDIX.....	i
 Chapter	
1. INTRODUCTION.....	1
1.1 Problem Statement.....	3
1.2 Objectives.....	4
1.3 Scope.....	4
1.4 Assumption.....	5
2. LITERATURE REVIEW.....	6
2.1 Rock and Fluid Interaction.....	6
2.2 GAGD Project .....	11
2.2.1 Performance and Prospect of GAGD Project.....	12
2.2.2 Theory Background of Gravity Drainage .....	14
2.2.3 Previous Investigation Done on GAGD Process.....	16
2.3 Simulation .....	18
2.3.1 ECLIPSE Simulator.....	21
2.4 Field Referred.....	23
2.5 Well Design.....	28
2.6 Summary .....	31
3. METHODOLOGY .....	32
3.1 Task Identification.....	32
3.2 Experimental Apparatus and Procedure.....	33
3.2.1 Apparatus.....	33
3.2.1.1 Models .....	33
3.2.1.2 Porous Media .....	36
3.2.2 Experiment Procedure.....	37
3.2.2.1 Flooding Test .....	37
3.2.2.2 Fluid Density Measurement.....	40

3.2.2.3 Fluid Viscosity Measurement .....	41
3.2.2.4 Packing, Cleaning, and Repacking.....	42
3.2.2.5 Porosity and Permeability Measurement.....	43
3.2.2.6 Simulation.....	46
4. RESULTS AND DISCUSSION .....	54
4.1 Fluid Properties Measurement .....	54
4.1.1 Density Measurement .....	54
4.1.2 Viscosity Measurement.....	55
4.2 Porous Media and Model Characterization .....	56
4.2.1 Gelama Merah Case Study.....	56
4.2.2 Laboratory Studies.....	59
4.2.3 Relative Permeability Curve .....	62
4.2.4 Minimum Miscible Pressure for Vaporizing Gas Drive Process	63
4.3 The Effect of $k_v/k_h$ on Gas Assisted Gravity Drainage Process.....	65
4.4 Visualization on Front Displacement .....	68
4.5 History Match .....	70
4.5.1 Sensitivity Test .....	71
4.5.2 Match the Well Bottom Hole Pressure .....	71
4.5.3 Match Recovery Factor.....	72
4.5.4 Match History Development Strategies .....	71
4.6 Development Strategy Optimization .....	74
4.7 Scaling of Production Time .....	84
4.8 Effect of Gravity Number on Recovery Factor.....	84
5. CONCLUSIONS AND SUGGESTIONS .....	86
5.1 Conclusions.....	86
5.2 Suggestions .....	87
REFERENCES.....	88
APPENDIX.....	96
Appendix A Fluid Viscosity Calculation.....	96
Appendix B Relative Permeability Calculation.....	98
Appendix C Porosity and Permeability Measurement .....	99
Appendix D Time Scaling .....	105
Appendix E Gravity Number Calculation .....	107
Appendix F Detail of Material and Equipments Used .....	109
Appendix G List of Publications.....	112
Appendix H ECLIPSE Data Overview .....	114
Appendix I Summary of Previous Research on GAGD Projects.....	134

## LIST OF TABLES

Table 2.1: Effect of Controlling Parameters on GAGD Projects (Sharma, 2005; Mahmoud, 2006; and Paidin, 2006) .....	16
Table 2.2: Gelama Merah Field Properties (Abdullah <i>et al.</i> , 2003, Shafi'i <i>et al.</i> , 2003 and Quek and Chang, 2004).....	25
Table 3.1: ECLIPSE Data File Sections.....	47
Table 4.1: Density of Mineral Oil and Brine at 25.8°C and 14.7psia.....	55
Table 4.2: Viscosity of Brine, Mineral Oil and Carbon Dioxide at 25.9°C, 14.7psia.....	56
Table 4.3: Porosity and Permeability for Homogeneous Model .....	60
Table 4.4: Porosity of Tightly-packed and Loosely-packed Model .....	60
Table 4.5: Porosity of Tightly-packed and Loosely-packed Model .....	60
Table 4.6: Average Porosity for Model with $k_v/k_h$ of 0.8, 0.9, and 1.0 .....	61
Table A.1: Viscosity Test Result.....	97
Table C.1: Viscosity Test Result .....	101
Table C.2: Porosity Results from Helium Porosimeter .....	101
Table C.3: Porosity Measurement from Measurement Model and Helium Porosimeter .....	101
Table C.4: Porosity, and Permeability for Heterogeneous Model.....	103
Table H.1: Minimal ECLIPSE Data for Simulation Run .....	114
Table I.1: Summary of GAGD Performance Based of Nine Fields (Kulkarni and Rao, 2004).....	134
Table I.2: Effect of Controlling Parameters on GAGD Projects (Sharma, 2005; Mahmoud, 2006; and Paidin, 2006) .....	135

## LIST OF FIGURES

Figure 1.1: Status of Crude Oil and Natural Gas Resources in Malaysia at 2011 (Kifni, 2011).....	1
Figure 2.1: Existing Porosity Measurement Techniques (Charles <i>et al.</i> , 1999; Torsaeter and Abtahi, 2003; and Bowen, 2003).....	7
Figure 2.2: Factors that Influence Permeability (Koederitz <i>et al.</i> , 1989).....	8
Figure 2.3: Average Permeability in Series Beads (Koederitz <i>et al.</i> , 1989).....	9
Figure 2.4: Average Permeability in Parallel Beads (Koederitz <i>et al.</i> , 1989) .....	10
Figure 2.5: Relative Permeability Correlation (Ahmed, 2001).....	11
Figure 2.6: Concept of the GAGD Process (Rao, 2001) .....	12
Figure 2.7: Findings from Kulkarni and Rao (Kulkarni and Rao, 2004) .....	13
Figure 2.8: Steps Followed in Reservoir Simulation (Ertekin <i>et al.</i> , 2001) .....	18
Figure 2.9: General Algorithm for Manual History Matching Along with Key Reservoir Data and Additional History-Matching Tools (Ertekin <i>et al.</i> , 2001) .....	20
Figure 2.10: Steps Followed in Reservoir Simulation (Ertekin <i>et al.</i> , 2001) .....	21
Figure 2.11: How ECLIPSE Sections Relate to the Flow Equation (Schlumberger Information Solutions, 2009) .....	22
Figure 2.12: Different Between Blackoil and Compositional Simulation (Schlumberger Information Solutions, 2009) .....	22
Figure 2.13: Location of Gelama Merah Field (Zainul <i>et al.</i> , 1999).....	24
Figure 2.14: Top of Sand Contour Map for Unit 3.2 (Abdullah <i>et al.</i> , 2003, Shafi'i <i>et al.</i> , 2003 and Quek and Chang, 2004) .....	25
Figure 2.15: Location of Gulfaks Field (Schlumberger Information Solution, 2010).....	26
Figure 2.16: : Reservoir Properties (Schlumberger Information Solution, 2010) ....	27
Figure 2.17: Oil Saturation at Segment Four at the end of Primary Production (Schlumberger Information Solution, 2010).....	28

Figure 2.18: Pressure Profile along Horizontal Well (Schlumberger Information Solution, 2010) .....	29
Figure 2.19: Segmented Density Calculation in Multi Segmented Well (Schlumberger Information Solution, 2010) .....	30
Figure 2.20: Inflow Control Valve (Schlumberger Information Solutions, 2010)....	31
Figure 3.1: Flow Chart for Methodology.....	32
Figure 3.2: Visual Physical Model (Model: VPM-G-02) .....	34
Figure 3.3: Measurement Model (Model: MM-G-01).....	34
Figure 3.4: Inner Dimension of Visual Physical Model .....	36
Figure 3.5: Inner Dimension of Measurement Model .....	36
Figure 3.6: Flow Chart for Flooding Test.....	38
Figure 3.7: Process Flow Diagram for Flooding Test .....	39
Figure 3.8: Flooding Test Set-up.....	39
Figure 3.9: Portable density meter (Model: DMA 35 <sub>N</sub> ) .....	40
Figure 3.10: OFITE Pressurized Viscometer Model 1100 .....	41
Figure 3.11: Flow Diagram for Packing, Cleaning, and Repacking (Ma, 2005) .....	42
Figure 3.12: Layered Models Set-up .....	43
Figure 3.13: Flow Diagram for Porosity and Permeability Measurement.....	44
Figure 3.14: Process Flow Diagram for Measurement Model.....	45
Figure 3.15: Measurement Model Set-up .....	45
Figure 3.16: Helium Porosimeter Test Set-up.....	46
Figure 3.17: Grid Block Size and Properties.....	48
Figure 3.18: Location and Condition of Injector and Producer .....	49
Figure 3.19: Schematic of Wells Orientation.....	50
Figure 3.20: Development Strategies Used for GAGD Process in Gulfaks Field ....	51
Figure 3.21: Well Design for PGAGD_ICD in Well Section Window.....	52
Figure 3.22: Well Design for PGAGD_ICD in Well Intersection Window .....	53
Figure 4.1: Density of CO <sub>2</sub> over Pressure (Vesovic <i>et al.</i> , 1990; Span and Wagner, 1996; Fenghour <i>et al.</i> , 1998) .....	55
Figure 4.2: West-East Cross Section of Gelama Merah Reservoir .....	57
Figure 4.3: Fluid Contact Indication from Formation Logs.....	58
Figure 4.4: Fluid Contact Calculation from Pressure Plot.....	58

Figure 4.5: Comparison of Porosity Value Obtained by the Measurement Model and Helium Porosimeter .....	59
Figure 4.6: Relative Permeability Generated from Wyllie-Garner Correlation .....	62
Figure 4.7: Slim Tube Displacement for CO <sub>2</sub> and N <sub>2</sub> .....	63
Figure 4.8: Phase Change during Vaporizing gas Drive Process using CO <sub>2</sub> .....	63
Figure 4.9: Ternary Diagram for CO <sub>2</sub> at Different Pressure.....	65
Figure 4.10: Ternary Diagram for N <sub>2</sub> at Different Pressure .....	65
Figure 4.11: Well Bottom Hole Pressure Profile for Different $k_v/k_h$ .....	66
Figure 4.12: The Effect of Different $k_v/k_h$ on Recovery Factor.....	67
Figure 4.13: The Fluid Displacement for Different $k_v/k_h$ .....	69
Figure 4.14: Front Displacement from Low to High Permeability.....	70
Figure 4.15: Front Displacement from High to Low Permeability.....	70
Figure 4.16: Spider Diagram Evaluation.....	71
Figure 4.17: Matching the Well Bottom Hole Pressure .....	72
Figure 4.18: Matching the Recovery Factor .....	73
Figure 4.19: Matched Oil Production Rate for Well P01 .....	74
Figure 4.20: Matched Gas Production Rate for Well P01 .....	74
Figure 4.21: Fluid Front Displacement for Two Vertical Wells.....	75
Figure 4.22: Fluid Front Displacement for Shallow Vertical Injector .....	76
Figure 4.23: Fluid Front Displacement for Deep Vertical Injector.....	76
Figure 4.24: Fluid Front Displacement for Horizontal Injector and Horizontal Producer .....	77
Figure 4.25: Oil Saturation Change along Horizontal Producer.....	78
Figure 4.26: Oil Saturation Change along Horizontal Producer with Inflow Control Valves.....	79
Figure 4.27: Recovery Factor for Different Well Arrangement over Pore Volume Injected.....	80
Figure 4.28: Recovery Factor for Different Development Strategy Implemented in Gulfaks Field.....	81
Figure 4.29: Change in Recovery Factor with Different Injected Gas Density.....	82
Figure 4.30: Recovery Factor for Different Injection Gas Used.....	83
Figure 4.31: Front Displacement during Miscible Displacement .....	83
Figure 4.32: The Effect of Gravity Number on Recovery Factor.....	85

Figure A1: Brine Viscosity at 600 RPM.....	96
Figure A2: Mineral Oil Viscosity at 600 RPM .....	96
Figure A3: Carbon Dioxide Viscosity at 25.9 °C and 14.7 psia (Vesovic <i>et al.</i> , 1990; Span and Wagner, 1996; Fenghour <i>et al.</i> , 1998) .....	97
Figure B1: Relative Permeability Calculation for $k_v/k_h=0.8, 0.9,$ and 1.0 from Excel Application.....	98
Figure C1: $k_v/k_h$ Calculation from Excel Application .....	103
Figure C2: Permeability Distribution for Gelama Merah 1 (PETRONAS CARIGALI, 2002–2003).....	104

## LIST OF ABBREVIATIONS

API	American Petroleum Institute
BSTB	Billion Stock Tank Barrels
BV	Bulk Volume
CGS	Centimetre-gram-second System of Units
CO <sub>2</sub>	Carbon Dioxide
EOR	Enhance Oil Recovery
E100	ECLIPSE Blackoil
E300	ECLIPSE Compositional
GAGD	Gas Assisted Gravity Drainage
GOC	Gas Oil Contact
ICD	In-flow Control Device
$k_v/k_h$	Vertical Permeability Over Horizontal Permeability Ratio
N <sub>2</sub>	Nitrogen
N <sub>G</sub>	Gravity Number
NTG	Net-to-gross
OOIP	Original Oil in Place
OWC	Oil Water Contact
PV	Pore Volume
PVC	Polyvinyl Chloride
PVT	Pressure Volume Temperature
ROIP	Residual Oil in Place

<b>TVDSS</b>	<b>True Vertical Depth Sub-sea</b>
<b>UTP</b>	<b>Universiti Technolgi PETRONAS</b>
<b>WAG</b>	<b>Water Alternating Gas</b>
<b>WBHP</b>	<b>Well Bottom Hole Pressure</b>

## LIST OF SYMBOLS

$A$	Cross-sectional Area
$B_o$	Formation Volume Factor
$d$	Grain Diameter
$h$	Height
$k$	Permeability
$L$	Length
$q$	Flow Rate
$S_{or}$	Residual Oil Saturation
$S_{wi}$	Initial Water Saturation
$t_d$	Dimensionless Time
$v_d$	Darcy Velocity
$\Phi$	Porosity
$\mu$	Viscosity
$\Delta p$	Pressure Different Across System
$\theta$	Dip Angle of Formation



## CHAPTER 1

### INTRODUCTION

In the early days of the petroleum industry, reservoirs were allowed to produce under the primary production phase until the production rates had become uneconomic, especially when expansion of the aquifer or gas cap was insufficient to maintain the reservoir pressure (Latil, 1980). The secondary phase of the recovery is implied by maintaining the reservoir pressure using water or gas injection (Latil, 1980). Enhanced oil recovery (EOR) is about advanced recovery techniques going beyond what are considered conventional methods at a given reference point of time with the recovery of 30-60% Original Oil in Place (OOIP) with compared with 20-40% OOIP using primary and secondary recovery (Latil, 1980 and Paidin *et al.*, 2010).

Figure 1.1 shows the end of giant field reserve recovery in Malaysia as per year 2011 whereby the new recovery is only 2% out of 21.2 Billion barrel of oil equivalent (Kifni, 2011). Thus, it is important to search for more efficient enhanced recovery methods.

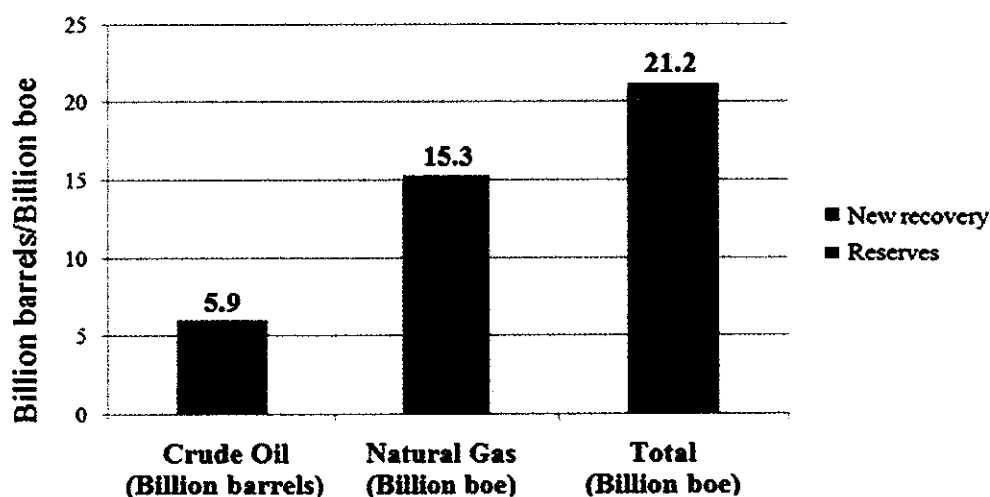


Figure 1.1: Status of Crude Oil and Natural Gas Resources in Malaysia as at 2011 (Kifni, 2011)

We have seen that water or gas injection in an oil reservoir resulted in a poor recovery due to partial sweep of the reservoir and oil trapped by capillary forces in the invaded zones. Thus, the successfulness of an EOR method requires the improvement of sweep efficiency by reducing the mobility ratio between injected and in-place fluids while improving displacement efficiency by eliminating or reducing the capillary forces simultaneously (Green and Willhite, 1998).

Though the gas injection process has been practiced since the turn of the last century, the large mobility of injected gas and density differences between gas, oil, and water have been the weakest link of the process performance. Caudle and Dyes (1958) noticed that the sweep efficiency of a gas injection process can be increased by decreasing the mobility behind the flooding front, in which the injected water reduces the mobility of the gas and helps stabilize the displacement front. Therefore, in order to achieve a better volumetric sweeps from gas injection process, it was initially proposed that gas and water should simultaneously inject into the reservoir. Later, to avoid injectivity problems and other operational limitations related to simultaneous injection, this method is then changed to Water Alternating Gas (WAG) process.

As noted by Rao *et al.*, (2004) a review of 59 field WAG projects have yield recovery improvement of only about of 5-10% OOIP, which is not lived up to its expectations. Gas Assisted Gravity Drainage (GAGD) process was developed as an EOR method that takes advantages of the naturally occurring gravity segregation due to the density differences between injected gas and oil in place (Paidin *et al.*, 2010). GAGD has been developed by Louisiana State University to overcome the limitation of the conventional gas injection process such as WAG and continuous gas injection (Sharma, 2005; Mahmoud, 2006; Paidin, 2006; Mahmoud and Rao, 2007).

An economic evaluation on GAGD process using Crystal Ball simulator that took Net Present Value, Internal Rate of Return, Performance Index, and Growth Rate Return into account showed that the implementation of GAGD has a high probability of being economic (Paidin *et al.*, 2010). Since WAG is widely applied in Malaysia oil fields, advantages of GAGD over WAG might offer a better solution in maximizing oil recovery.

## 1.1 Problem Statement

After the secondary and tertiary recovery method, 60% of the original oil in place is still left in the reservoir (Baviere, 1991 and Paidin *et al.*, 2010 and). It is hope to maximize the oil production by implement a better recovery method. EOR was introduced, by injecting appropriate agent that is not normally present in the reservoir, which was aimed to increase ultimate oil recovery.

Refer to the pros and cons of gas injection, WAG, and GAGD process which is discussed in the previous section, it seems that GAGD is more encouraging than WAG and gas injection process (Holm and Josendal. 1982; Christensen *et al.*, 1998; Kulkarni and Rao, 2004; Rao *et al.*, 2004; Sharma, 2005; Mahmoud, 2006). However, there are still many uncertainties in GAGD technique that require further studies. For example, the effect of different vertical permeability over horizontal permeability ratio ( $k_v/k_h$ ) on the oil recovery, the effect of different well design on oil recovery, and the effect of different injected gas type on oil recovery.

From the previous research done on GAGD (Holm and Josendal, 1982; Christensen *et al.*, 1998; Kulkarni and Rao, 2004; Rao *et al.*, 2004; Sharma, 2005; Mahmoud, 2006; Paidin *et al.*, 2010; Kasiri and Bashiri, 2011), it appears that the researchers only concentrate on uniform permeability reservoir. However, in reality, the  $k_v/k_h$  is usually unique for the reservoir. In this research, effect of different  $k_v/k_h$  on the oil recovery in GAGD process was investigated by using ECLIPSE simulator for field level studies and glass beads for laboratory pilot studies.

One of the items to be considered in a field development plan is the well design. For example, the length of the injector and producer, the well orientation, and if there is any inflow control valve needed in the producer. This is one of the determining factors of the successfulness of GAGD process. However, this has never been investigated by all the previous reported researches. Thus, it is worth to study the effect of different well design on GAGD process which can then be a reference for others during a field development plan.

Sharma (2005) and Paidin (2006) have difference research outcome on the effect of using different type of injection gas during GAGD process on the oil recovery.

Sharma did not see any increase in the oil recovery by replacing the injection gas with nitrogen gas while Paidin observed that there is an increment of 10.9%OOIP when the injection gas was replaced by using nitrogen gas. This is a conflict that worth investigating in order to select the best gas type for GAGD injection.

## 1.2 Objectives

The objectives of the research are:

- i. To history match the simulated results from ECLIPSE simulator with respect to the observed laboratory result for simulation model validation
- ii. To investigate the effect of  $k_v/k_h$  on gravity segregation in GAGD process by using ECLIPSE simulator
- iii. To propose different development strategies on GAGD process for an optimum recovery which cover different well design and different selection of injection gas
- iv. To investigate the feasibility of implementing GAGD process in the field level on Gulfaks field by using Petrel pre-processor and ECLIPSE simulator.

## 1.3 Scope

The scope of the study covers the laboratory investigations as well as the simulation studies. Laboratory investigation is a need to visualize the fluid displacement and study the basic concept of GAGD process. However, there are some limitations in the laboratory investigations such as the visual physical model cannot withstand a pressure higher than 25psi, the  $k_v/k_h$  than can be packed by the visual physical model is very limited, and it is impossible to mimic the well design used in the field level to the visual physical model. Thus, to overcome this weakness, ECLIPSE simulator was used to simulate a more realistic condition for the field level implementation of GAGD process which is based on Gulfaks field. Gulfaks field will be the only field selected because of the availability of all the data.

For the development strategies investigation on Gulfaks field, the research will only cover:

- i. The effect of having different recovery strategy on the oil recovery (continue the prediction by using the existing wells, continue the prediction by drill more water injector, continue the prediction by implementing WAG process, or continue the prediction by using GAGD process)
- ii. The effect of injecting different injection gas ( $\text{CO}_2$  and  $\text{N}_2$ ) on the oil recovery because these are the common gas which will be injecting to the reservoir
- iii. The effect of implement inflow control vales to the producer well

#### **1.4 Assumption**

Since GAGD process is very sensitive to heterogeneity, which effects might not present in small diameter cores used in laboratories (Mahmoud, 2006). The laboratory investigation was done in a visual physical model. The weakness of this research is the porous media cannot be compress until reservoir condition. Thus, we need to assume that the porous media exhibits the flow mechanism in reservoir rock. This is the basic assumption that used by researcher that did investigation by using glass beads (Rao *et al.*, 2004; Sharma, 2005; Mahmoud, 2006; Paidin *et al.*, 2010). Since wettability test is not possible in the visual physical model, the model was assumed to be oil wet.

As a best effort, the packing procedure proposed by Ma in 2005 was followed in order to establish a standard packing technique. Gravity segregation and recovery were monitored by changing the value of  $k_v/k_h$  (0.8, 0.9, and 1.0). For all these process, gravity number (NG) has been taken into account. Since there are only limited  $k_v/k_h$  that can be created by the visual physical model, this weakness will be overcome by running more cases using ECLIPSE simulator to generate more  $k_v/k_h$  (0.1, 0.2, 0.3, 0.4, 0.5, 0.6, 0.7, 0.8, 0.9, 1.0).

## CHAPTER 2

### LITERATURE REVIEW

This chapter lists some of the main concerns in investigating the successfulness of GAGD process. This chapter also give the definition of GAGD process, the performance and prospect of GAGD process, theoretical background, and previous investigations that has been done on GAGD process. Apart from laboratory measurement, this chapter also cover the important of simulation investigation on GAGD process and scale the laboratory measurement results to field level. Finally, this chapter include the description on Gulfaks field in North Sea and the options available of well design which was used to investigate the performance of GAGD process in real field level.

#### **2.1 Rock and Fluid Interaction**

This section explains some of the parameters that will influence the interaction between rock and fluid. This is important because small-scale laboratory measurements of fluid flow in porous media have showed that fluid displacement is a function of the properties of the solid material (Fanchi, 2001). This section has explained the important to measure the porosity and permeability in this research

To measure the potential hydrocarbon in place, we need to measure the porosity of the rock. This is the potential storage volume for hydrocarbons between the pore spaces in the rock as show in Equation 2.1 (Charles et al., 1999 and Ahmad, 2001):

$$\text{Porosity} = \frac{\text{Pore Volume}}{\text{Bulk Volume}} = \frac{\text{Bulk Volume} - \text{Mineral Volume}}{\text{Bulk Volume}} \quad (2.1)$$

Harari (1995) stated that porosity measurements at ambient conditions are usually adequate since the resulting decrease in porosity is normally very small ( $\pm 2\%$ ). Harari did his research by using core plug that has been compacted over a long time. This may be not true for glass beads system, the porosity might be increase when subjected to pressure (Wang, 2011) and thus require a further verification.

Among the existing techniques (Figure 2.1), Liquid Saturation Method was chosen to measure the pore volume of glass beads system because it is compatible to apply in glass beads system (Charles *et al.*, 1999; Torsaeter and Abtahi, 2003; and Bowen, 2003). The flow diagram and the detail description of the procedure are available in Section 3.2.2.5 and Appendix C, respectively.

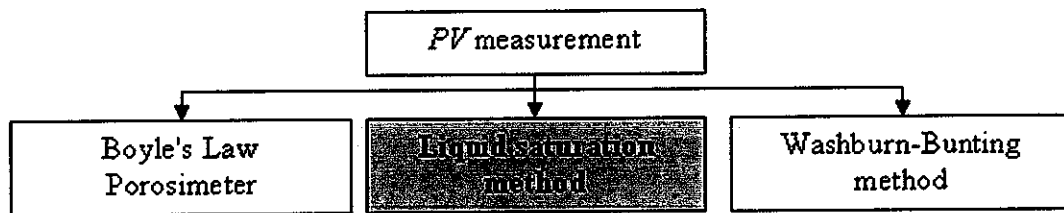


Figure 2.1: Existing Porosity Measurement Techniques (Charles *et al.*, 1999; Torsaeter and Abtahi, 2003; and Bowen, 2003)

Permeability is a rock property that relates on how much the rate change as a effect of pressure difference. The hydrocarbon can be recovered in the rock where the permeability value is above 0.01mD (Charles *et al.*, 1999 and Ahmad, 2001). Since packing of glass beads was done in the visual physical model during the laboratory investigation. It is important to know the impact of glass beads properties and packing technique on the investigation result. From the research done by Koederitz *et al.*, in 1989, as far as the rock properties and packing technique concern, the factors that will influence the permeability measurement are show in Figure 2.2. From Figure 2.2, we can see the important of following a standard packing procedure. Thus, as a best effort, the packing procedure proposed by Ma in 2005 was followed in order to establish a standard packing procedure (please refer to Appendix C for detail description on step-by-step packing, cleaning, and repacking procedure as proposed by Ma, 2005).

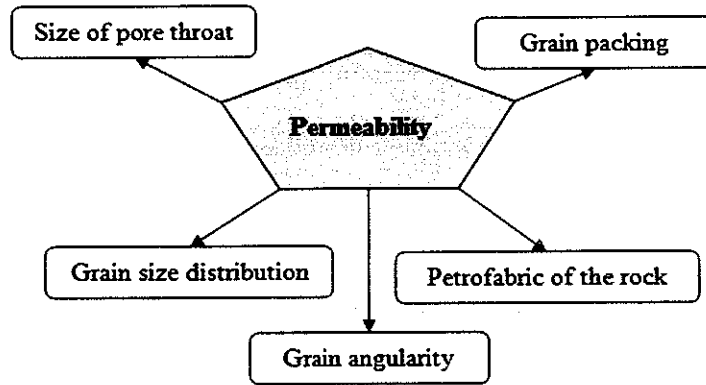


Figure 2.2: Factors that Influence Permeability (Koederitz *et al.*, 1989)

Different approaches have been reported to measure the permeability of a porous media. Kozeny-Carman equation (Equation 2.2) suggested to calculate the permeability from grain diameter and porosity approach. However, since the porosity of the glass beads system is not uniform due to the different in grain diameter and compaction limitation in visual physical model, Darcy equation (Equation 2.3) was chosen to calculate the permeability of laboratory model. Darcy equation proposed to calculate permeability depending on the injectivity done during the flooding process (Koederitz *et al.*, 1989 and Charles *et al.*, 1999).

$$k = \frac{3.631 \times 10^9 d^2 \phi^3}{(1 - \phi)^2} \quad (2.2)$$

Where,

- $k$  = Permeability, md
- $d$  = Grain diameter, in
- $\phi$  = Porosity, fraction

$$k = \frac{-q\mu L}{A\Delta p} \quad (2.3)$$

Where,

- $k$  = Permeability, darcies,
- $q$  = Outlet flow rate, cm<sup>3</sup>/sec,
- $\mu$  = Fluid viscosity at temperature of the system, cP
- $L$  = System length, cm
- $A$  = System cross-sectional area, cm<sup>2</sup>, and
- $\Delta p$  = Pressure differential across system, atm.

Heterogeneity in the porous media will create a lot of havoc to projects with horizontal gas floods by creating early breakthroughs and thus resulting in a poor reservoir sweep (Jackson *et al.*, 1985; Rao, 2001). However, in gravity stable gas floods, heterogeneous stratification can delay gas breakthrough due to physical dispersion, and reduced gas channelling through the high permeability layer. Thus, improve the sweep efficiency. According to Kulkarni (2005), the vertical-to-horizontal permeability ratio is a major factor generally used to represent heterogeneity in a reservoir as per permeability concern.

To investigate the  $k_v/k_h$  of a layered laboratory model, the reciprocal average permeability ( $k_v$ ) and arithmetic average permeability ( $k_h$ ) need to be calculate first. The system for which the reciprocal average permeability technique and arithmetic average permeability are applicable are illustrate by Figure 2.3 and Figure 2.4 respectively (Koederitz *et al.*, 1989). From Figure 2.3 and Figure 2.4, it was noted that permeability and length of each layer need to be known first. Thus, a measurement model was designed to measure the permeability of each glass beads set before stack them up to a series beads.

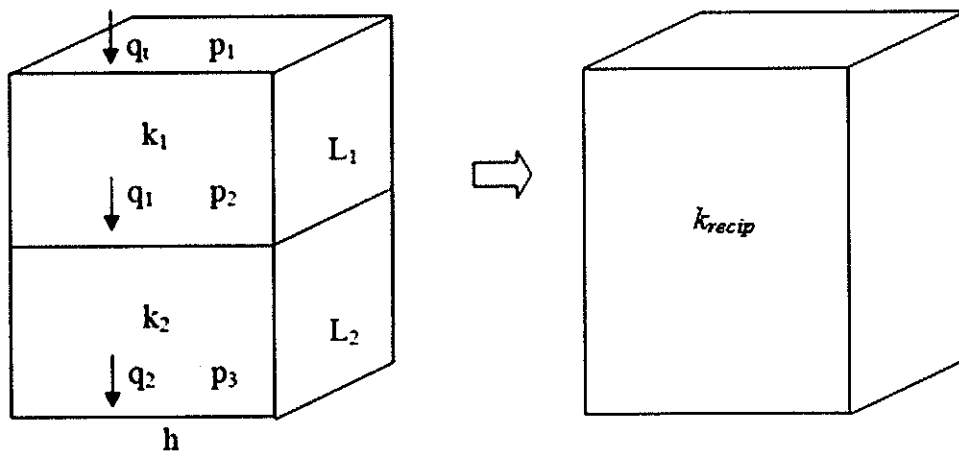


Figure 2.3: Average Permeability in Series Beads (Koederitz *et al.*, 1989)

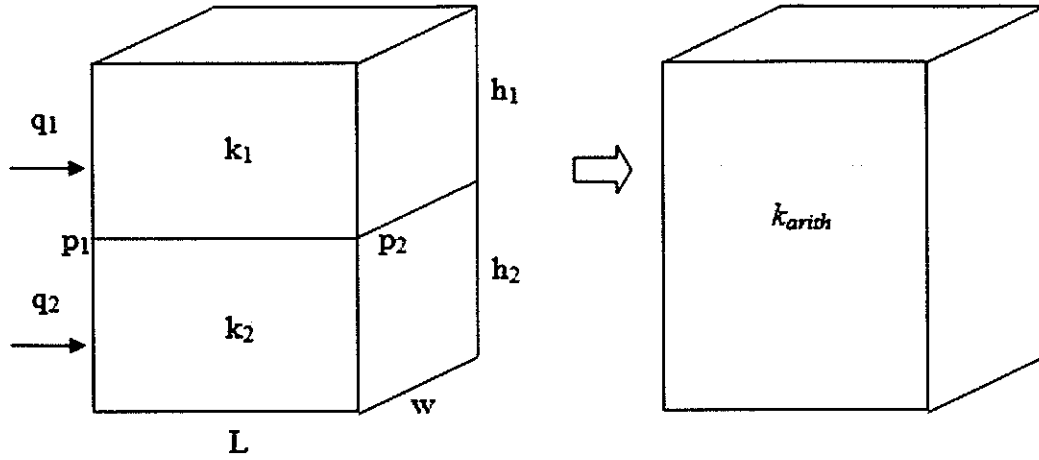


Figure 2.4: Average Permeability in Parallel Beds (Koederitz *et al.*, 1989)

From Koederita *et al.*, (1989), the reciprocal average permeability technique and arithmetic average permeability can then be calculate using Equation 2.4 and Equation 2.5.

$$k_{recip} = \frac{\sum_{i=1}^n L_i}{\sum_{i=1}^n (L_i/k_i)} \quad (2.4)$$

Where,

$k_i$  = absolute permeability of bed  $i$ , md

$L_i$  = length of section  $i$ , ft

$n$  = number of sections

$$k_{arith} = \frac{\sum_{i=1}^n (k_i h_i)}{\sum_{i=1}^n h_i} \quad (2.5)$$

Where,

$k_i$  = absolute permeability of bed  $i$ , md

$h_i$  = thickness of bed  $i$ , ft

$n$  = number of beds

In GAGD process, gas will be injected into the reservoir, in many of the cases, it involved multiple phase flow. Wyllie and Gardner correlation was chosen to estimate the relatively permeability for each of the phase in the porous media

(Ahmed, 2001). Figure 2.5 shows Wyllie and Gardner correlation for relative permeability calculation under different porous media conditions (Ahmed, 2001). This method was chosen because the respective relative permeability can be calculated after connate water saturation and the critical oil saturation are determined. The information was then used as an input data in ECLIPSE 100 Blackoil simulation (E100) and ECLIPSE 300 Compositional simulation (E300) under PROPS section. This is the section of the input data which contains the pressure and saturation dependent properties of the reservoir fluids and porous media.

<b>Drainage Oil-Water Relative Permeabilities</b>		
<b>Type of formation</b>	<b><math>k_{ro}</math></b>	<b><math>k_{rw}</math></b>
Unconsolidated sand, well sorted	$(1 - S_w^*)$	$(S_w^*)^3$
Unconsolidated sand, poorly sorted	$(1 - S_w^*)^2(1 - S_w^{*1.5})$	$(S_o^*)^{3.5}$
Cemented sandstone, oolitic limestone	$(1 - S_o^*)^2(1 - S_w^{*2})$	$(S_o^*)^4$

<b>Drainage Gas-Oil Relative Permeabilities</b>		
<b>Type of formation</b>	<b><math>k_{ro}</math></b>	<b><math>k_{rg}</math></b>
Unconsolidated sand, well sorted	$(S_o^*)^3$	$(1 - S_o^*)^3$
Unconsolidated sand, poorly sorted	$(S_o^*)^{3.5}$	$(1 - S_o^*)^2(1 - S_o^{*1.5})$
Cemented sandstone, oolitic limestone, rocks with vugular porosity	$(S_o^*)^4$	$(1 - S_o^*)^2(1 - S_o^{*2})$

Figure 2.5: Relative Permeability Correlation (Ahmed, 2001)

## 2.2 GAGD Project

Gravity drainage is defined as a recovery process in which gravity acts as the main driving force and where gas replaces the voidage volume (Kulkarni, 2004). It occurs in primary phases of oil production through gas cap expansion as well as in the later stages where gas is injected from the external source (Kulkarni, 2004).

Due to the consistently success field applications of the gravity stable gas injection, Louisiana State University has proposed GAGD process. The concept of GAGD is shows in Figure 2.6 (Rao, 2001). A horizontal producer is place at the bottom of the pay zone while CO<sub>2</sub> is inject through existing vertical wells at the top

(into gas cap) to provide gravity stable displacement and uniform reservoir sweep. As the CO<sub>2</sub> chamber grows downward and sideways, more oil will be recover without any increases in the reservoir water saturation. The efficiency displacement efficiency can be further maximize by maintaining the injection pressure near minimum miscible pressure which helps in lowering the reservoir capillary forces and finally the residual oil saturation.

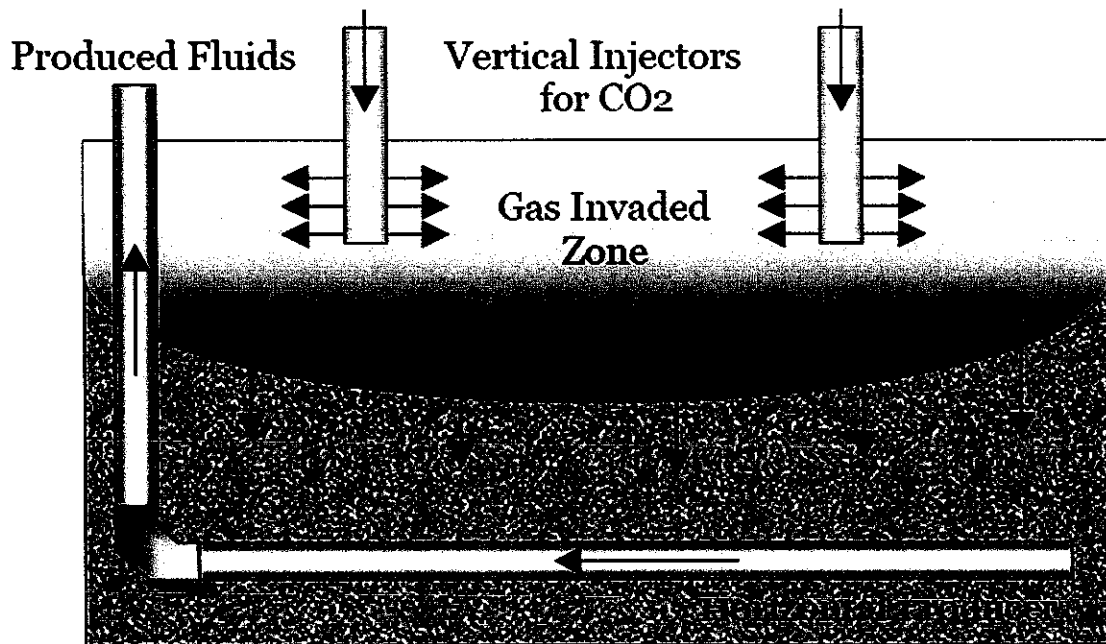


Figure 2.6: Concept of the GAGD Process (Rao, 2001)

### 2.2.1 Performance and Prospect of GAGD Project

Study on the performance and prospect on the previously done GAGD project is important before we decide to implement it in any of our field. This section has listed some of the successful story of the GAGD project and as the advantages of GAGD project over the conventional WAG project.

Kulkarni and Rao (2004) have summarized the performance of GAGD based on nine fields, namely, West Hackberry, Hawkins Dexter Sand, Weeks Island SRB-Pilot, Bay St. Elaine, Wizard Lake D3A, West Pembina Nisku D, Wolfcamp Reef, Intisar D, and Handil Main Zone, respectively. Outcomes from the research are show in Figure 2.7 (refer to Appendix I for all the field performance). According to the

research, GAGD projects have an average recovery factor of 82.33%OOIP compare to WAG projects which only have an average recovery of 5-10%OOIP.

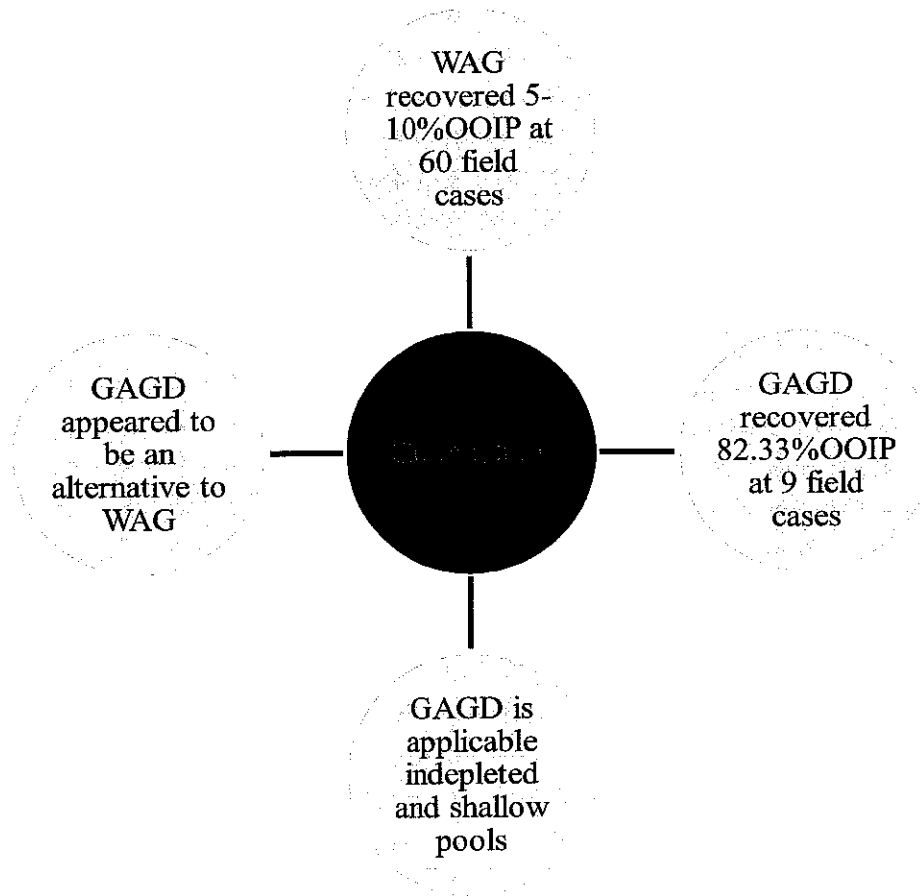


Figure 2.7: Findings from Kulkarni and Rao (Kulkarni and Rao, 2004)

According to Mahmoud (2006), for a GAGD project where the vertical drainage is controlled by gravity and the CO<sub>2</sub> is injected in a miscible mode, there will a very short transition zone between the miscible CO<sub>2</sub> and the original oil zone. Thus, nearly 100%OOIP of oil recovery could be achieved.

WAG was introduced by Caudle and Dynes back in 1958 and is widely apply worldwide however, GAGD that was introduced later in 1960 did not get as much attention until it was started to be developed by Lousiana State University. Based on Kulkarni and Rao (2004) findings, GAGD should have a better displacement and sweep efficiency than WAG provided that, gravity segregation phenomena were well controlled. This can be achieve by working with nature by use of buoyancy rise of injected gas to displace oil downwards. Thus, this research has studied the relationship on of gravity number ( $N_G$ ) with the oil recovery in GAGD process.

The field applications show ultimate oil recoveries as high as 85-95%OOIP. However, all the fields studied were based on pinnacle reef type reservoirs and gravity drainage using vertical wells might not yield similar recoveries when implemented in horizontal type reservoirs (Kulkarni and Rao, 2004).

Gravity drainage can yield a high oil recovery but a conventional vertical well provides less effective means of recovery especially in none dipping reservoirs compare to horizontal well. The main advantage of placing the horizontal well at the bottom of the payzone is the usefulness gravity forces after the depletion of gas cap or solution drive. The second advantage of horizontal well is that they able to delay the gas breakthrough and the encroachment of water (Joshi, 1991).

### 2.2.2 Theoretical Background of Gravity Drainage

Water, oil and gas co-exist in many reservoirs but these three phases cannot be all mixed together. Due to the density different at reservoir conditions of temperature and pressure, gas will always be on top, follow by oil and water with some transition zones. Gravity drainage makes use of gravity force and pressure gradient of respective fluids to recover the oil in place (Koederitz *et al.*, 1989). In a steeply dipping bed, low viscosity and high permeability, oil recovery by gravitational segregation can be on the order of 75%OIIP (Koederitz *et al.*, 1989). According to Koederitz (1989), gravity segregation phenomena must be controlled as expressed by Equation 2.6 for the higher oil production rate.

$$q_o = \frac{1.127k_o A(0.433\Delta\gamma \sin \theta)}{1000\mu_o B_o} \quad (2.6)$$

Where,

$q_o$  = flow rate, STB/D

$k_o$  = effective permeability to oil, md

$\mu_o$  = reservoir oil viscosity, cP

$\Delta\gamma$  = (sg oil - sg gas)

$B_o$  = formation volume factor, RVB/STB

$A$  = cross sectional area, perpendicular to formation dip which fluid flows, ft<sup>2</sup>

$\theta$  = dip angle of formation

From the equation, a higher flow rate can be achieved by choosing a suitable injection gas and controlling the production pressure. By choosing a suitable gas, we can reduce the density difference between the oil and gas while controlling the production pressure, we can keep the pressure below the formation volume factor and achieve a higher flow rate.

To make the research study meaningful, time scaling is an important part for real field interpretation. The equation that was used in time scaling was taken from Sharma, 2005 (Equation 2.7). Equation 2.7 enables the scale-up of run time in the laboratory Visual Physical model to the dimensionless time and later the time required in the real reservoir level to achieve the same recovery as the .

$$t_d = \frac{kk_{ro}^o \Delta \rho g t}{h \phi \mu g_c (1 - S_{or} - S_{wi})} \quad (2.7)$$

Where,

$t_d$  is the dimensionless time

$t$  is the real time, s

$k$  is the absolute permeability of the porous media, m<sup>2</sup>

$k_{ro}^o$  is the end-point relative oil permeability

$\Delta \rho$  is the density contrast between the displaced and displacing phase, kg/m<sup>3</sup>

$g$  is the gravitational force, 9.81 m/s<sup>2</sup>

$g_c$  is the gravitational force conversion factor, 1

$\mu$  is the oil viscosity, Pa.s

$h$  is the height of the porous media, m

$\phi$  is the porosity of the porous media, fraction

$S_{or}$  is the residual oil saturation, fraction

$S_{wi}$  is the initial water saturation, fraction

$N_G$  is the ratio of gravity force to viscous force, the relationship is described by Sharma (2005) in Equation 2.8. There is a conflict between Mahmoud (2006) and Sharma (2005) regarding to the usefulness of  $N_G$  to determine the recovery in

GAGD process. According to Sharma (2005), there is an approximate logarithmic relationship between the recovery performance and the gravity numbers but finding from Mahmoud (2006) does not agree with Sharma’s statement. Mahmoud (2006) did not see any significant relationship between  $N_G$  and the recovery factor. However, this might be because Mahmoud’s (2006) experimental range was not wide enough to be able to establish a relationship that is clear.

$$N_G = \frac{\Delta\rho g K}{\Delta\mu v_d} \tag{2.8}$$

Where,

$K$  is the absolute permeability of the porous medium,  $m^2$

$\Delta\mu$  is the viscosity different between oil and gas, Pa.s

$v_d$  is the Darcy Velocity, m/s

$\Delta\rho$  is the density different between oil and gas,  $kg/m^3$

$g$  is the gravitational acceleration,  $m/s^2$

### 2.2.3 Previous Investigation Done on GAGD Process

For maximum recovery, it is important to find the optimum condition for GAGD application. Table 2.1 summarized and discussed several controlling parameters that have been investigated by the past researchers which is a very important guide line for the research (refer to Appendix I for more controlling parameters that have been investigated by the previous researchers). From Table 2.1, it appears that there is no yet any reported work that investigates the effect of reservoir heterogeneity on GAGD. Thus, there is a need to investigate the effect of  $k_v/k_h$  on GAGD since many reservoirs are actually layered and thus, the  $k_v/k_h$  is definitely different.

**Table 2.1:** Effect of Controlling Parameters on GAGD Projects (Sharma, 2005; Mahmoud, 2006; and Paidin, 2006)

Controlling parameter	Previous investigation results				Remarks
	Sharma, 2005	Mahmoud, 2006	Paidin, 2006	Mahmoud and Rao, 2007	
Porosity	8.5-32.9 %	45.7 %	32.9-41.0 %	8.5-32.9 %	The porosity can go very high (45.7 %)

<b>Injected gas composition</b>	Did not affect the oil recovery in immiscible mode	-	Increment of (10.9 % OOIP)	-	More investigation need to be done on investigating the effect of using N <sub>2</sub> as an injection gas
<b>Injection depth</b>	-	Did not affect oil recovery	-	Did not affect oil recovery	Provided with vertical communication between layers
<b>Gravity number, N<sub>G</sub></b>	Logarithmic relationship between gravity number and recovery	-	-	Field: 1-30; visual model: 0.2-1.1	An important parameter since GAGD make use of gravity
<b>Vertical permeability, k<sub>v</sub></b>	Most important parameter	Not an important parameter	-	-	The conflict may due to the differences in flow rate used
<b>k<sub>v</sub>/k<sub>h</sub></b>	-	-	-	-	No research has been reported yet
<b>Well design</b>	Horizontal well	Horizontal well	Horizontal well	Horizontal well	Previous research concentrate on horizontal wells

Previous researchers showed that the porous medium which is packed by glass beads has shown a relatively high porosity value with the highest recorded by Mahmoud (2006) with the value of 45.7%. This is one of the weaknesses of glass-beads-packed porous medium but the model has shown its value to visualize the front displacement during the flooding test. There is a contrast in the research outcome between Sharma (2005) and Paidin (2006) on the oil recovery increase by using N<sub>2</sub> as an injection gas during GAGD process. More research needs to be done on investigating the usability of N<sub>2</sub> as an injection gas during GAGD process. Mahmoud (2006) conclude that the gas injection depth does not have an influence on oil recovery and GAGD process is more favourable in a fractured reservoir. N<sub>G</sub> is a parameter that need to be take into account when investigating GAGD process since it involve the effect of gravity stability during the gas injection. If the viscous force

is dominated during the GAGD process, the horizontal producer might experience an early gas breakthrough on the higher permeability zone. All the previous researchers advice a similar recommendation, which is to investigate the effect of reservoir heterogeneity in GAGD process. Since GAGD process involves horizontal producer, it might worth to investigating the effect of different well design on GAGD process for an optimum well design during the field development.

### 2.3 Simulation

The pilot test and laboratory test are necessary to investigate the feasibility of GAGD process but they are too expensive. Thus, it is good to run some test such as simulation for a faster investigation. According to Wang (2011), the benefits of simulations are:

- i. To understand the reservoir.
- ii. To examine the reservoir performance and recovery mechanism.
- iii. To study the feasibility of EOR technologies.
- iv. To optimize the key reservoir development parameters.

Simulation means the construction and operation of a model whose behaviour assumes the appearance of actual reservoir behaviour (Teknica, 2001). It is generally performed by following the steps as showed in Figure 2.8 (Ertekin *et al.*, 2001).

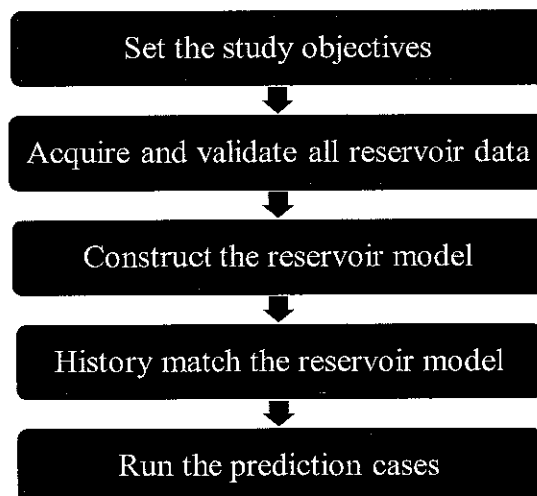


Figure 2.8: Steps Followed in Reservoir Simulation (Ertekin *et al.*, 2001)

Before once can continue to run any prediction with the constructed reservoir model, it is important to run a history match evaluation on the created model. The primary objective of history matching is to improve and to validate the reservoir simulation model results are match with the observed well production data (Ertekin *et al.*, 2001). There is no single, universally accepted strategy for performing a history match (John, 2006). Several authors have presented history matching guidelines including Crichlow (1977), Thomas (1982), Mattax and Dalton (1990), Saleri *et al.* (1992), and Carlson (2003). Ten golden rules for engineers who work on reservoir simulation studies have been listed by Aziz in his report in 1984.

Figure 2.9 shows the general algorithm for adjusting reservoir data to match historical production behaviour. Although every reservoir study is different, the guidelines provide a first pass for most petroleum reservoir (Ertekin *et al.*, 2001).

The same workflow was applied in this research so that the pressure and saturation is match between the laboratory test results and ECLIPSE simulation results. The match is very important since we require a valid and representative simulation model for prediction process.

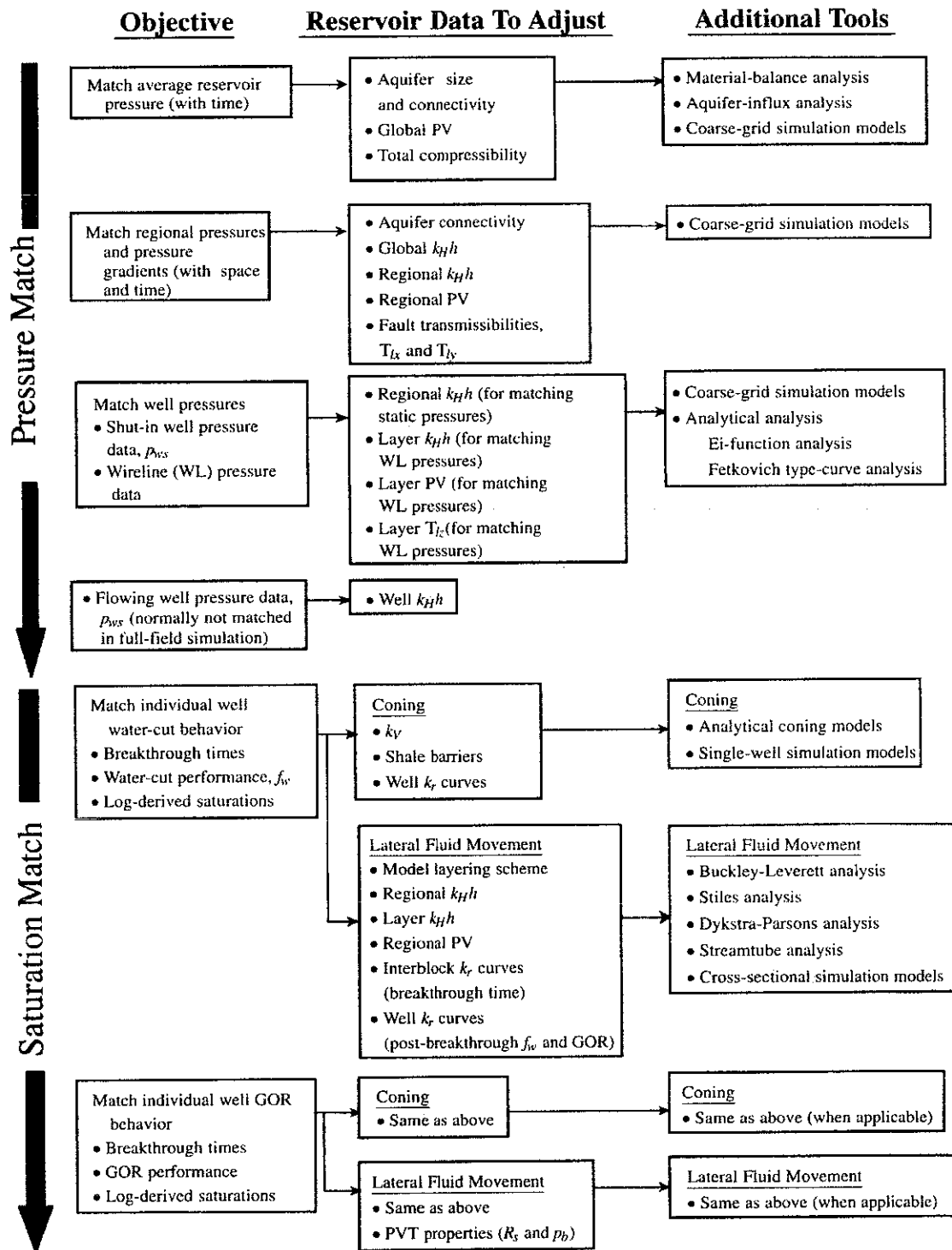


Figure 2.9: General Algorithm for Manual History Matching Along with Key Reservoir Data and Additional History-Matching Tools (Ertekin *et al.*, 2001)

### 2.3.1 ECLIPSE Simulator

Since ECLIPSE was used as a simulator for this research, it is important to describe the simulator in detail. Within the category of the finite difference solution technique, there is also the consideration of handling of fluid composition. The two options that available in ECLIPSE family are E100 and E300, respectively.

The E100 assumes that the oil and gas phases can each be represented as one component through time. The properties of the component can change with pressure and temperature, but the composition does not change. On the other hand, E300 tracks each component (methane, ethane, and so forth) of the oil and gas in the reservoir (Figure 2.10). This method is used to model fluids near the critical point where changes in the pressure and temperature of the compositional system can result in very different fluid behaviour (Bobek, 1990).

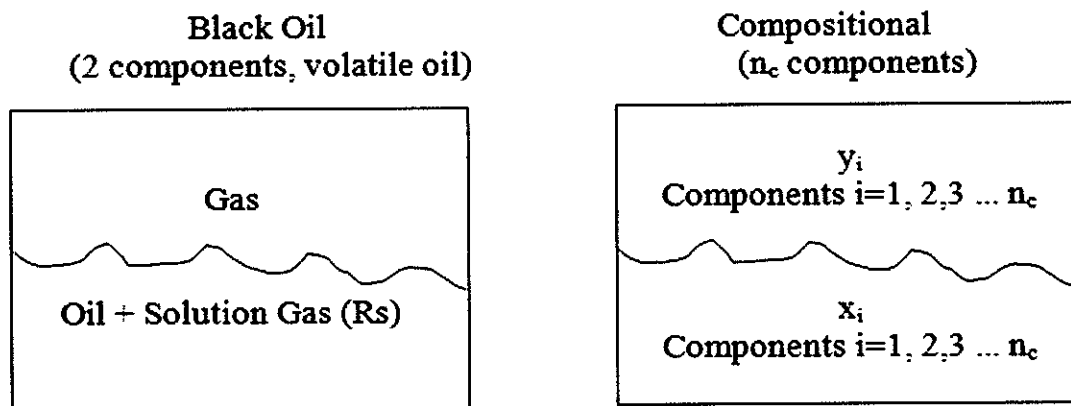


Figure 2.10: Comparison of Blackoil and Compositional Model (Bobek, 1990)

The engineer need to first describe the reservoir model in a input data file in which it consists of fluid and rock property description, initial conditions, wells and their phase flow rates and surface facilities. Figure 2.11 shows how each section in ECLIPSE is map to the flow equation (Schlumberger Information Solutions, 2009).

$$\text{Flow} = \text{Transmissibility} * \text{Mobility} * \text{Potential Difference}$$

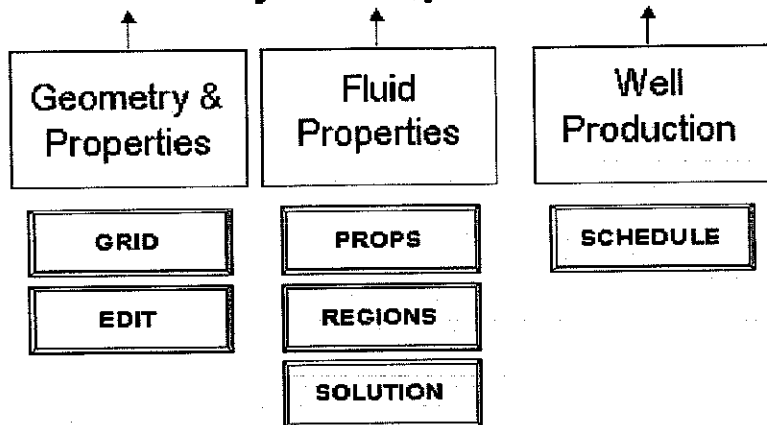


Figure 2.11: How ECLIPSE Sections Relate to the Flow Equation (Schlumberger Information Solutions, 2009)

When the reservoir geometry is in place, cell properties must be defined. This includes, but not restricted to, porosity, permeability in three dimensions and net-to-gross. The reservoir is also usually subdivided into distinct regions (Schlumberger Information Solutions, 2009):

- i. Reporting flows and fluids in place.
- ii. Specifying regions of distinct fluid contact.
- iii. Specifying regions in which fluids have different PVT properties, such as different API.
- iv. Specifying regions in which rock properties are distinct, such as connate or irreducible water saturation.

The different of E100 and E300 is summarized in Figure 2.12. Apart from how each phase been defined, there is also different in the fluid definition in which E100 is from PVT data lookup while E300, is from an iterative solution of equation of state. Thus, E300 requires more effort on regressing the equation of state to get a more robust and valid reservoir model.

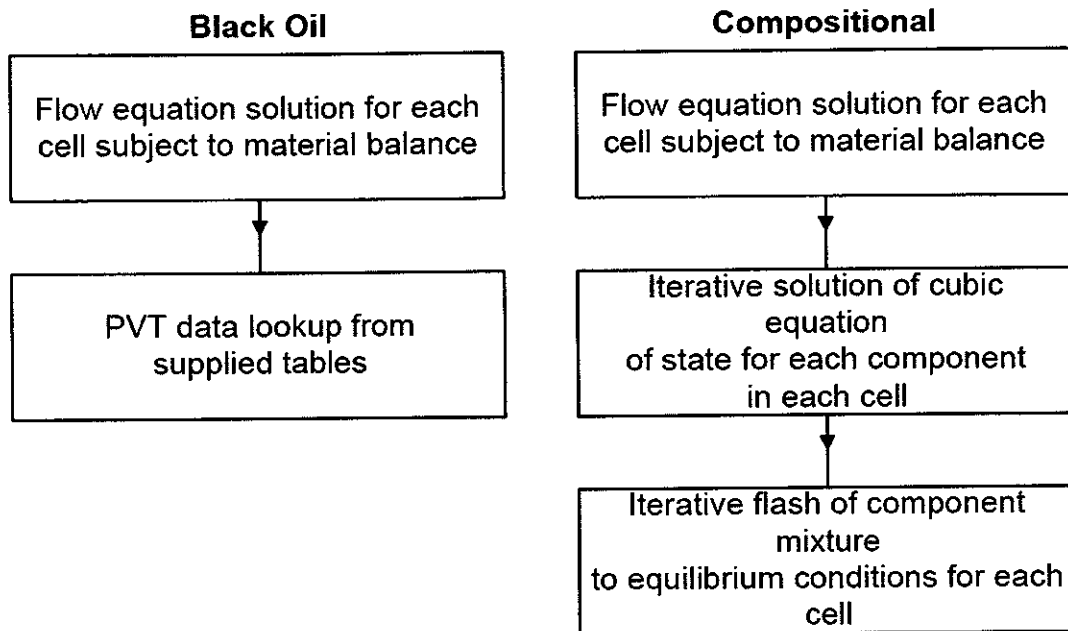


Figure 2.12: Different Between Blackoil and Compositional Simulation  
(Schlumberger Information Solutions, 2009)

## 2.4 Field Referred

There are two field that was referred in this research, which are Gelama Merah field and Gulfaks field. Gelma Merah is used as the reference prototype for Visual Physical model dimension and dimensionless time scaling purpose while Gulfaks field is used for field development investigation for the implementation of GAGD in real field level.

Gelama Merah field is located in Block SB-18-12 offshore West Sabah, Malaysia (Figure 2.13) at Latitude:  $05^{\circ} 33' 49.98''$  N and Longitude:  $114^{\circ} 59' 06.34''$  E. It is 141076ft NW from Labuan, 426509ft SW from Kota Kinabalu, and 140.4ft in water depth (Abdullah *et al.*, 2003, Shafi'i *et al.*, 2003 and Quek and Chang, 2004). Due to the confidential issue, the ECLIPSE model created will not be release to UTP until green light has been granted from PETRONAS.

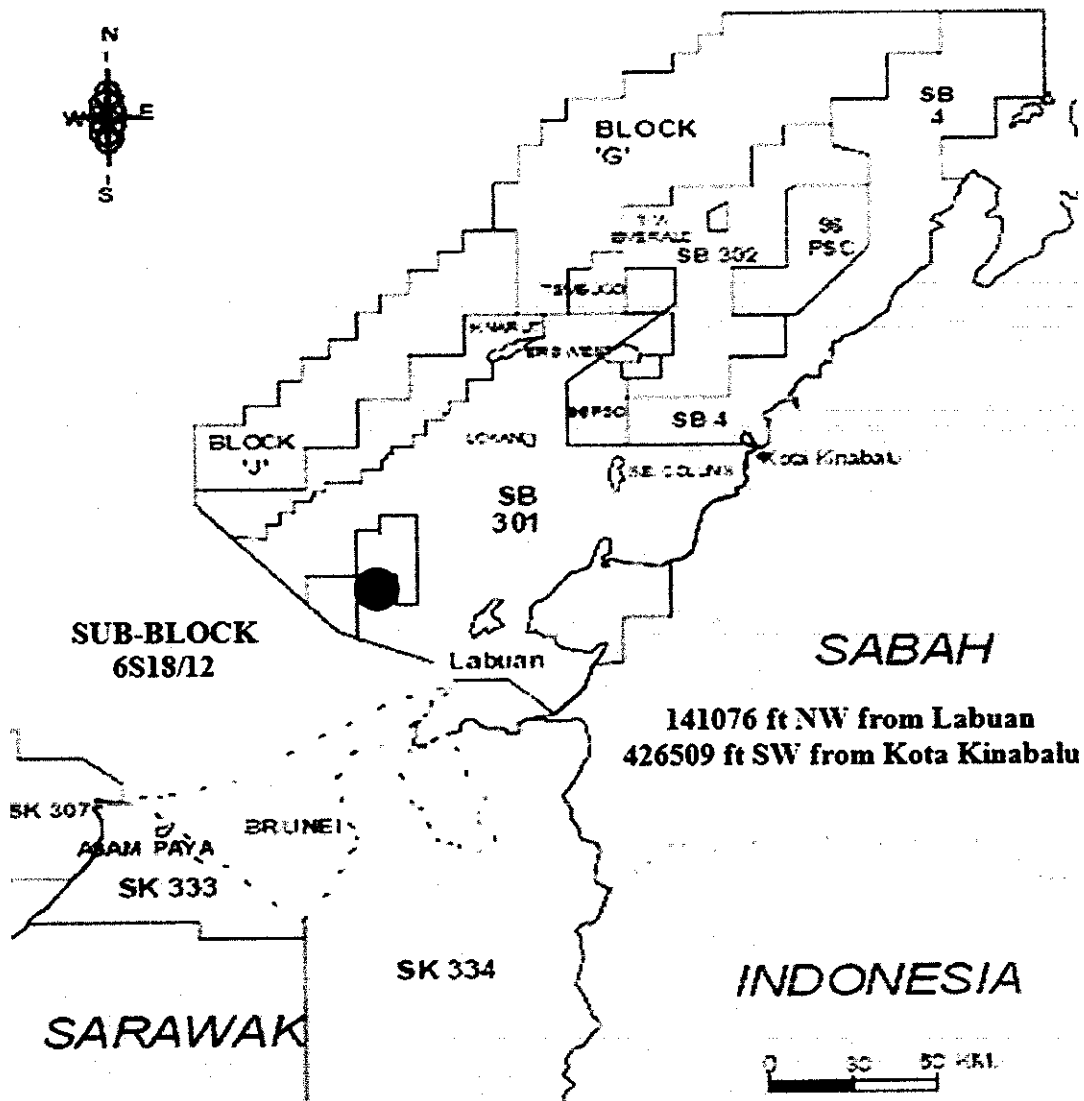


Figure 2.13: Location of Gelama Merah Field (Zainul *et al.*, 1999)

A total of nine targeted sand units is available, namely 3.2 (Figure 2.14), 4.0, 5.0, 6.0, 7.0, 8.0, 9.0, 9.1, and 9.2, respectively. After interpreted all the available contour map, a West-East cross section of the Gelama Merah reservoir is showed in Figure 4.2. For this research, Sand 9.2 is used as the target sand for full field GAGD field study because of the good sand quality (highest average permeability, highest average porosity, and highest residual oil saturation).

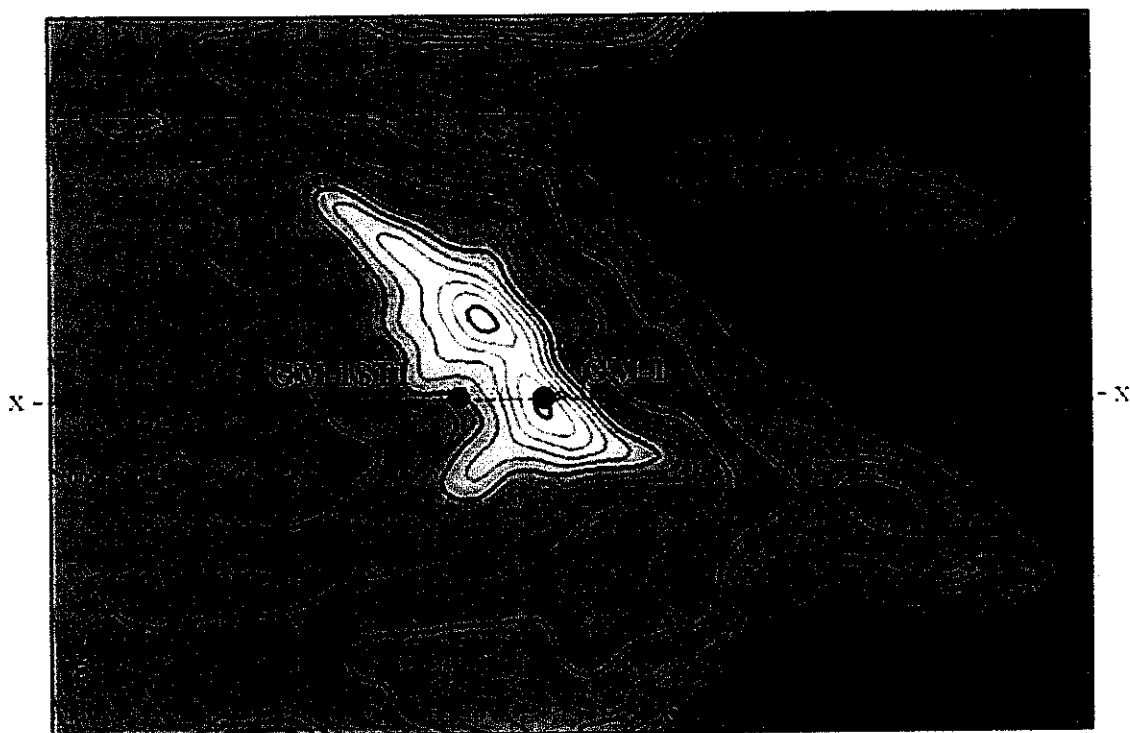


Figure 2.14: Top of Sand Contour Map for Unit 3.2 (Abdullah et al., 2003, Shafi'i et al., 2003 and Quek and Chang, 2004)

Table 2.2 summarizes all the Gelama Merah field properties which were then used in time scaling calculation please refer to Appendix E for time scaling application from laboratory scale to the real field scale.

Table 2.2: Gelama Merah Field Properties (Abdullah et al., 2003, Shafi'i et al., 2003 and Quek and Chang, 2004)

Property	Value
Absolute permeability	100mD
End-point relative oil permeability	0.48
Average porosity	27%
Reservoir thickness	115ft
Oil density	51.69Ib/ft <sup>3</sup>
Carbon dioxide density	8.73Ib/ft <sup>3</sup>
Initial water saturation	36%
Residual oil saturation	20%
Oil viscosity	1.36cP

The second field that was referred in this study is Gulfaks field (Figure 2.15) which is a major oilfield in North Sea. Data from Gulfaks was a commercially released by Statoil to Schlumberger for training purpose. Feasibility of implement GAGD in field level was investigated based on Gulfaks field.

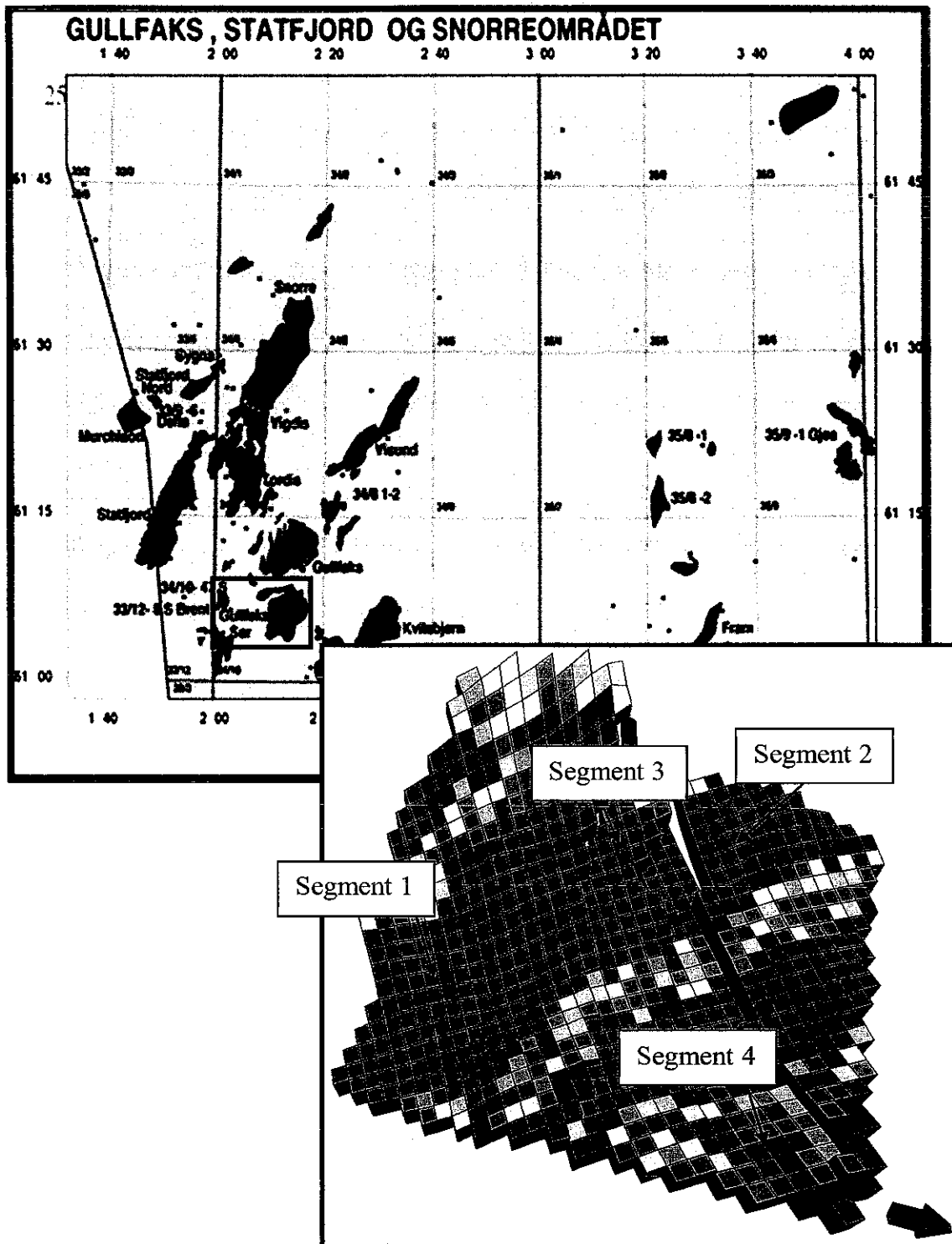


Figure 2.15: Location of Gullfaks Field (Schlumberger Information Solution, 2010)

Horizontal permeability of Gullfaks field range from 33-4905mD while the vertical permeability range from 3-490mD. The maximum  $k_v/k_h$  ratio of the reservoir is around 2.42 (Figure 2.16). Since the reservoir is deep down, the condition made Gullfaks field a good candidate for GAGD implementation.

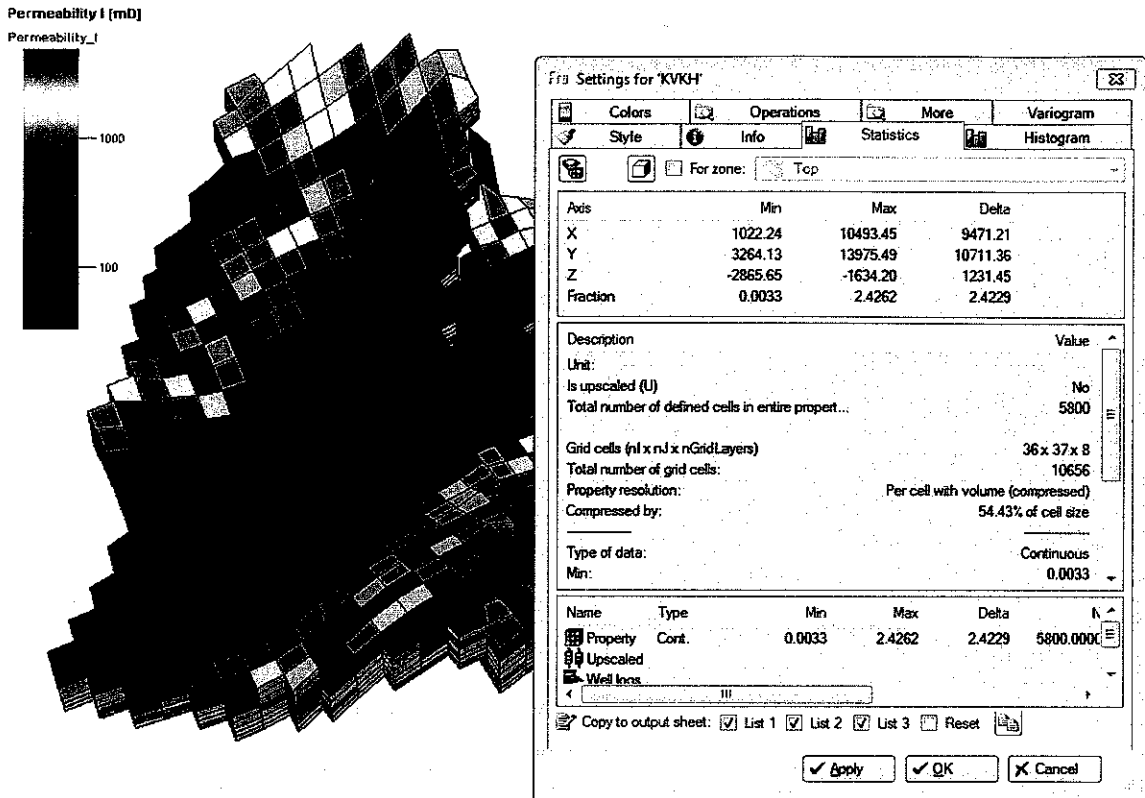


Figure 2.16: Reservoir Properties (Schlumberger Information Solution, 2010)

Gulfaks field was subdivided into four major segments because of the faults. Segment four was initially produced with only a vertical producer (P01) from 1<sup>st</sup> of February 2005 to 7<sup>th</sup> of July 2009. Refer to Figure 2.17, at the end of the primary production period, segment four of Gulfaks field was still left with high oil saturation. Thus, investigation of difference recovery techniques is needed to recover the left over oil.

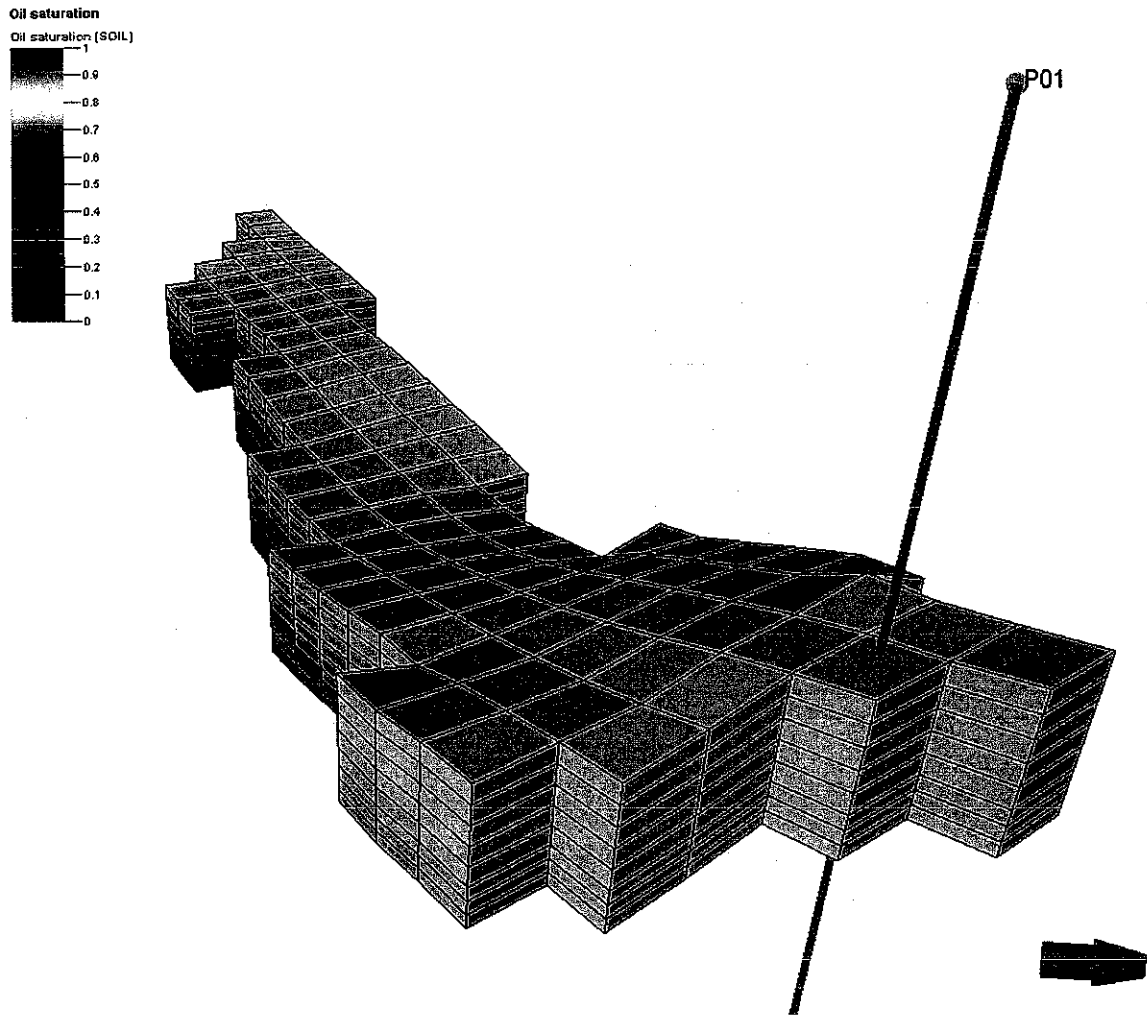


Figure 2.17: Oil Saturation at Segment Four at the end of Primary Production (Schlumberger Information Solution, 2010)

## 2.5 Well Design

Refer to Figure 2.18, there will be some frictional pressure losses along the tubing in a horizontal well that caused the coning at the well heel due to increased draw down in comparison to the toe (Schlumberger Information Solution, 2010). It is an industry practice to introduce inflow control devices in horizontal well to impose an additional pressure drop between the tubing and the sand face, which varies along the well's length in proportion to the in-tubing pressure losses. However, to capture this scenario correctly, the wells need to be model as multi-segment wells.

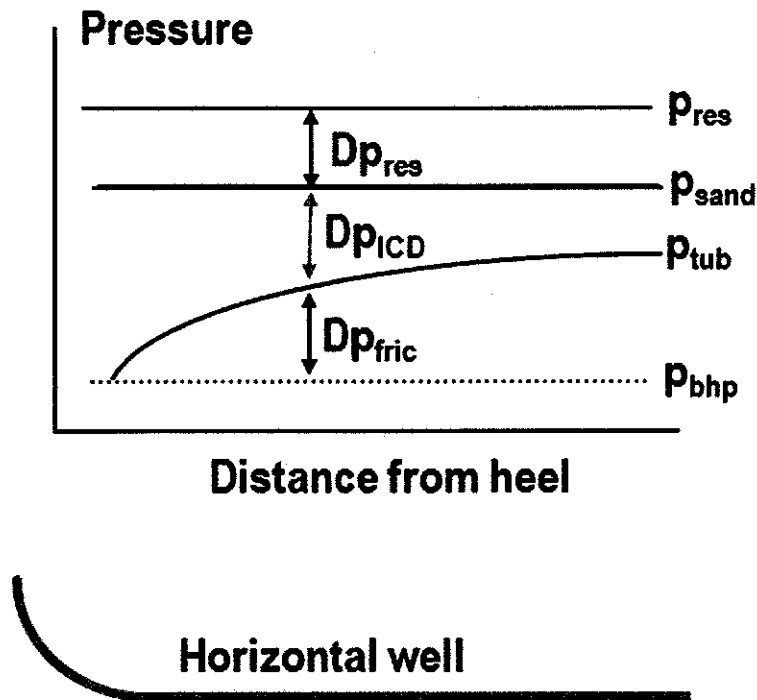


Figure 2.18: Pressure Profile along Horizontal Well (Schlumberger Information Solution, 2010)

The multi-segment well model is a special extension, which is available in both E100 and E300. It provides a detailed description of fluid flow in the well bore. The facility is specifically designed for horizontal and multi-lateral wells, although it can of course be used to provide a more detailed analysis of fluid flow in standard vertical and deviated wells. Like the standard well model, the equations are solved fully implicitly and simultaneously with the reservoir equations, to provide stability and to ensure that operating targets are met exactly (Holmes *et al.*, 1998).

In the standard well model, ECLIPSE will only consider the pressure drop between the bottom hole pressure and the tubing head pressure (Equation 2.9) while for multi segmented well, the well is divided into segments to compute the fluid density. Since an average density is computed for each segment, the formation volume factors are based on the average pressure for each segment and the density is allowed to vary along the wellbore (Schlumberger Information Solution, 2010). Once the density is computed, the pressure drop can be computed since we know the connection depths (Figure 2.19).

$$\Delta p = \Delta p_{hyd} = \rho g h \quad (2.9)$$

Where,

$\Delta p$  is the pressure different between bottom hole pressure and tubing head pressure,

$\Delta P_{hyd}$  is the hydrostatic pressure drop,

$\rho$  is the density of the wellbore content,

$g$  is the gravitational acceleration, and

$h$  is the connection depth

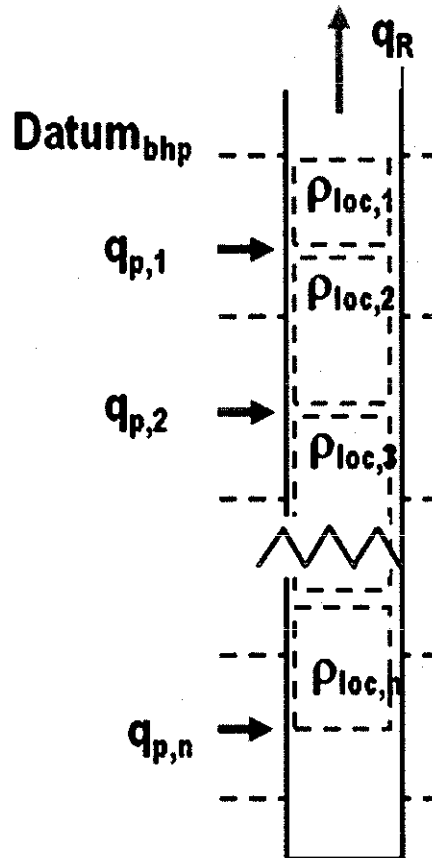


Figure 2.19: Segmented Density Calculation in Multi Segmented Well (Schlumberger Information Solution, 2010)

The description of inflow control valve that provided by Schlumberger is show in Figure 2.20. The inflow control valve was used to investigate the optimum design of GAGD process in real field implementation. The inflow control valve has four opening. With an opening area of 4mm each, this made the effective opening of 0.314in for each in flow control valve.

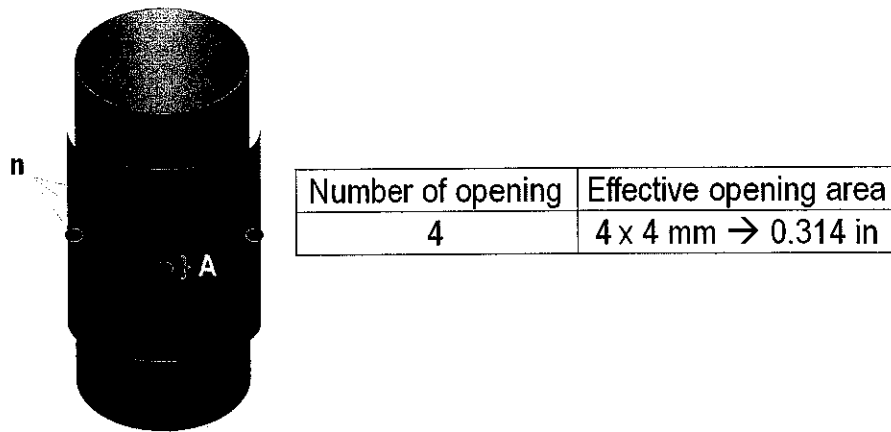


Figure 2.20: Inflow Control Valve (Schlumberger Information Solutions, 2010)

## 2.6 Summary

Field implementation of GAGD project has showed its usefulness in recovering more oil (54%OOIP) compared to WAG project (5-10%OOIP). GAGD project made use of the effect of gravity which tends to segregate fluids in the reservoir in order to maintain the density equilibrium. Gravity drainage is defined as a recovery process in which gravity acts as the main driving force and where gas replaces the voidage volume. Heterogeneity plays havoc with horizontal gas floods leading to early breakthroughs and poor reservoir sweeps but in gravity stable gas floods, heterogeneous stratification can delay gas breakthrough due to physical dispersion, and reduced gas channelling through the horizontal deposited high permeability layer. Thus, improve the sweep efficiency.  $k_v/k_h$  is generally used to represent the extent of permeability heterogeneity in a reservoir. Recent advances in horizontal well technology has demonstrated the usefulness of horizontal well in minimizing the gas coning. Laboratory investigation and pilot test is a must in investigating the usefulness of GAGD project but they are too time consuming and not cost effective. Thus, simulation is a good option to close this gap. For a more reasonable comparison, we need to scale the laboratory model to field scale so that it will be more representative, which in this research, Gelama Merah field. For GAGD feasibility study in field level, Gulfaks field was chosen and different development strategies can then be studied based on simulation.

## CHAPTER 3

### METHODOLOGY

#### 3.1 Task Identification

The description for apparatus and procedures are present in this chapter. Figure 3.1 summarizes the overview for methodology in order to achieve the objectives. The research is divided into two main parts, the simulation studies and the laboratory studies. The laboratory studies were used as a compliment to the simulation because of the limitation in the laboratory apparatus. Outcome from the laboratory studies was used as an input to study the effect of  $k_v/k_h$  on gravity segregation in GAGD process by using ECLIPSE simulator. In order to propose different development strategies on GAGD process and as a feasibility screening on implementing GAGD process in field level, simulation studies were done based on Gulfaks field.

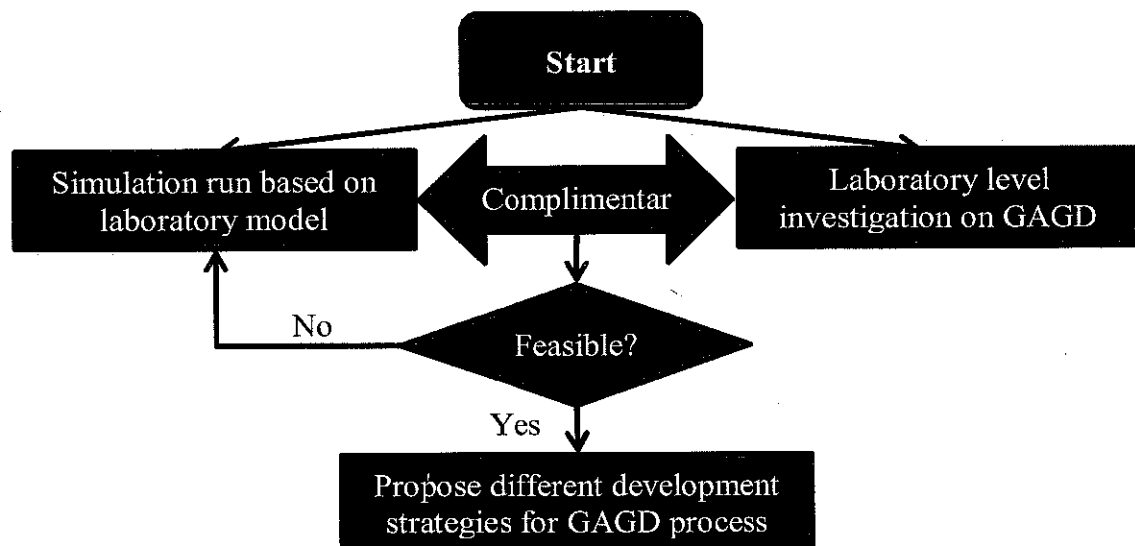


Figure 3.1: Flow Chart for Methodology

## 3.2 Experimental Apparatus and Procedure

This section summarizes all the apparatus and procedures involved in laboratory investigation. Experiments were conducted to visualize the GAGD process of recovery by CO<sub>2</sub> injection. The experimental laboratory design for this study was aimed on investigating the effect of  $k_v/k_h$  on gravity segregation as a compliment to the ECLIPSE simulation. Different values of  $k_v/k_h$  were created by using glass beads in the visual physical model and the oil recovered from the model was recorded. The model's dimension, fluid properties, grid properties, and production data were recorded so that simulation can be run for a better development strategy in GAGD process. Prior to the development strategy run, the simulation model was first history match to make sure that the simulation model is representing the laboratory model. For a more detail description, please refer to Appendix C and Appendix D.

### 3.2.1 Apparatus

A Hele-Shaw visual physical model was made from Perspex while a measurement model was made from PVC. All the specification and limitation for the equipments have to be taken into account for a better measurement. The details of the models are described in section 3.2.1.2 while the details of all of the equipments used are described in Appendix F.

#### 3.2.1.1 Models

Two models were fabricated for use in the present research, namely, the visual physical model (Model: VPM-G-02) and the measurement model (Model: MM-G-01), as show in Figure 3.2 and 3.3, respectively. They were used to visualize the displacement process and to measure the permeability and porosity of the glass beads.



Figure 3.2: Visual Physical Model (Model: VPM-G-02)



Figure 3.3: Measurement Model (Model: MM-G-01)

There are several steps to be followed to construct the visual physical model which are important for structural and sealant purposes. During the test run, the original visual physical model which was made from 100% Perspex was cracked when the system's pressure reached 25psi. To increase the strength, the frame of visual physical model was further enhanced with metal frame and the system pressure can sustain until 40psi.

Chloroform was used to stick the Perspex together. For a leak free model, epoxy glue was applied between the metal frame and Perspex plates. To avoid the glass beads from entering the injector or producer and cause any flow assurance issue, metal screen was placed at the perforated area for glass beads control.

Finally, silicone was applied to all the joins prior to the leaking test. Different from the visual physical model, piping tape was wrapped on all the joints for leaking prevention. It is a very important to create a leak free environment for pressure consistency.

Mineral oil was chosen over crude oil because of visibility reason. Mineral oil which was manufactured by Sigma-Aldrich was dyed with blue dye so that the fluid displacement can be clearly observed in the visual physical model. More detail on the mineral oil is available in Appendix F.

Brine which is 30000ppm was prepared by manually mixing tap water with sodium chloride. Since brine is insoluble with the mineral oil and the dye is only soluble in the mineral oil, it created a contrast between the fluids. Thus, the fluid displacement can easily visualize.

It is important to know the dimension of the measurement model and visual physical model since it is an important parameter for permeability and porosity calculation. The detail calculation on the permeability and porosity is shows in Appendix C. The inner dimension of the visual physical model and measurement model are showed in Figure 3.4 and Figure 3.5 respectively. The dimension has to be known for calculation. Visual physical model was made from perspex and steel while the measurement model was made from PVC pipe.

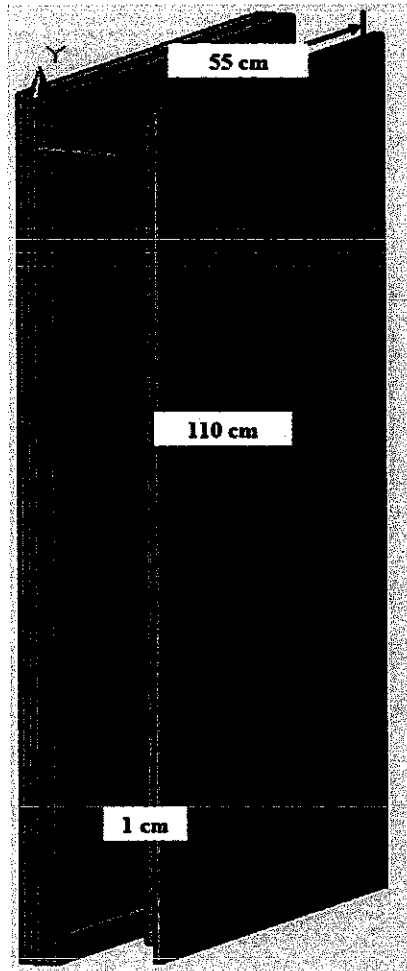


Figure 3.4: Inner Dimension of Visual Physical Model

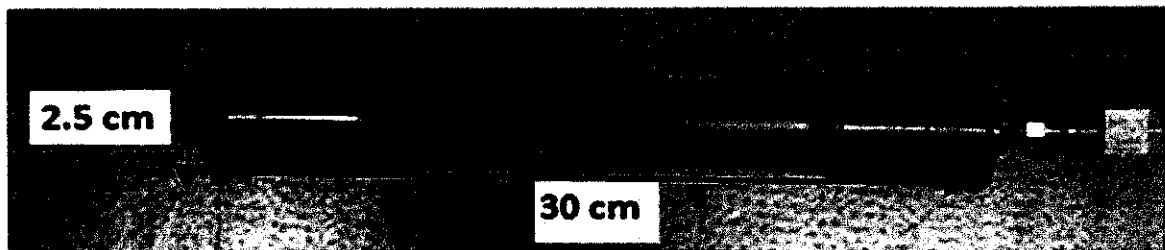


Figure 3.5: Inner Dimension of Measurement Model

### 3.2.1.2 Porous Media

Glass beads with size of 30-60, 90-150, 212-400, and 425-600 $\mu\text{m}$  were used. Details of the glass beads were listed in Appendix F. Glass beads was chosen because it could enhance the observation and chemically inert. It is realized that the pore structure of heterogeneous and random on a microscopic scale. Even for the same

packs of spheres, regularity in pore shapes would at best be localized. Thus, it is necessary to assume the uniform of the individual pores.

### **3.2.2 Experiment Procedure**

This section described all the experiments procedure involved by using flow chart, process flow diagram, and set-up. The experiment procedure was replicated from the previous researchers for a standardized investigation methodology. The procedure has to be strictly followed for a consistent result. Detail description on the step-by-step experiment procedure is shows in Appendix C.

#### *3.2.2.1 Flooding Test*

Figure 3.6 shows the flow chart for flooding test in laboratory investigation. The equipment was setup according to the flow chart which is shows in Figure 3.6. The set-up allows an automatic recoding of inlet and outlet pressure throughout the experiment run by connecting all the pressure gauges to Matlab software. A webcam was used to record the fluid displacement throughout the injection and displacement process. The recorded video was used to compare with the simulated fluid displacement to ensure a uniform fluid displacement. A step-by-step procedure for the flooding test is shows in Appendix C.

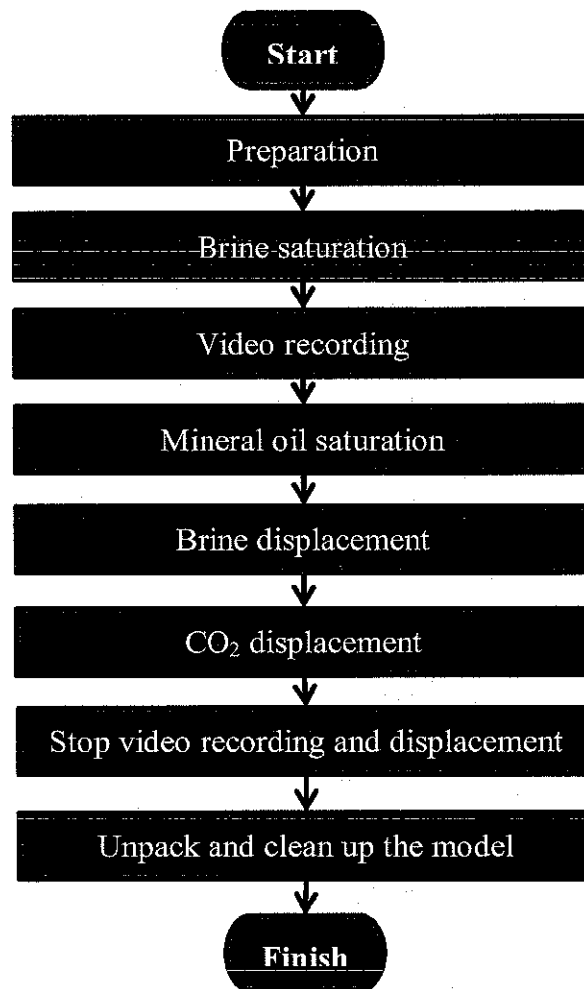


Figure 3.6: Flow Chart for Flooding Test

The flooding test was setup as Figure 3.7 and 3.8. Injected CO<sub>2</sub> has to go through a moisture removal trap to avoid any corrosion. The instruments used can resist the pressure of 100psi, in which all the instruments can still be utilize when the visual physical model can sustain a higher pressure. All the instruments used were calibrated against the existing TEMCO RPS-800-10000 HTHP Relative Permeability Test System prior to system setup to validate the accuracy and robustness of all the instruments. The in house model is in fact easier to operate and much cheaper than the existing TEMCO RPS-800-10000 HTHP Relative Permeability Test System. However, the in house model can only operate to 40psi with the current visual physical model. The visual physical model has been certified by Universiti Teknologi PETRONAS post graduate department during Engineering Design Exhibition year 2011.

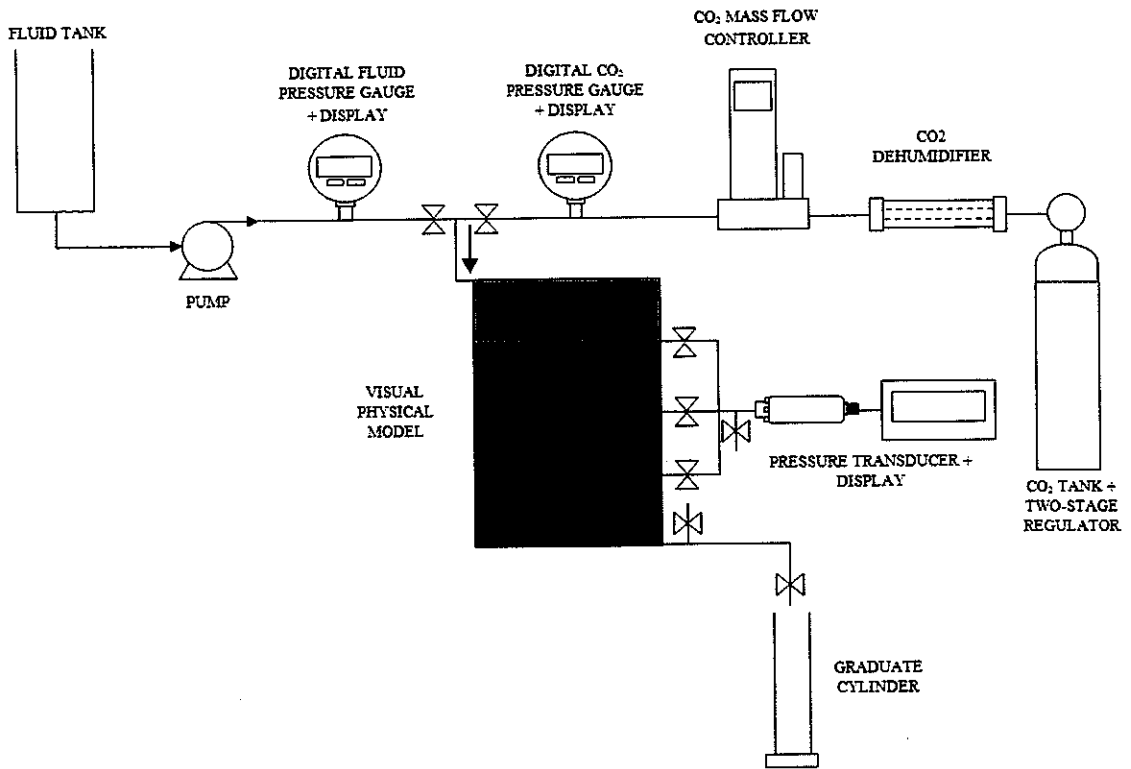


Figure 3.7: Process Flow Diagram for Flooding Test

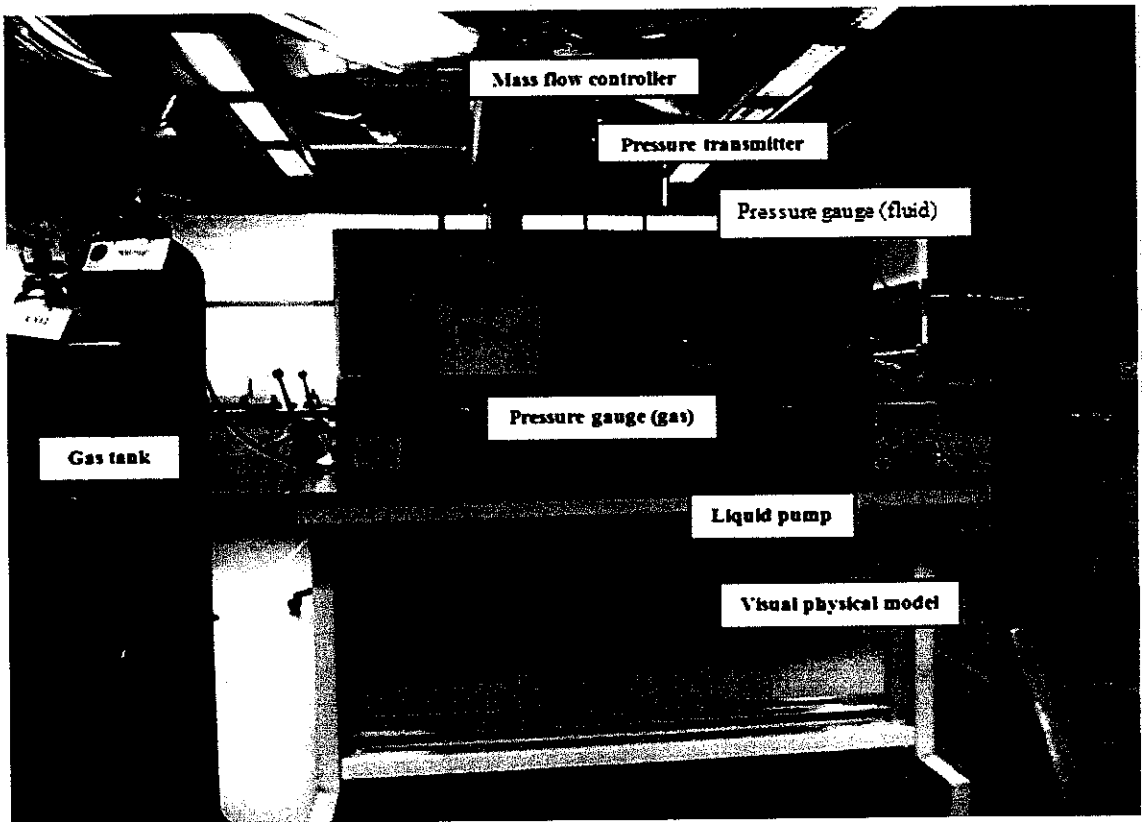


Figure 3.8: Flooding Test Set-up

### 3.2.2.2 Fluid Density Measurement

Portable density meter (Model: DMA 35<sub>N</sub>) which is manufactured by Anton Paar GmbH (Figure 3.9) was used for density measurement (refer to Appendix G for description of density meter DMA 35<sub>N</sub>). DMA 35<sub>N</sub> was designed for use in the most demanding industry, it can be used to measure the density, specific gravity or percentage concentration of the fluid sample. Based on the harmonic oscillator technology, the DMA 35<sub>N</sub> is light with only 275g which is come very handy for enormous amount of fluid data. The DMA 35<sub>N</sub> can also store up to 1024 data points which can then transfer to a computer or printer later.

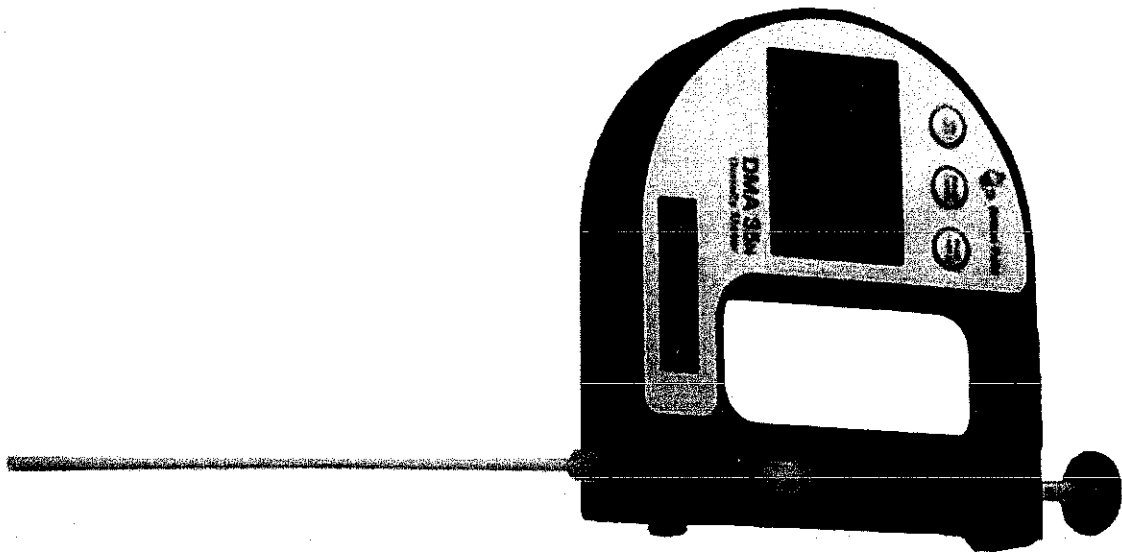


Figure 3.9: Portable density meter (Model: DMA 35<sub>N</sub>)

DMA 35<sub>N</sub> was used to determine the density or relative density of crude according to the U-tube principle. Prior to any fluid density measurement, the density meter has to be calibrated using the distilled water before it can be use to measure other fluid. The density meter needs to be flash with distilled water before that next fluid density is measure. For a more representative measurement, a total of five reading was taken and an average number was taken as the final density measurement. Equation 3.1 was used for density calculation (Torsaeter and Abtahi, 2003).

$$\rho_{avg} = \frac{1}{n} \sum_{i=1}^n \rho_i \quad (3.1)$$

### 3.2.2.3 Fluid Viscosity Measurement

Viscosity of all the liquid used in the research was determined by using OFITE Pressurized Viscometer Model 1100 (Figure 3.10). Detail description on OFITE Pressurized Viscometer Model 1100 is available in Appendix F. The viscometer measured fluid viscosity (cP) at a given shear rate and displayed according to CGS system. This is a fully-automated system which accurately determines the fluids characteristics of stimulation fluids, completion fluids, drilling fluids, and cement in term of shear stress, shear rate, time and temperature at pressure up to 2500psi.

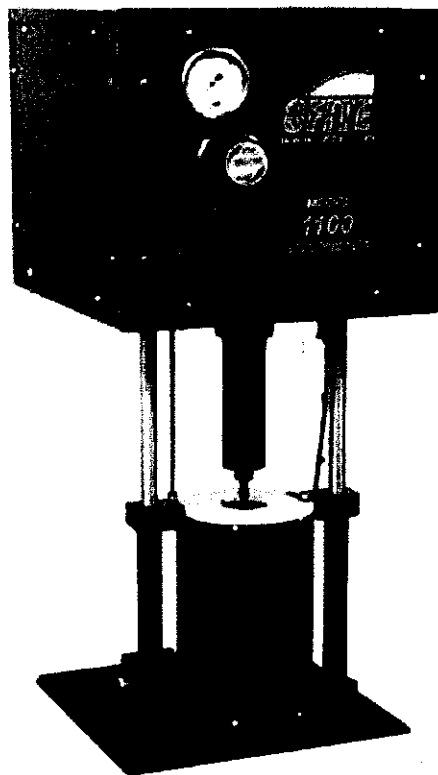


Figure 3.10: OFITE Pressurized Viscometer Model 1100

Using the exclusive ORCADATM software, a computer novice can operate the viscometer, and yet the system is versatile enough for advanced research and demanding test parameters. The viscometer is suitable for laboratory and field use. The viscometer was used to measure the brine and mineral oil viscosity at 600RPM.

### 3.2.2.4 Packing, Cleaning, and Repacking

Packing is the most crucial and yet hardest part of this research. Even for packs of spheres, regularity in pore shapes would at best be localized. Leaking test has to be done prior to pack the glass beads. This is a very crucial step since a leaky model will result in pressure loss and all the pressure recorded will not be valid anymore. The visual physical model was injected with compress gas and the system pressure was continuously monitored. Epoxy and silicon is applied to any leaking point of the visual physical model in the case of any pressure reduction was observed. After the epoxy and silicon were cured, soapy water was then applied to the weak point and compress gas was reinjected for pressure monitor purpose. After the leaking test, the visual physical model was placed on the table for packing purpose. After the desired flooding test was run, the visual physical model was unpacked and clean up for the next run. The used glass beads need to be wash with soap and acetone before can be dehumidified and reuse in next measurement. To get a consistent permeability, steps used by Ma (2005) were modified and followed (Figure 3.11). A detail description on how  $k_v/k_h$  was calculated is shown in Appendix C.

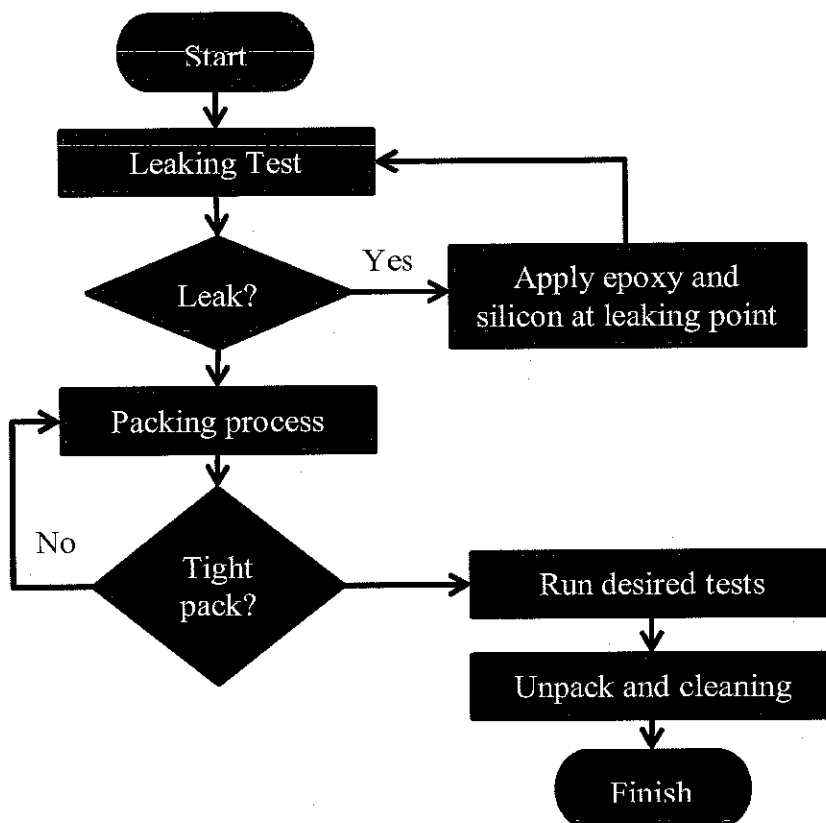
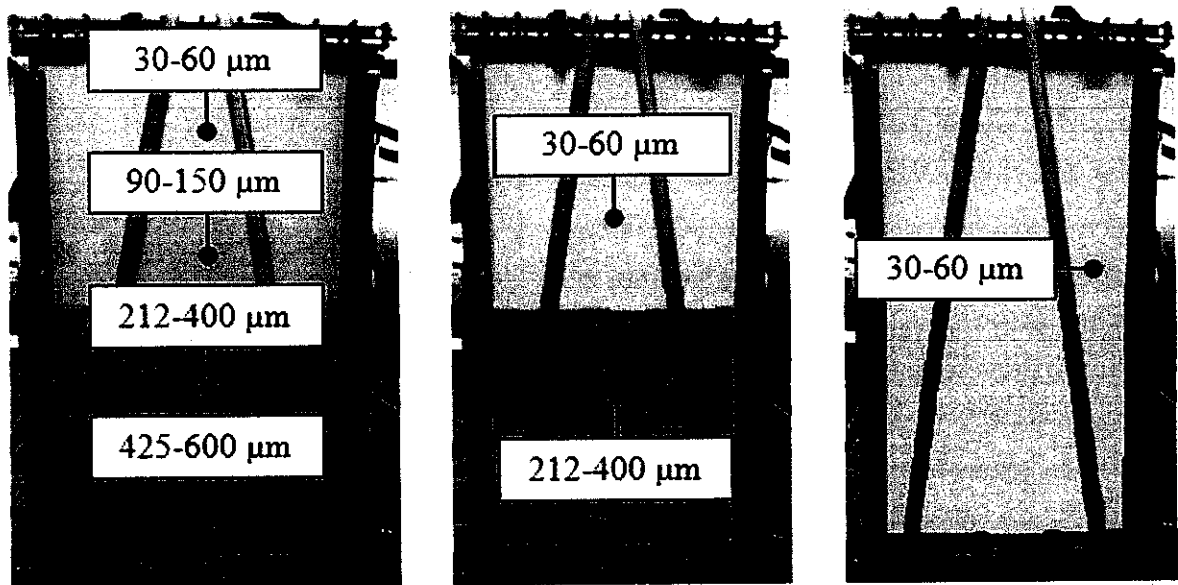


Figure 3.11: Flow Diagram for Packing, Cleaning, and Repacking (Ma, 2005)



(a)  $k_v/k_h=0.8$

(b)  $k_v/k_h=0.9$

(c)  $k_v/k_h=1.0$

Figure 3.12: Layered Models Set-up

### 3.2.2.5 Porosity and Permeability Measurement

Prior to setup the visual physical model, we need to know the porosity and permeability that the specific group of glass beads can create. To meet that purpose, a measurement model was design (Figure 3.3) by using PVC. The flow chart is shows in Figure 3.13.

For porosity calculation, we need to record the dry weight and the wet weight of the measurement model while for porosity calculation while the inlet pressure, outlet pressure, flow rate and model's dimension for permeability calculation. Detail description for the calculation of pore volume, porosity, and permeability are explained in Appendix C. After the calculation has been done, the same batch of glass beads were re-measured using Helium Porosimeter. Comparison between measurement model and Helium Porosimeter is shows in Table C3 (Appendix C). To make sure the measurement design is up to the standard, the custom-made-measurement model needs to be further modify if the different is more than 2%.

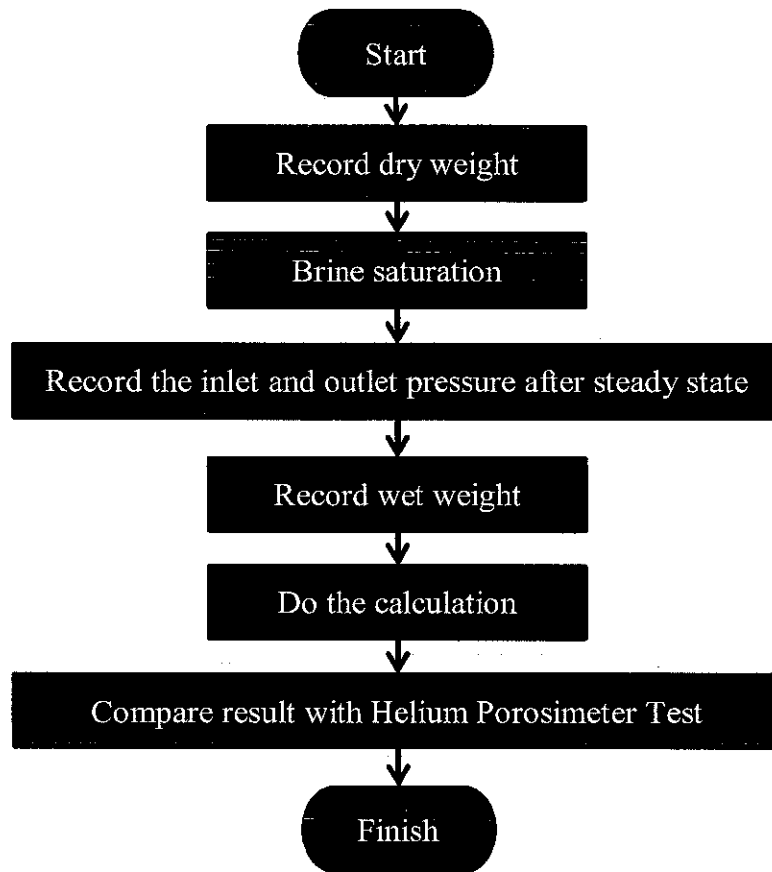


Figure 3.13: Flow Diagram for Porosity and Permeability Measurement

Process flow diagram for the porosity and permeability measurement is shown in Figure 3.14. The dry weight and wet weight of the model need to be measured for porosity calculation (detail description of the calculation is available in Appendix C). Depend on the type of the injection type (gas or liquid), the injection part can be changed between a pump or a gas tank. For permeability calculation, the flow rate, fluid viscosity, model's measurement, inlet and outlet pressure need to be recorded during the calculation (please refer to Appendix C for detail description). For a better visualization on the measurement model design, the measurement model set-up is shown in Figure 3.15. Detail description on the materials and equipment used is provided in Appendix F.

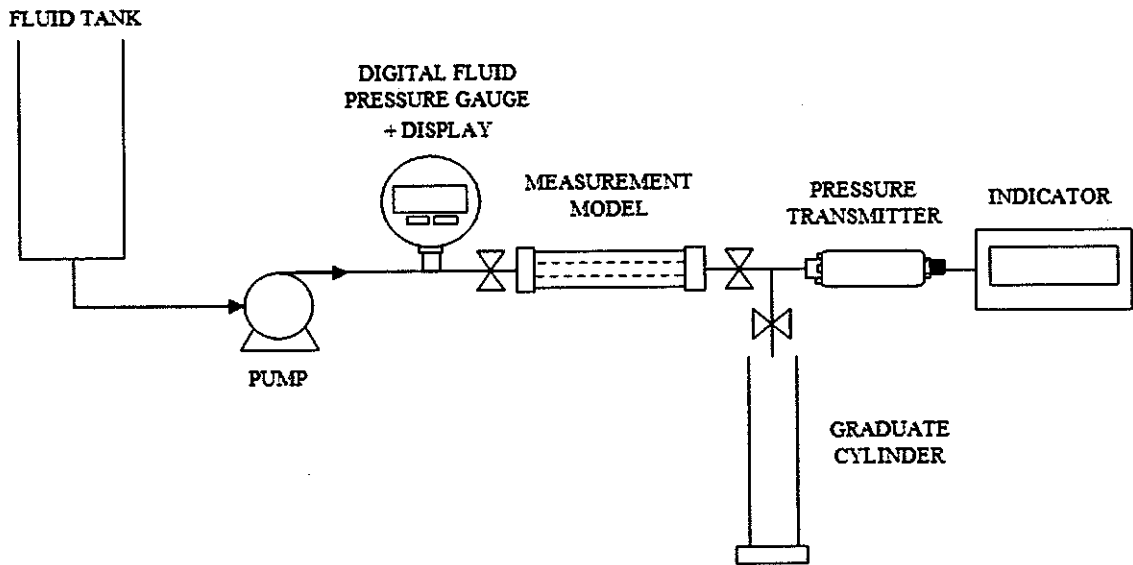


Figure 3.14: Process Flow Diagram for Measurement Model

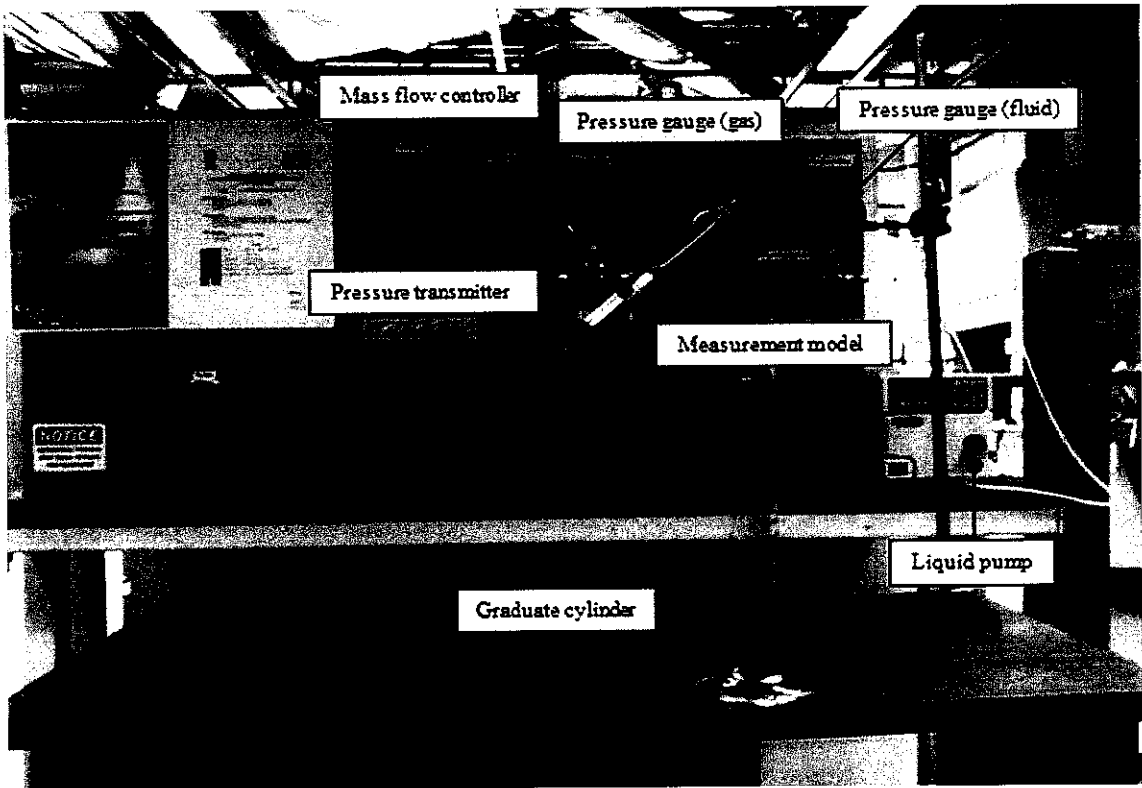


Figure 3.15: Measurement Model Set-up

Porosity measurement results from measurement model were compared over Helium Porosimeter test in which the set-up is shown in Figure 3.16. Helium Porosimeter test applies Boyle-Mariotte's Law to measure the porosity. The glass beads were filled in the matrix cup prior to the porosity measurement. The operating manual can be found in the manual prepared by Vinci Technologies (1997).

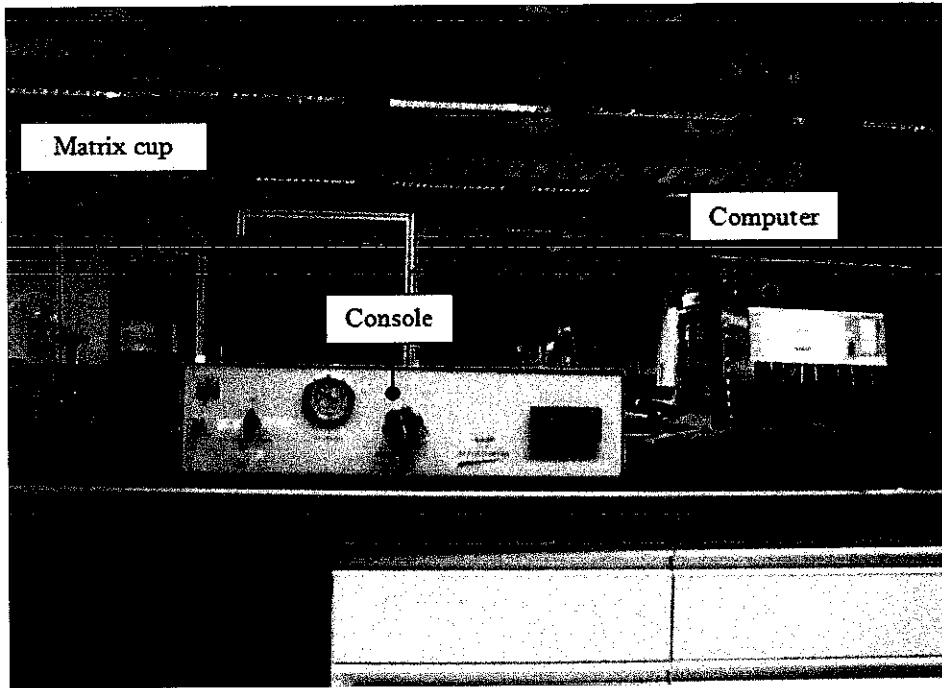


Figure 3.16: Helium Porosimeter Test Set-up

### 3.2.2.6 Simulation

Prior to deployment of any newly develop injection method, it needs to go through some laboratory measurements or pilot test. However, these processes are time and cost consuming. It took two months to complete only a single cycle in the laboratory investigation for one value of  $k_v/k_h$ . Thus, it is important to carry out simulation run during this research. Simulation was run by using Schlumberger ECLIPSE Blackoil (E100) and ECLIPSE Compositional (E300) Reservoir Simulation software. An ECLIPSE data input file is split into sections, each which introduced by keyword.

A list of all section-header keywords is summarizes in Table 3.1 together with a brief description of the contents of each section. A more detail breakdown of the section contents may be found in ECLIPSE reference manual which come with ECLIPSE Launcher while a quick overview on minimal data for ECLIPSE simulation run are summarized in Appendix H. The fluid component properties which have been used in the PROPS section were adapted from previous project used for WAG (Musa, 2004). While the grid's dimension that was used in the GRID section which is in the same scale as the laboratory model is shows in Figure 3.17.

Table 3.1: ECLIPSE Data File Sections

Section Name	Description
RUNSPEC	Title, problem dimensions, switches, phases present, components etc.
GRID	Specification of geometry of computational grid (location of grid block corners), and of rock properties (porosity, absolute permeability, etc.) in each grid block.
PROPS	Tables of properties of reservoir rock and fluids as functions of fluid pressures, saturations and compositions (density, viscosity, relative permeability, capillary pressure, etc.). Contains the equation of state description in compositional runs.
SOLUTION	<p>Specification of initial conditions in reservoir - may be:</p> <ul style="list-style-type: none"> <li>• Calculated using specified fluid contact depths to give potential equilibrium</li> <li>• Read from a restart file set up by an earlier run</li> <li>• Specified by the user for every grid block (Not recommended for general use)</li> </ul>
SCHEDULE	Specifies the operations to be simulated (production and injection controls and constraints) and the times at which output reports are required. Vertical flow performance curves and simulator tuning parameters may also be specified in the SCHEDULE section.

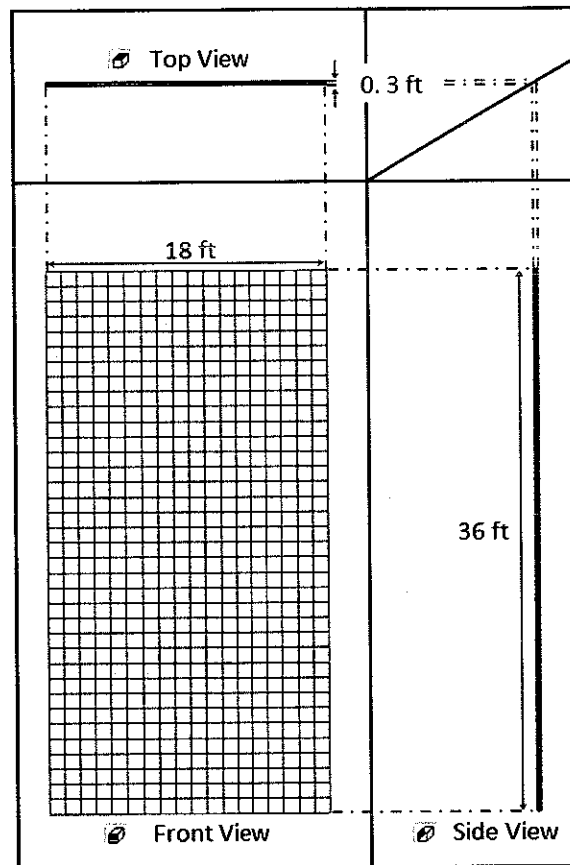


Figure 3.17: Grid Block Size and Properties

The location for injector and producer is shown in Figure 3.18 (red color). For the completion status, both of the wells were perforated at the x-direction (indicated by green oval) but shut at the z-direction (indicated by red color). This is the base case condition that was used to mimic the condition in laboratory test. After the results from simulation model (both for E100 and E300) was history matched with the laboratory measurement results, further investigation was done by using different combination of well design. The minimum miscible pressure for CO<sub>2</sub> and N<sub>2</sub> injection were also investigated using the slim tube apparatus. This was run using E300 simulation run because of the limitation of visual physical model to handle too extreme pressure and there is no slim tube apparatus facility in Universiti Teknologi PETRONAS. The recovery factor for different type of injection gas (CO<sub>2</sub> and N<sub>2</sub>) was recorded to investigate the effect of different type of injection gas in GAGD process. The recovery factor for each of the cases was recorded to investigate the most effective development strategy for GAGD process implementation.

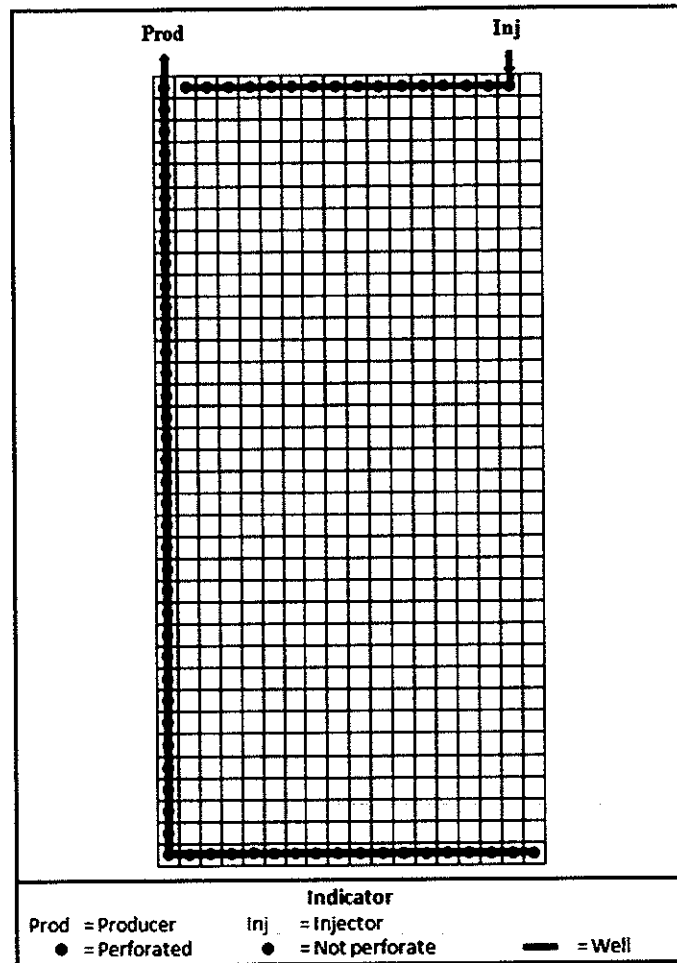
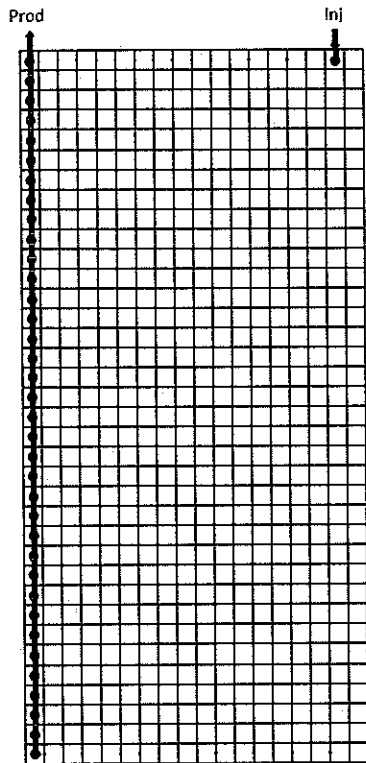


Figure 3.18: Location and Condition of Injector and Producer

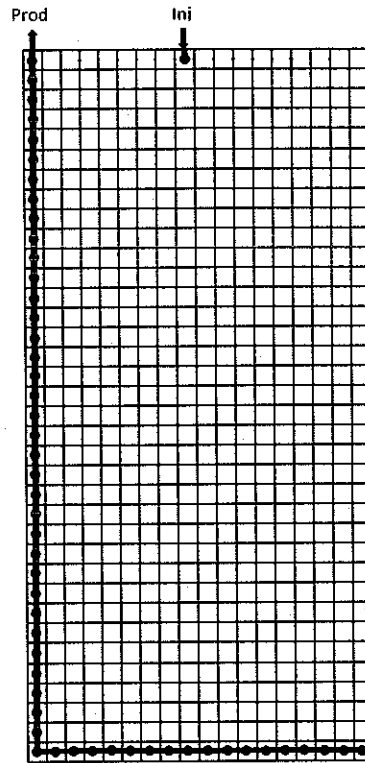
Visualization during gas injection was simulated using FloViz application. The wells orientation (injector and producer) were also investigated to make sure the best orientation was used for the candidate (reservoir investigated). Types of orientation that have been investigated were (Figure 3.19 (a), (b), (c), and (d)):

- a) Two vertical wells.
- b) Shallow vertical injector with horizontal producer.
- c) Deep vertical injector with horizontal producer.
- d) Two horizontal wells.

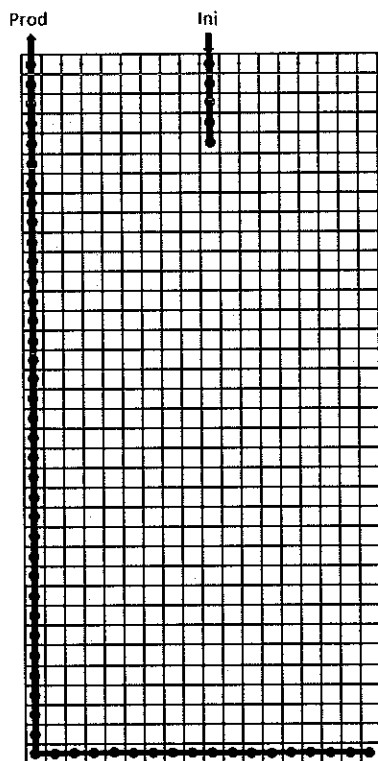
Optimum well location is very crucial because gas need to has enough time to migrate to the top of the reservoir. If the injector is located too near to the producer, early gas breakthrough might happen but if it is too far, it will take longer time to observe the oil production.



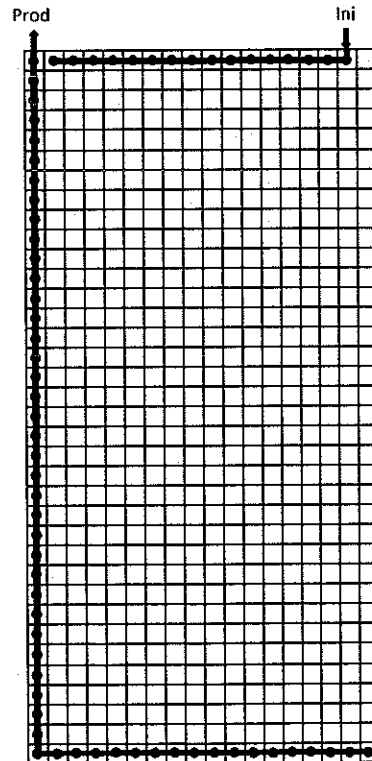
(a) Two Vertical Wells



(b) Shallow Vertical Injector with Horizontal Producer



(c) Deep Vertical Injector with Horizontal Producer



(d) Two Horizontal Wells

Figure 3.19: Schematic of Wells Orientation

After the best well orientation was found for GAGD process, investigations were then run to find the best well control and development strategies for GAGD application in Gulfaks field. The well control and development strategies that were investigated were (Figure 3.20):

- a) Continue the production with existing producer well (Case A).
- b) Continue the production by introducing *WAG* process (Case B).
- c) Continue the production by introducing *GAGD* process (Case C).
- d) Continue the production by introducing *GAGD* process with inflow control valve (Case D).

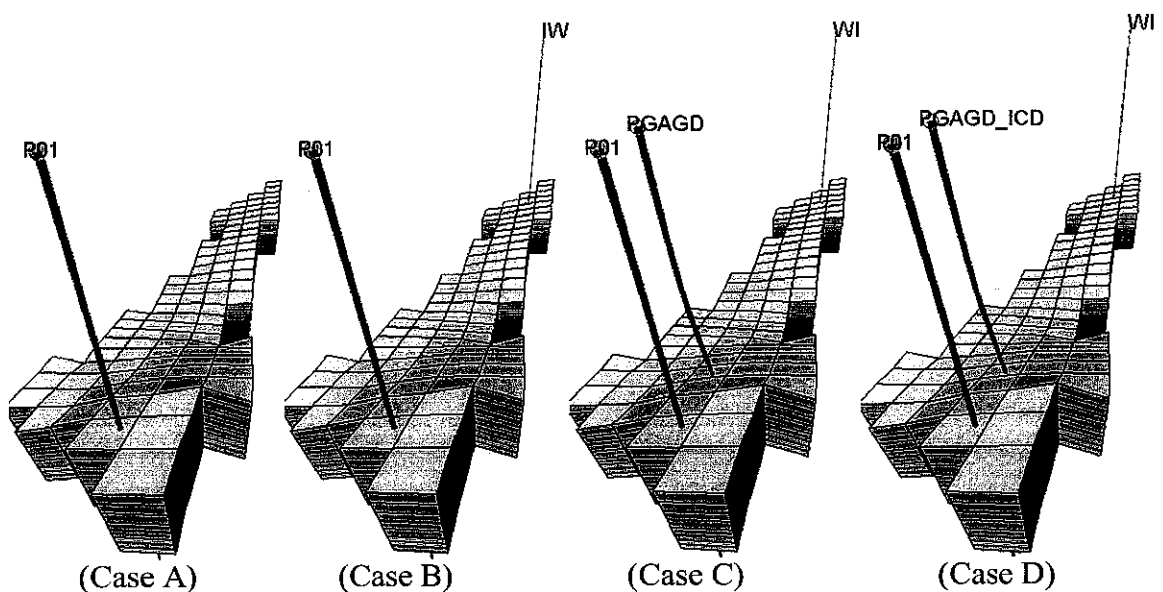


Figure 3.20: Development Strategies Used for GAGD Process in Gulfaks Field

For Case A, the case was used as a base case where the well (P01) was left to produce without introducing any external supporting force. For Case B, investigation was made by introducing a new well (IW) which will alternatively inject water and gas to segment four of Gulfaks field for pressure support. For Case C, investigation was done by implement GAGD process at Gulfaks field. PGAGD was the horizontal producer well while WI was the water injector. Case D used the same development strategy but there is some difference in the horizontal producer's well design. For well PGAGD\_ICD, research has been done by introducing some inflow control valve throughout the producer. Figure 3.21 shows the well design in well section view while Figure 3.22 shows the well design in well intersection window which were both design in Petrel software. Figure 3.22, shows the inflow control device's

location throughout the horizontal well. The inflow control device is indicated as blue color while the packer is indicated as red color.

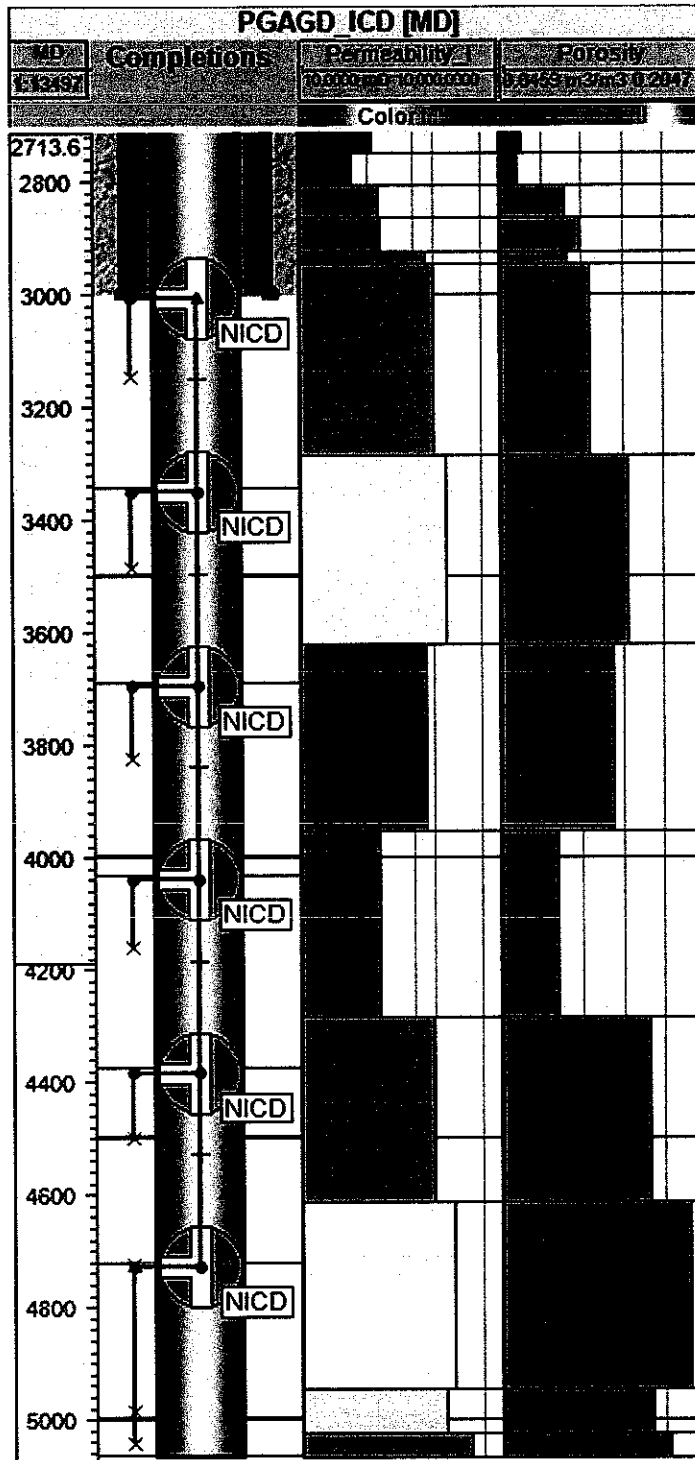


Figure 3.21: Well Design for PGAGD\_ICD in Well Section Window

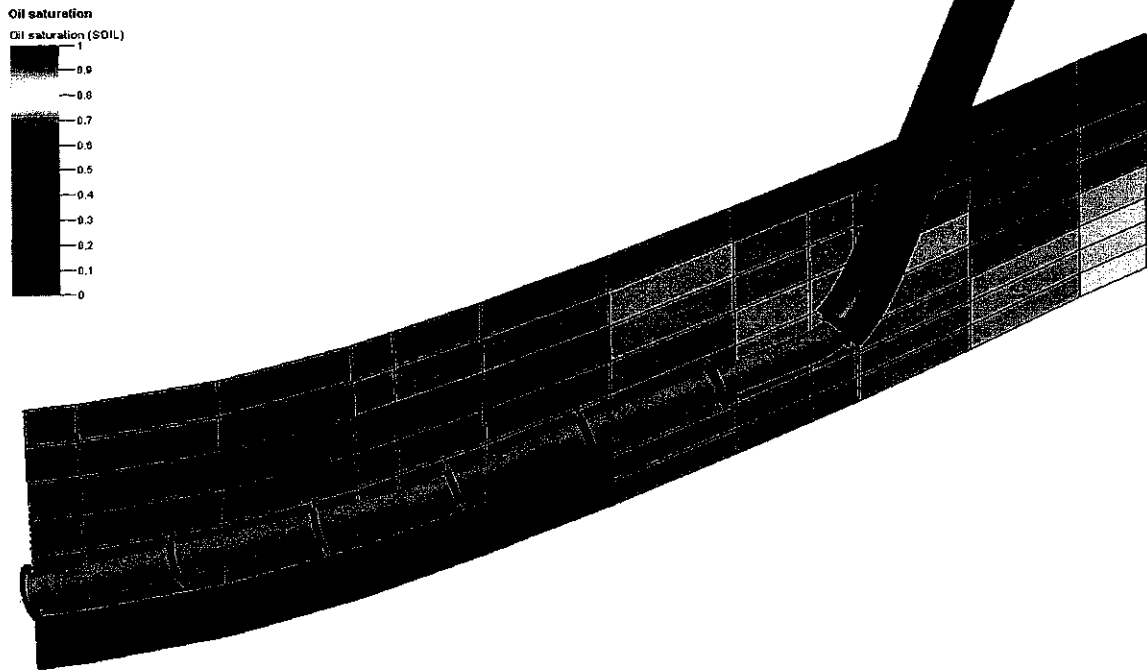


Figure 3.22: Well Design for PGAGD\_ICD in Well Intersection Window

All these investigations will answer the question of:

1. Do the simulation models able to simulate and predict as how the laboratory model vice versa?
2. What is the effect of  $k_v/k_h$  on gravity segregation in GAGD process that is predicted by using ECLIPSE simulator?
3. What is the best development strategy for GAGD process and which gas should be chosen as injection gas?
4. From simulation outcome, is GAGD feasible to be implement Gulfaks field?

## CHAPTER 4

### RESULTS AND DISCUSSION

This research aimed to character the effect of reservoir heterogeneity on GAGD process by simulation and laboratory experiments. The ECLIPSE model was compared with the observed laboratory measurements before it was then run for more prediction cases to full fill the study's objectives.

#### 4.1 Fluid Properties Measurement

##### 4.1.1 Density Measurement

Since GAGD process employs the advantage of density difference between the phases, it is important to know the density difference between all of the fluids (Mahmoud, 2006). The density of mineral oil and brine were measured in the laboratory while the density for CO<sub>2</sub> was taken from the handbook (Vesovic *et al.*, 1990; Span and Wagner, 1996; Fenghour *et al.*, 1998). Since the laboratory condition is very stable, no change in humidity, temperature, and pressure, it was assumed that the data taken from the handbook is representative enough. All these information was input to ECLIPSE as a gas reference density at specific depth and pressure while it will be scale to the current pressure as simulation proceed. Table 4.1 shows the density for mineral oil and brine while Figure 4.1 shows the density for CO<sub>2</sub> over pressure all at room temperature. The density different between CO<sub>2</sub> and mineral oil at 78.4°F and 14.7psia is as much as 0.84g/cm<sup>3</sup> the big density different will help to keep the gravity force dominant which is an advantage of GAGD process (Kulkarni, 2004).

Table 4.1: Density of Mineral Oil and Brine at 25.8°C and 14.7psia

$\rho_{\text{Mineral Oil, g/cm}^3}$	$\rho_{\text{Brine, g/cm}^3}$
0.84	1.02
0.84	1.02
0.83	1.02
0.84	1.02
0.83	1.02
$\rho_{\text{avg}} = 0.84\text{g/cm}^3$	$\rho_{\text{avg}} = 1.02\text{g/cm}^3$

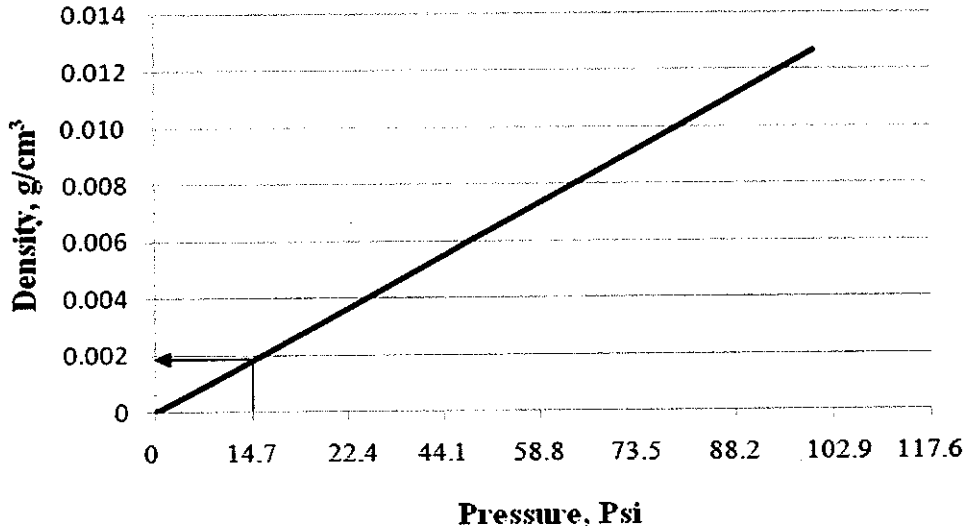


Figure 4.1: Density of CO<sub>2</sub> over Pressure (Vesovic *et al.*, 1990; Span and Wagner, 1996; Fenghour *et al.*, 1998)

#### 4.1.2 Viscosity Measurement

Table 4.2 shows the viscosity of brine, mineral oil and CO<sub>2</sub> that have been used by this research. This information was further applied in calculation. The results and calculations are available in Appendix A. Refer to the oil category by Richard and Wallace (1990), the mineral oil used in the study is categorise as light oil, in which the specific density is less than 0.93 and the viscosity is less than 100cP. Light oil is used because the crude oil will inherit the visualization purpose of investigation using the visual physical model during laboratory investigation.

Table 4.2: Viscosity of Brine, Mineral Oil and Carbon Dioxide at 25.9°C, 14.7psia

<b>Fluid</b>	<b>Viscosity, cP</b>
Brine	2.50
Mineral Oil	25.00
Carbon Dioxide	0.01

## **4.2 Porous Media and Model Characterization**

This section describes the reservoir properties for Gelama Merah field, the visual physical model, the simulation model, and Gulfaks field. This investigation is important to describe all the reservoir condition since the results might be different in different condition. Properties from Gelama Merah were collected from field report and static model which was inherited from the geologist. Visual physical model's properties were measured from laboratory investigation which was then implemented in the simulation model.

### **4.2.1 Gelama Merah Case Study**

After interpreted all the available contour map, the West-East cross section of Gelama Merah reservoir is shown in Figure 4.2. This is done by record the cross plot of contour map on a graph paper and then transfer to PowerPoint. From the interpretation, we can see that there is around 115ft of oil zone. Characterization on the candidate is important in order to obtain enough information for time scaling (refer to Appendix E). Sand U9.1 was used as the referred sand in Gelama Merah because Sand U9.1 is the sand where oil is located. This is the sand where the gas-oil-contact and potential oil-water-contact cut off, the area where the potential oil located near well GM-1.

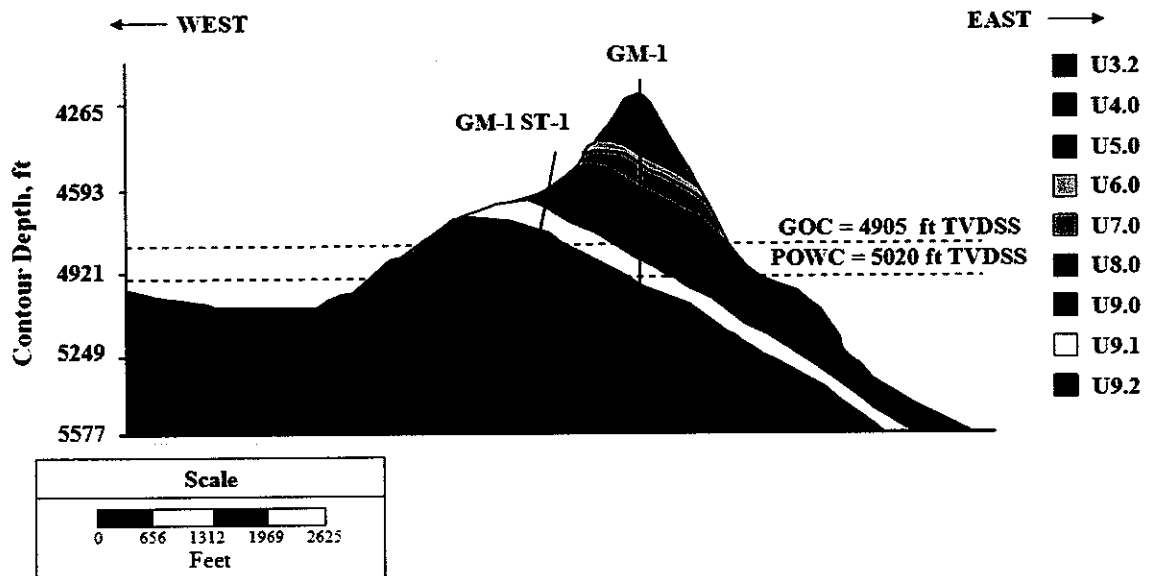


Figure 4.2: West-East Cross Section of Gelama Merah Reservoir

Figure 4.3 and 4.4 show partially on how to determine the depth of gas oil contact (GOC) and oil water contact (OWC) in order to determine the reservoir pressure and reservoir fluid properties at target zone. The cross plot between Neutron and Density were plotted to determine the potential hydrocarbon zone which were then confirmed with the Resistivity log (Figure 4.3). Based on log interpretation GOC and OWC were located around 4905ft and 5020ft, respectively. Neutron logs measure the hydrogen content in the formation and it will give a high reading if there is high content of water because water was made from two hydrogen atom and one oxygen atom. Density log on the other hand measure the density in the formation. As the return high energy gamma rays were measured, it will show the bulk density. In this research, we cross plotted the two logs and Butterfly Effect can be clearly observe in Figure 4.3. Resistivity log was then used to confirm the potential hydrocarbon zone.

To make the final confirmation on the oil zone, this research applied the single well's pressure plot technique (Figure 4.4) in which the formation pressure gradient was plotted with depth the wellbore. Based on the different pressure gradient, the GOC and OWC can be determined. The values calculated from the Pressure Plot agree with the results from the logs which validate both of the technique used. It is very important to set the correct the initial GOC and OWC since it will be used by ECLIPSE to calculate the in-place, and all the phase content in all the grids.

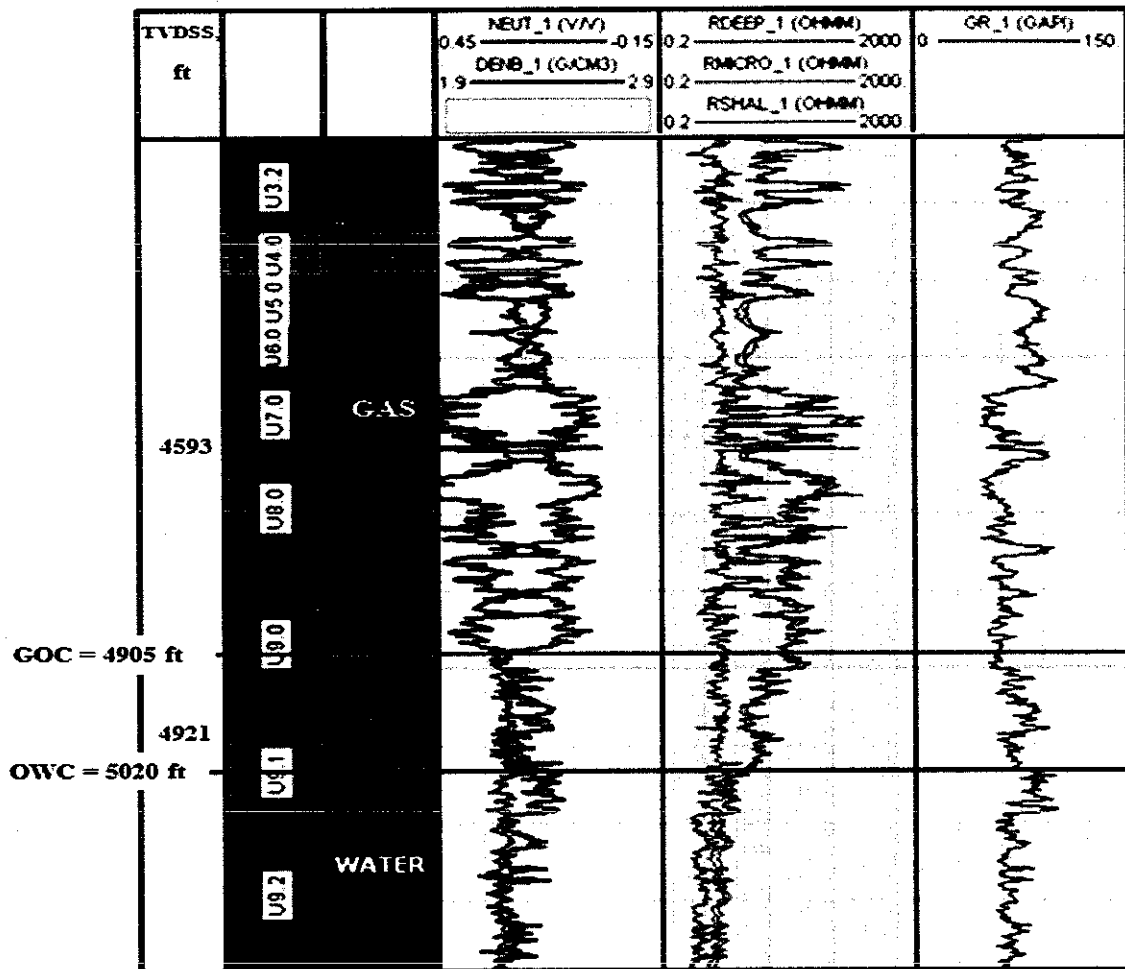


Figure 4.3: Fluid Contact Indication from Formation Logs

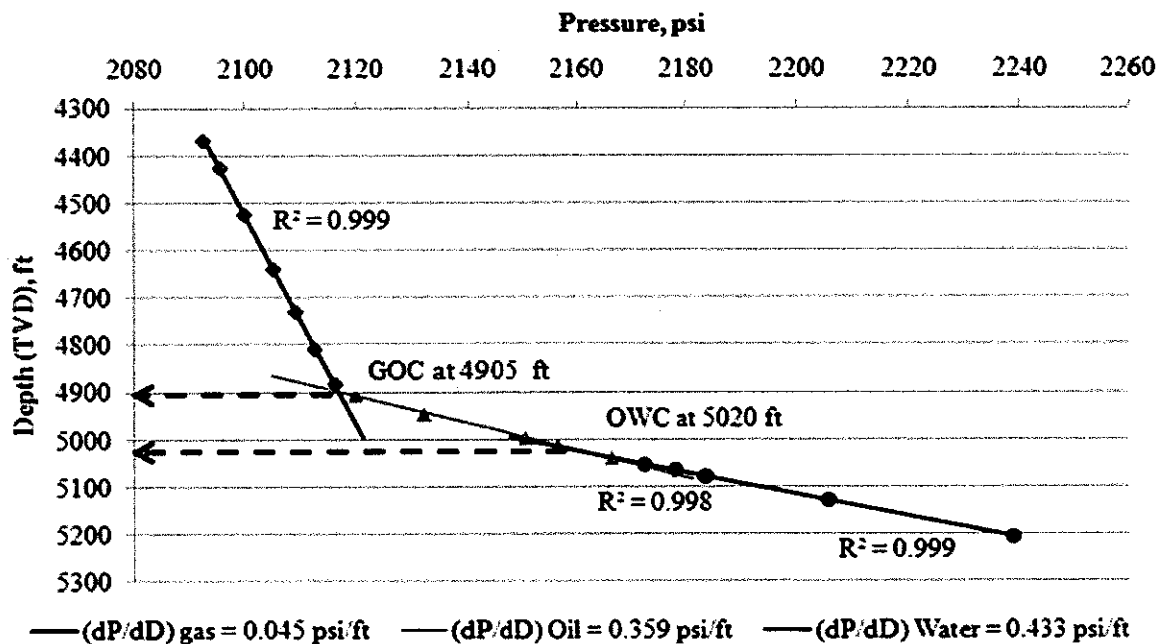


Figure 4.4: Fluid Contact Calculation from Pressure Plot

## 4.2.2 Laboratory Studies

Figure 4.5 shows that the measurement model is an effective tool to measure the porosity for glass beads. Measurement from the measurement model only shows a small difference (2.8%) when compare to results from Helium Porosimeter test. Table 4.3 shows the porosity and permeability for homogeneous model when the measurement model is pack with glass beads with different class of grain size. The results were within the acceptable range reported by previous researchers (Blackwell *et al.*, 1960; Sharma, 2005; and Mahmoud, 2006) which range from 20–45%. Packing technique is a very important factor that affects the porosity outcome. Thus, it is very important to follow a consistent packing technique. It is also realized that there is some irregularity in the glass beads size which will cause the microscopic level heterogeneity. According to Institute of Petroleum Engineering (2010), permeability is found generally to be lower with smaller grain size if other factors such as surface tension effects are not influential. Pore channels become smaller as the size of the grains is reduced, and it is more difficult for fluid to flow through smaller channels.

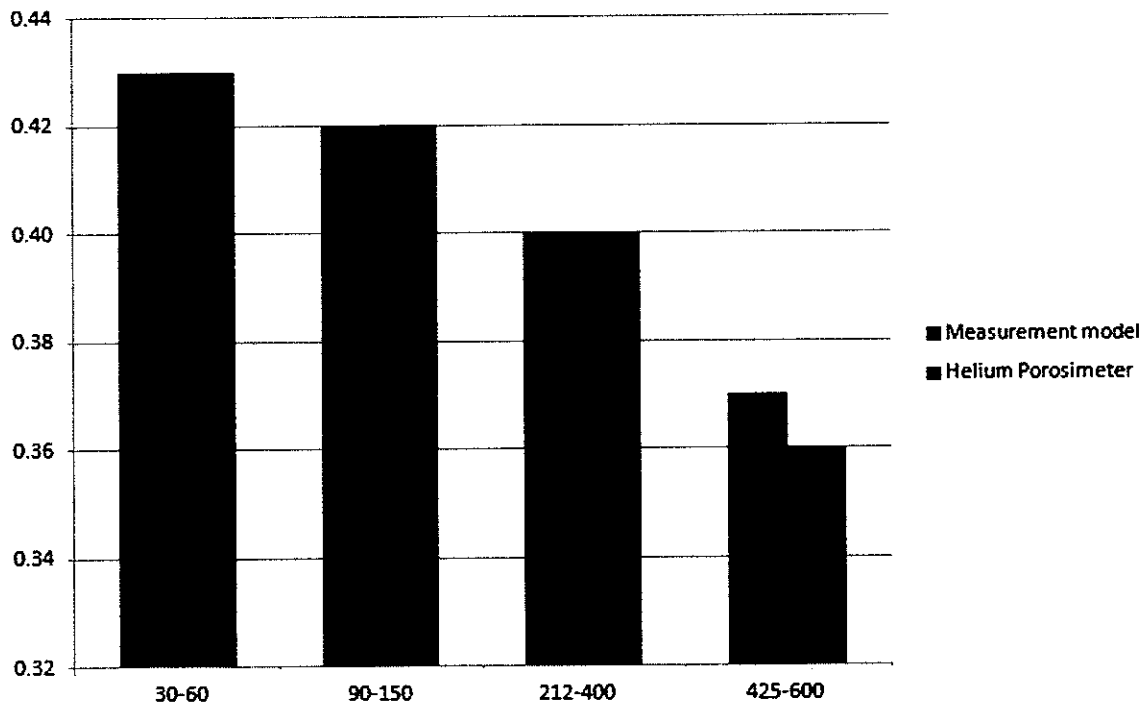


Figure 4.5: Comparison of Porosity Value Obtained by the Measurement Model and Helium Porosimeter

Table 4.3: Porosity and Permeability for Homogeneous Model

Glass Beads Size, $\mu\text{m}$	Porosity, %	Permeability, mD
30-60	0.43	12483
90-150	0.42	14979
212-400	0.40	24965
425-600	0.37	37448

Laboratory investigation was done to investigate the effect of different packing technique porosity and permeability measured. Table 4.4 shows the porosity difference between tightly-packed and loosely-packed model. The maximum different is 5% which reflect the important of consistency in packing the porous media during laboratory investigation. This happened because the structure of packing depends in detail on the forces acting between the grains during rearrangement of grains in which different rearrangement protocols can lead to either random close packed or random loose packed systems (Makse *et al.*, 2008).

Table 4.4: Porosity of Tightly-packed and Loosely-packed Model

Size, $\mu\text{m}$	Porosity of tightly packed model, %	Porosity of loosely-packed model, %	Different, %
30-60	0.41	0.43	4.88
90-150	0.40	0.42	5.00
212-400	0.39	0.40	2.56
425-600	0.37	0.37	0.00

\*\* Results from tightly-packed model were used as the base reference in porosity calculation

Table 4.5 shows the permeability of tightly-packed and loosely-packed model. The packing technique gives a higher impact on the permeability when the glass beads size is reduced, with a maximum of 20% difference between a tightly packed and loosely packed model. It can be observe that the packing technique will give a higher impact to the permeability of the porous media in comparison with the porosity when the glass beads is small but when the glass beads reach certain value (in this case from  $212\mu\text{m}$ ), the effect is very minor. By vibrating the model on a shaker table, a decrease in the glass beads will be observed for if there is any loosely packed area available. Glass beads are added in the model until the glass beads level is constant. The loosely-packed model does not undergo the shaking so the porous media was loosely packed.

Table 4.5: Permeability of Tightly-packed and Loosely-packed Model

Glass beads size, $\mu\text{m}$	Permeability of tightly packed model, mD	Permeability of loosely-packed model, mD	Different, %
30-60	12483	14979	17
90-150	14979	18724	20
212-400	24965	24965	0
425-600	37448	37448	0

\*\* Results from tightly-packed model were used as the base reference in permeability calculation

From Table 4.6 the average porosity with for  $k_v/k_h$  of 0.8, 0.9, and 1.0 are 0.41, 0.42, and 0.43, respectively (please refer to Appendix B for how the models with different  $k_v/k_h$  value were packed). The average porosity for each model was calculated by volumetric-weighted average porosity method (see Appendix C). From Table 4.6, the porosity different between homogeneous model ( $k_v/k_h = 1.0$ ) and heterogeneous model ( $k_v/k_h = 0.8$ ) is 3.1%. This has set an agreement with the stamen done by Izgec *et al.*, (2007) whereby reservoir heterogeneity will have a small impact on porosity.

Table 4.6: Average Porosity for Model with  $k_v/k_h$  of 0.8, 0.9, and 1.0

$k_v/k_h$	Average Porosity, %
0.8	0.41
0.9	0.42
1.0	0.43

According to Amyx *et al.*, (1960), the porosity for cubical packing is 47.6%, and the porosity of the models were still within in the range. Packing procedure by Ma (2005) has been followed, for a better packed model, the visual physical model will need to be place on the shaker table for a longer time during the vibration process (please refer to Appendix C for packing, cleaning, and repacking procedure). It is also realized that there is some irregularity in the glass beads size which will cause the microscopic level heterogeneity. However, this is something unavoidable since the only the manufacture has the control on the uniform of the produced glass beads.

### 4.2.3 Relative Permeability Curve

After all the measurements have been done with the measurement model, the critical water saturation was measured. By using Wyllie-Garner correlation (Figure 2.5), the relative permeability curve is then calculated, detail description on how to generate the relative permeability curve is available in Appendix B. Figure 4.6 shows the relative permeability curve for oil-water and oil-gas system, which is generated using Wyllie-Garner Correlation (refer to Appendix B). The relative permeability curve values were then input to ECLIPSE 100 simulation under PROPS section. The connate water saturation, connate gas saturation, maximum water saturation, and maximum gas saturation (the one circle using red color in Figure 4.6) were used to populate the initial saturation for each phase in each cell while the relative permeability data are used to calculate fluid mobility. Finally, solve the flow equations between cells and from cells to the well. The connate water saturation is the lowest water saturation value in any given water saturation function or the unmoveable water saturation which is also term as in-situ water saturation.

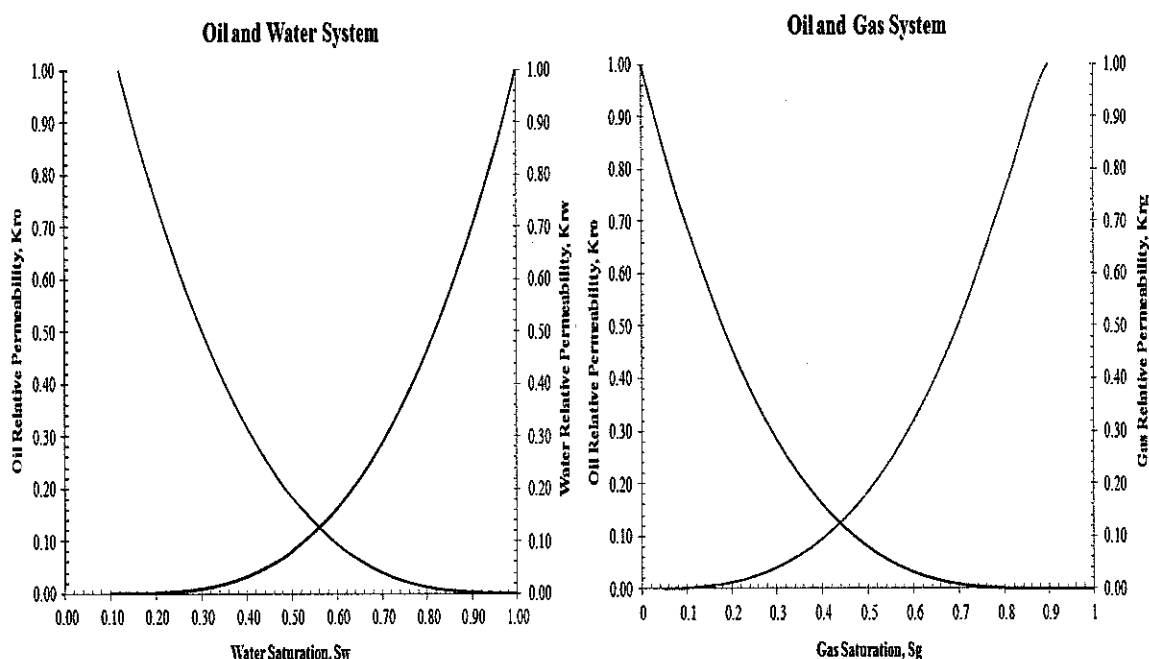


Figure 4.6: Relative Permeability Generated from Wyllie-Garner Correlation

#### 4.2.4 Minimum Miscible Pressure for Vaporizing Gas Drive Process

To select the best injection gas between CO<sub>2</sub> and N<sub>2</sub> for GAGD process, simulation investigation was done by using E300. Figure 4.7 shows the result for slim tube displacement for CO<sub>2</sub> and N<sub>2</sub> from E300 simulation run. The aim of this simulation run is to get the minimum miscible pressure for CO<sub>2</sub> and N<sub>2</sub> displacement. This was done by increasing the pressure until almost 100% ROIP was achieved. Result from slim tube test indicated that the minimum miscible pressure for CO<sub>2</sub> to be miscible with the reservoir oil is 200psi while there is no indication of any miscibility for N<sub>2</sub> with the reservoir oil, not even in an extreme high pressure.

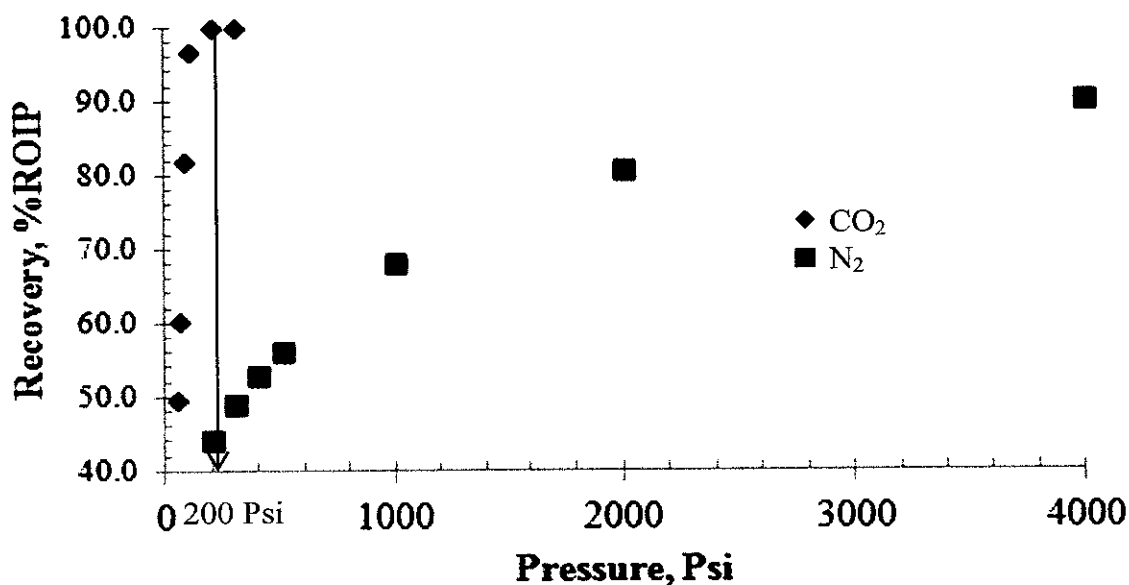


Figure 4.7: Slim Tube Displacement for CO<sub>2</sub> and N<sub>2</sub>

During CO<sub>2</sub> injection in a miscible mode, the injected CO<sub>2</sub> will enrich the oil in the light intermediate range and at the same time stripe the heavier fractions. Refer to Figure 4.8, forward moving gas (like a vaporizing gas drive) becomes richer in the middle intermediates and heavier fractions and at the same time losses the light intermediates fractions. There is a big transition zone in between where the front transition zone act as vaporizing gas drive while the tail of transition zone act as condensing gas drive.

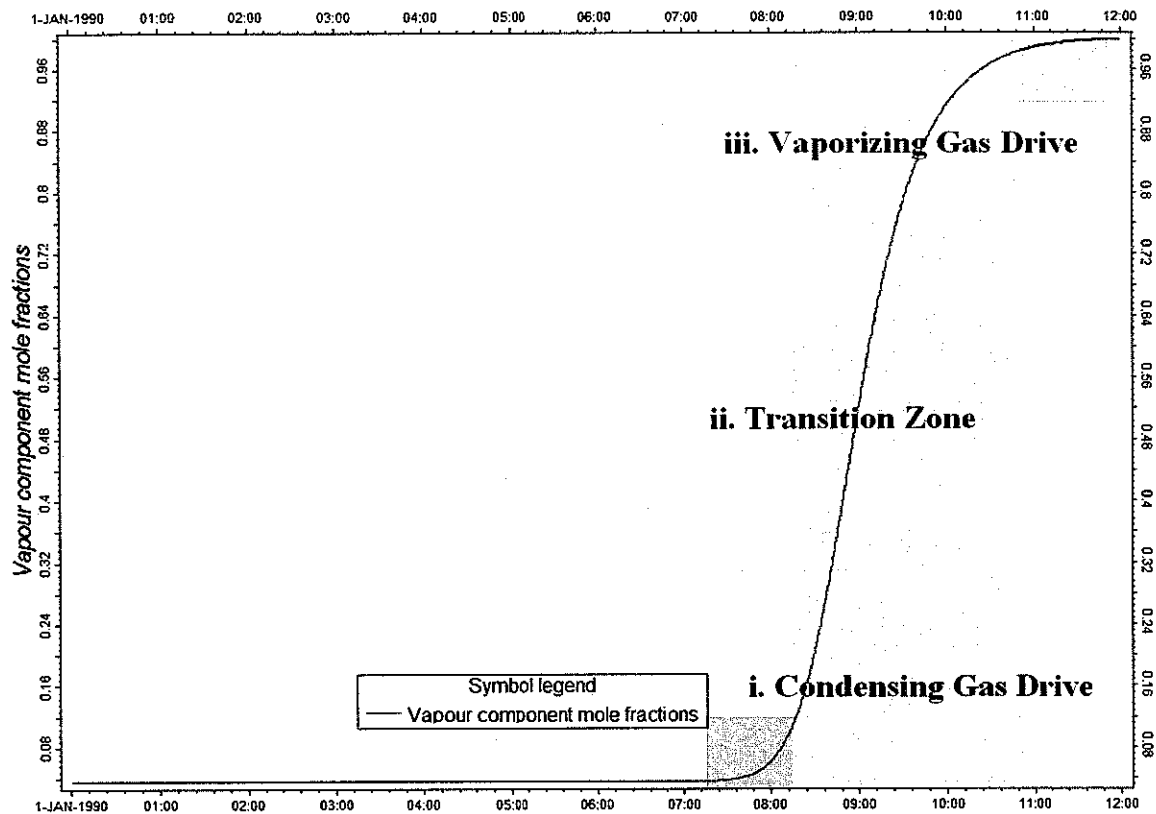


Figure 4.8: Phase Change during Vaporizing gas Drive Process using CO<sub>2</sub>

Apart from the slim tube test, the minimum miscible pressure can also be observed from the ternary diagram. At the initial pressure (50psi), the reservoir oil is lying on the two phase envelop and thus, the CO<sub>2</sub> injected is not miscible with the reservoir oil. At the pressure of 100psi, it can be observe that the reservoir oil is moving towards the Plat point. However, the line joining the enriched gas with the original oil still crosses the two phase region and this is still in an immiscibility condition. Refer to Figure 4.9, miscibility occurs at the pressure of 200psi. At this pressure, the oil point is on the critical line, which is the minimum pressure for the reservoir to become miscible. Once the reservoir oil is inside the single phase zone, GAGD process will happen in a miscible condition.

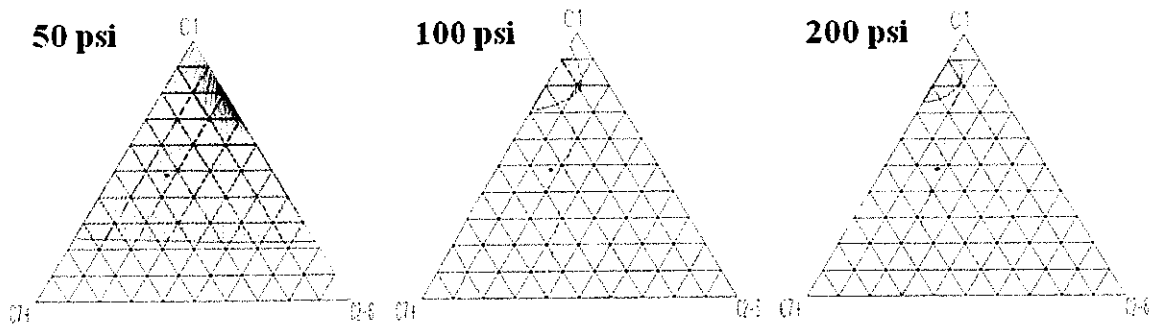


Figure 4.9: Ternary Diagram for CO<sub>2</sub> at Different Pressure

In Figure 4.10, it can be observed that miscibility is very hard to achieve with N<sub>2</sub> injection. Even under the pressure of 4000psi, the reservoir oil still at the left side of the extension of the tie line which means that the reservoir oil is still within the two phase envelope. This made N<sub>2</sub> not a favourable injection gas if a miscible displacement is desirable.

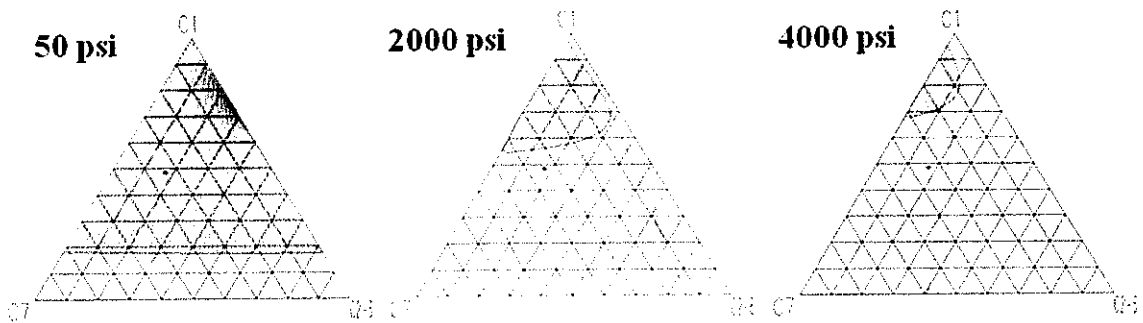


Figure 4.10: Ternary Diagram for N<sub>2</sub> at Different Pressure

From the slim tube measurement run and ternary diagram plot, it can be concluded that, to achieve a miscible displacement during GAGD process, it is recommended to use CO<sub>2</sub> as an injection gas. Miscible displacement will be achieved in a lower pressure compared to N<sub>2</sub> injection.

### 4.3 The Effect of $k_v/k_h$ on Gas Assisted Gravity Drainage Process

Three different  $k_v/k_h$  (0.8, 0.9, and 1.0) were created using glass beads as a transport medium. The experiment set up for the laboratory investigation took about two months for a single run, thus, to reduce the experiment run time, simulation using

ECLIPSE was selected. Simulation run also allow a more realistic investigation because of the pressure constrain to run the experiment at reservoir pressure.

Refer to Figure 4.11, different well bottom hole pressure profile can be observe from different  $k_v/k_h$  models. It can be observed that different settling time is required for different  $k_v/k_h$  models. However, all the well bottom hole pressure settle down after 1.1 pore volume of  $CO_2$  been injected in which the homogeneous model settle down first and the higher  $k_v/k_h$  ratio settle down slower. This can be supported with the finding from Mackay (2009), in which the time to establish a steady state field pressure is determined by the magnitude of the diffusivity constant,  $D$  (Equation 4.1). As the magnitude of the diffusivity constant decreases the time taken for a pressure fluctuation to transmit a given distance increases. For the case with  $k_v/k_h$  of 0.9, the permeability in vertical direction is low. This has resulted in a lower diffusivity constant and longer time to establish a steady state field pressure. The faster the fluid front achieve a steady pressure and a piston like front displacement, the lower the risk of having an early gas breakthrough in GAGD process.

$$D = \frac{k}{\phi\mu c} \tag{4.1}$$

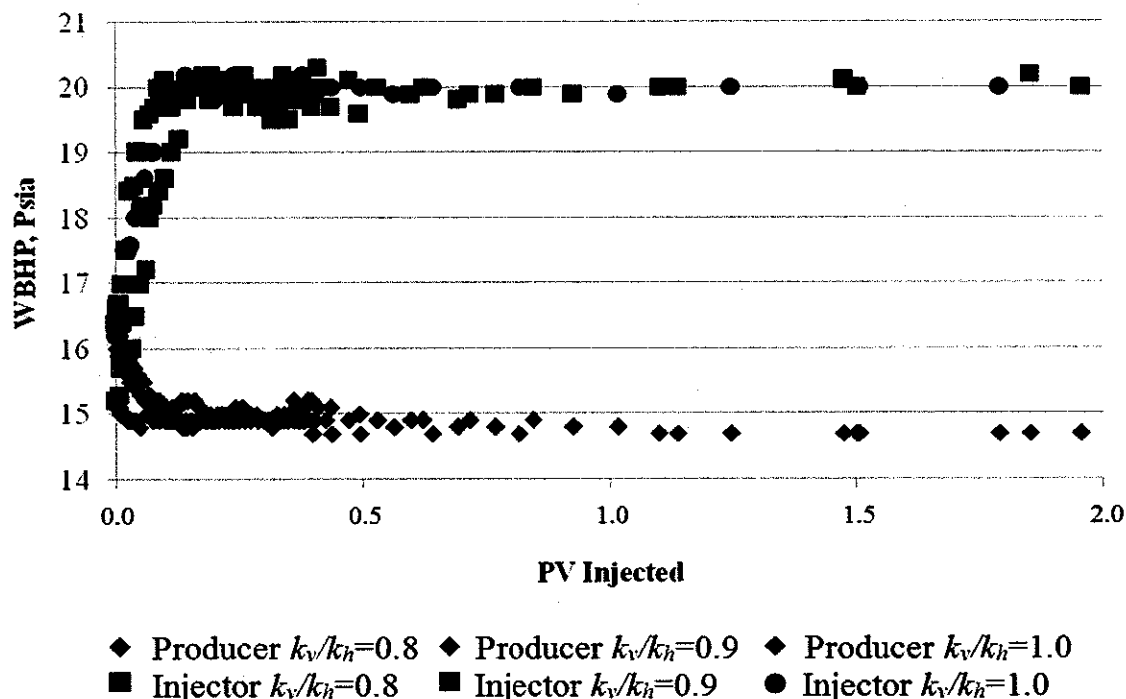
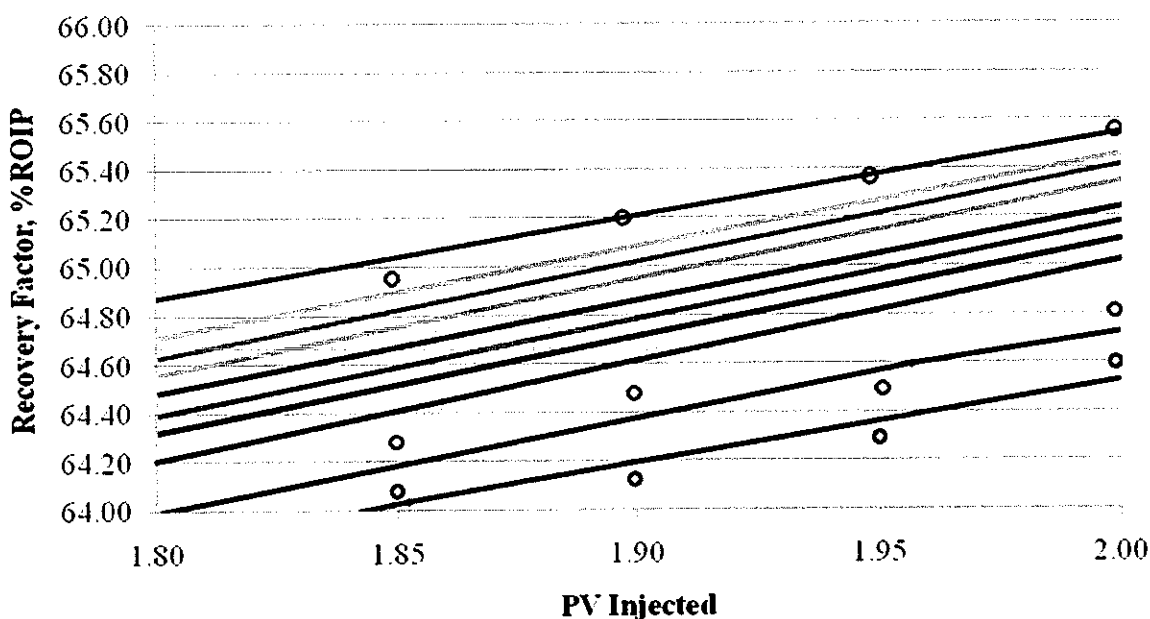


Figure 4.11: Well Bottom Hole Pressure Profile for Different  $k_v/k_h$

Due to the difference in  $k_v/k_h$  ratio, the resulted recovery factor for each case is slightly different. Laboratory investigation from the visual physical model shows that the recovery factor for  $k_v/k_h$  of 0.8, 0.9, and 1.0 were 64.73%ROIP, 64.53%ROIP, and 65.53%ROIP, respectively (Figure 4.12). For heterogeneous cases ( $k_v/k_h = 0.8$  and  $k_v/k_h = 0.9$ ), a dominant in vertical permeability will yield a higher recovery. For homogeneous reservoir ( $k_v/k_h = 1.0$ ), the vertical and horizontal permeability were the same. Thus, gas sweeps the reservoir more uniformly to give a higher recovery. Refer to Figure 4.12, the simulation results are match with the laboratory results. The simulated results also agree with the laboratory investigation where the dominant in the vertical permeability will yield a higher recovery. However, this is only true when a stable front displacement can be well control for a piston-like front displacement. This will be further explain under the real field implementation of GAGD process section in which inflow control valves are place in the horizontal well.



Laboratory observed data:

○  $k_v/k_h=0.8$    ○  $k_v/k_h=0.9$    ○  $k_v/k_h=1.0$

Simulated result:

—  $k_v/k_h=0.1$    —  $k_v/k_h=0.2$    —  $k_v/k_h=0.3$    —  $k_v/k_h=0.4$    —  $k_v/k_h=0.5$   
 —  $k_v/k_h=0.6$    —  $k_v/k_h=0.7$    —  $k_v/k_h=0.8$    —  $k_v/k_h=0.9$    —  $k_v/k_h=1.0$

Figure 4.12: The Effect of Different  $k_v/k_h$  on Recovery Factor

Provided with a good well control for a stable piston-like front displacement, research show that GAGD process is more favourable in a reservoir with more dominant in vertical permeability.

#### 4.4 Visualization on Front Displacement

Figure 4.13 (a), (b), and (c) show the fluid displacement for model with  $k_v/k_h$  of 0.8, 0.9, and 1.0, respectively. A darker color indicates that there was a higher liquid saturation while a lighter color indicates that gas has invaded the respective zone. It can be observed that the front displacement for homogeneous model ( $k_v/k_h = 1.0$ ) is comparatively more stable (near horizontal displacement) than heterogeneous model. For the model with  $k_v/k_h$  of 0.8, due to more dominant of vertical permeability, a long tongue-like displacement can be observed.  $\text{CO}_2$  is more favourable to move vertically downward than horizontally. As the  $k_v/k_h$  increases to 0.9, a more stable displacement can be observed. Thus, in Figure 4.13, gas tends to bypass the side area of the visual physical model. It was proven that gas will always displace the higher permeability zone first. For the homogeneous model ( $k_v/k_h = 1.0$ ), there are a few spots that were not fully swept by the gas. Naami *et al.*, (1999) stated that this phenomenon might be caused by the local heterogeneities in homogeneous model. A natural porous medium has intrinsic local heterogeneities that led to the formation of fingers even during the displacement of a mobility ratio of unity.

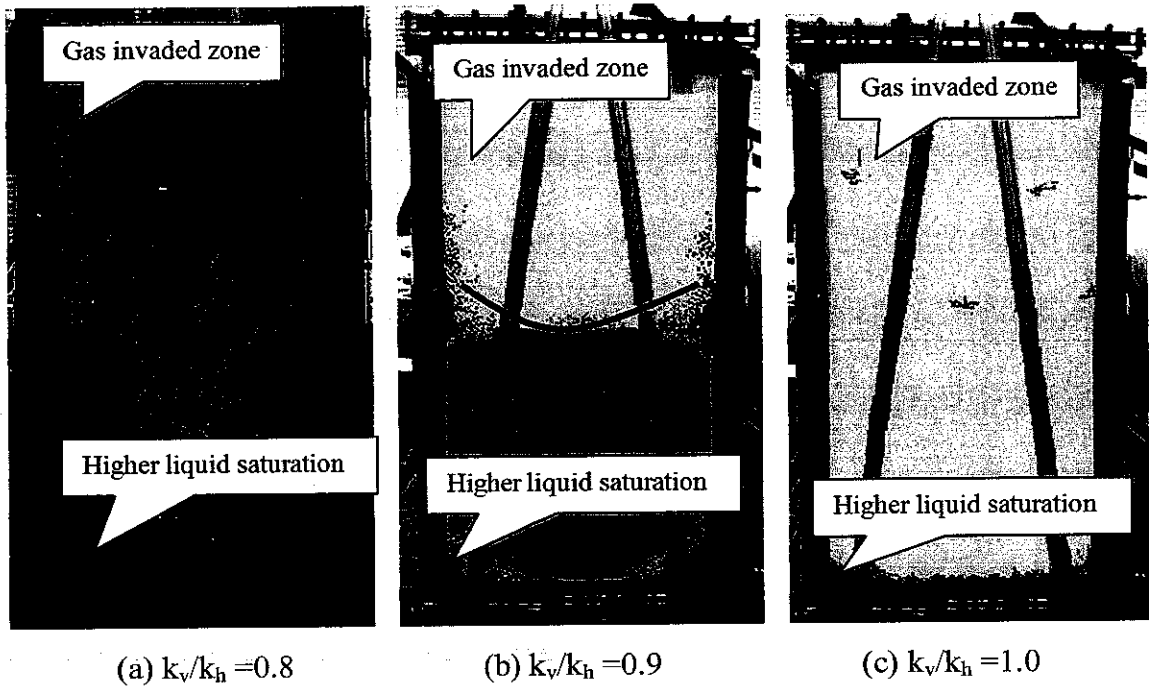


Figure 4.13: The Fluid Displacement for Different  $k_v/k_h$

Snapshots from ECLIPSE simulation shown in Figure 4.14 and 4.15 show the fluid displacement across different permeability layers. Figure 4.14 shows that when the gas move from a lower permeability layer to a higher permeability layer, multiple viscous fingering will be observed. The capillary force is reduced when gas flow from a smaller to bigger pore size. Thus, gas is more dominant to move downward. For cases where gas moves from high to low permeability layer, the back pressure encountered has caused the gas prefer to move sideways (Figure 4.15). During this mechanism, the un-swept area will be reduce.

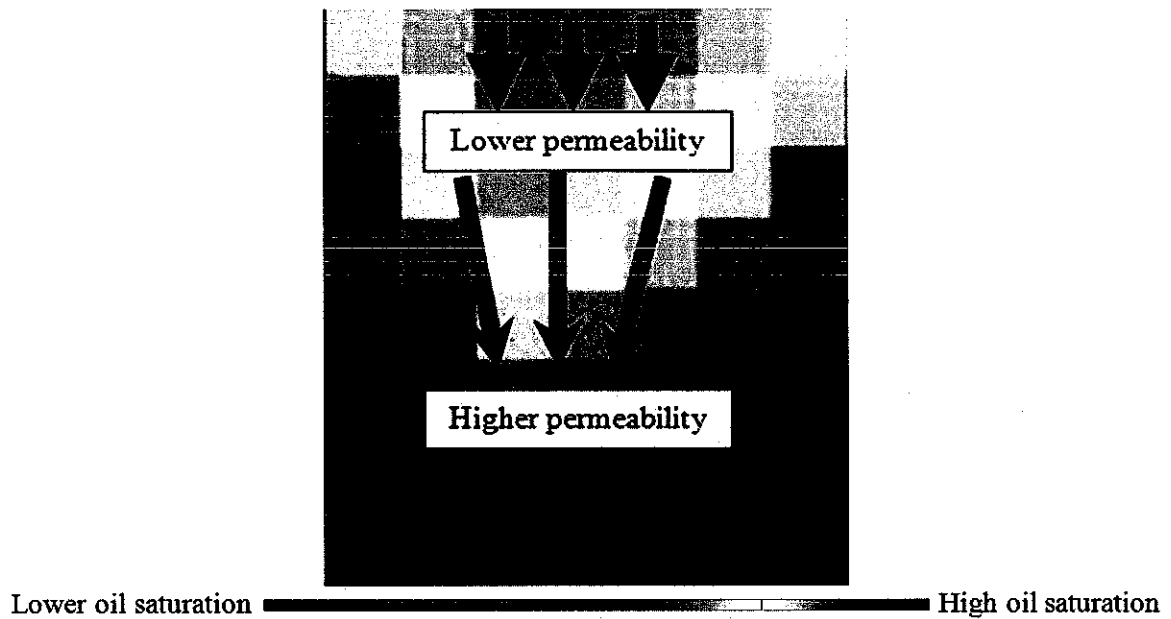


Figure 4.14: Front Displacement from Low to High Permeability

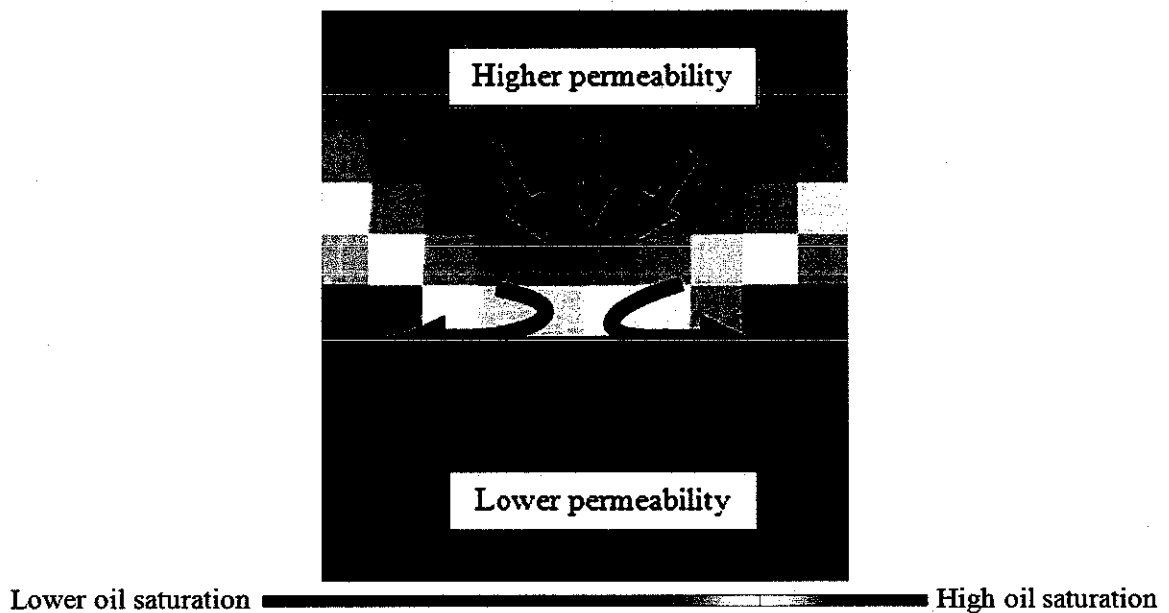


Figure 4.15: Front Displacement from High to Low Permeability

#### 4.5 History Matching

Before continue with any prediction, the ECLIPSE model need to be validate so that it will predict like the real-case scenario. Three subsections in history matching are sensitivity test, well bottom hole pressure matching, recovery factor matching and uncertainty optimisation, respectively.

### 4.5.1 Sensitivity Test

Figure 4.16 shows sensitivity of recovery factor to uncertainties towards reservoir characters and operating parameters such as gas density, net-to-gross (NTG), injector pressure, and injector rate. A higher line gradient means that the operating parameter will give a higher impact on the oil recovery. It is clearly highlight that injector pressure as the most important input quantity (of those considered) and has the most impact on the change in recovery. Thus, it is very important to control the injection pressure for a higher recovery in GAGD process to prevent a negative effect on the recovery factor. No change is observed when the density of injection gas change. Thus, it is suggest to use compress air as injection gas in GAGD process. However, further investigation is a must to use compress gas as an injection gas.

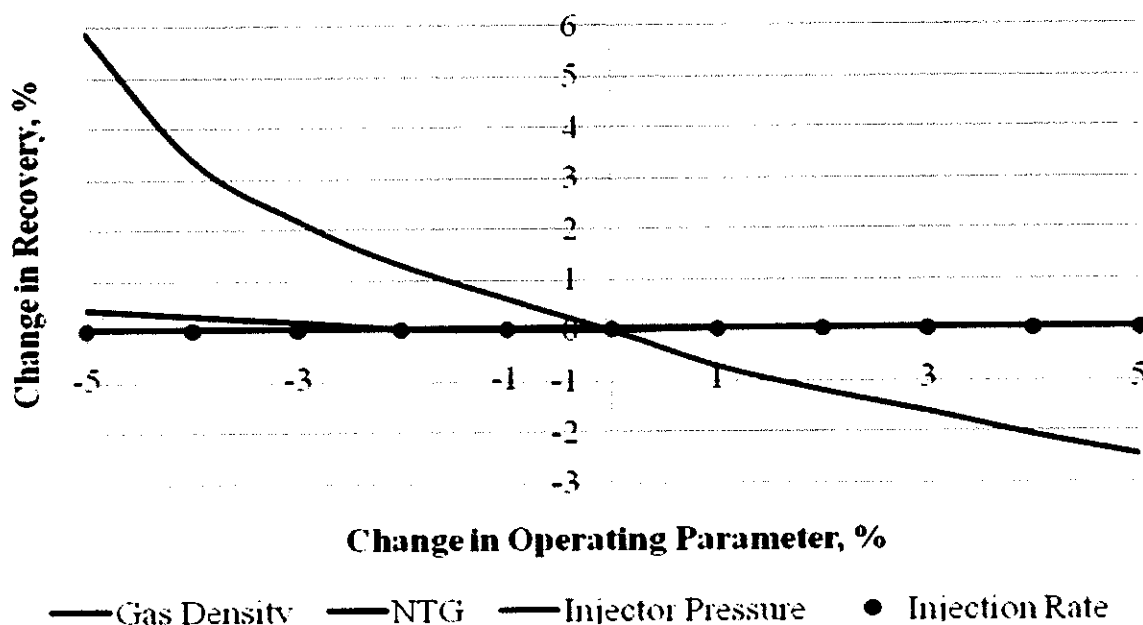


Figure 4.16: Spider Diagram Evaluation

### 4.5.2 Match the Well Bottom Hole Pressure

Results from sensitivity test shows that injector pressure has the highest weight on recovery factor. Thus, it is important to match the injector pressure from simulation to laboratory result. Injector pressure of 20psia gave the closest fit to history data as shown in Figure 4.17. An error bar of 1% was applied to history data for error correction.

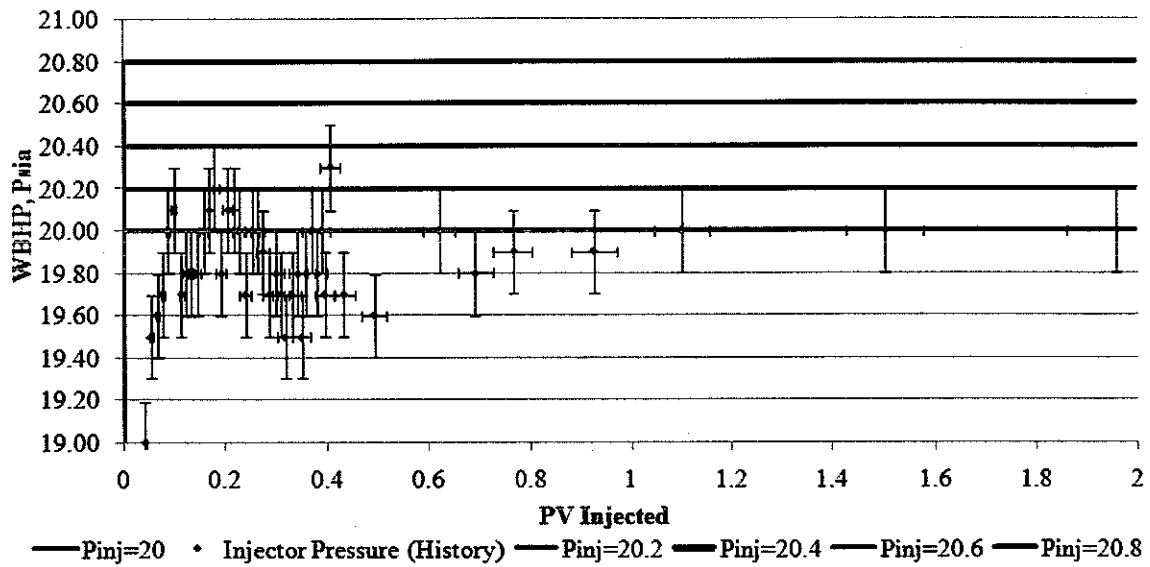


Figure 4.17: Matching the Well Bottom Hole Pressure

#### 4.5.3 Match Recovery Factor

After confirming that the injection pressure could give the most impact on the recovery factor, it is important to history match the injection pressure that will give the same recovery factor between the laboratory result and simulation result. Laboratory record of recovery factor has been termed as history data while the objective of history matching is to match the recovery factor from simulation to history data. An error bar of 1% has been applied to the history data for error correction. Figure 4.18 shows that by apply the injector pressure of 20psia in the simulation will give the best fit to the recovery factor that recorded in laboratory investigation.

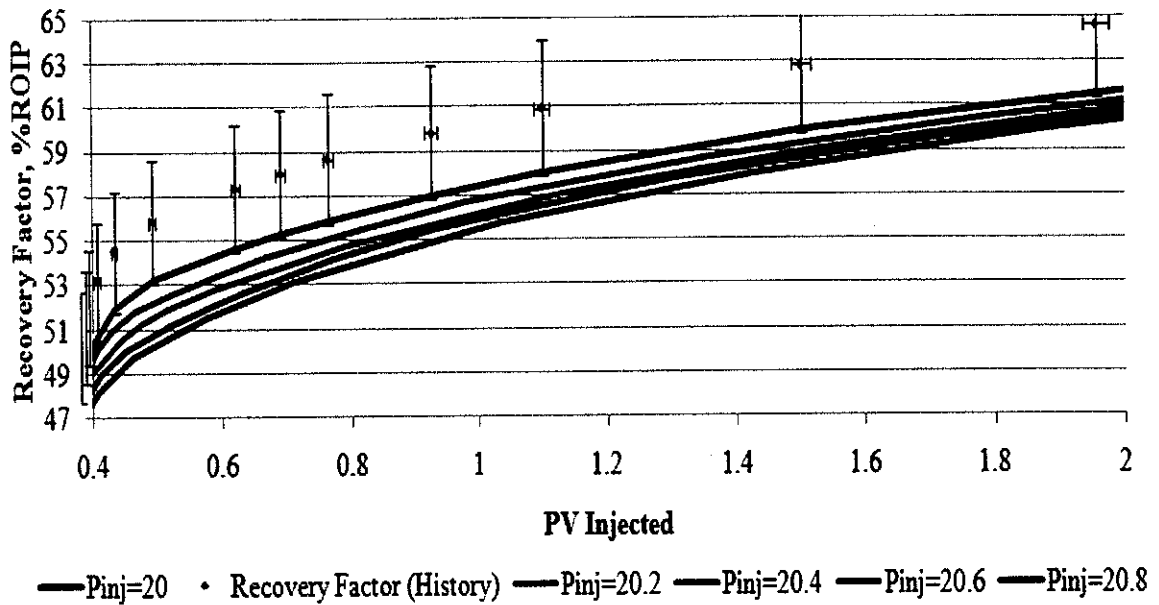


Figure 4.18: Matching the Recovery Factor

#### 4.5.4 Match History Development Strategies

Figure 4.19 and 4.20 show the history matched result for the producer, P01. P01 is the only producer in segment four of Gulfaks field which has been produced from 1<sup>st</sup> February 2005 to 7<sup>th</sup> January 2009. P01 is a vertical well that has been perforated in the first three layer of Gulfaks field which is a total of 181ft. This research has matched the actual production history with the simulated history. Geological, geophysical and petrophysical input were used to build a reservoir description, and then a simulation model was build. Refer to Figure 4.19 and 4.20, it can be observed that the oil production rate and gas production rate has been matched. The prediction step can now be run on the model to investigate the best development strategy of GAGD process in Gulfaks field.

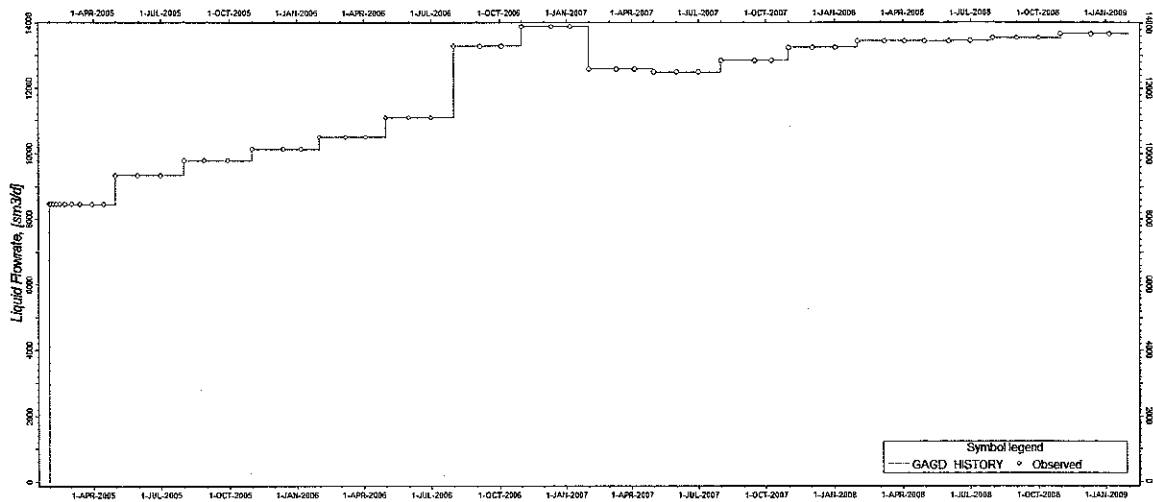


Figure 4.19: Matched Oil Production Rate for Well P01

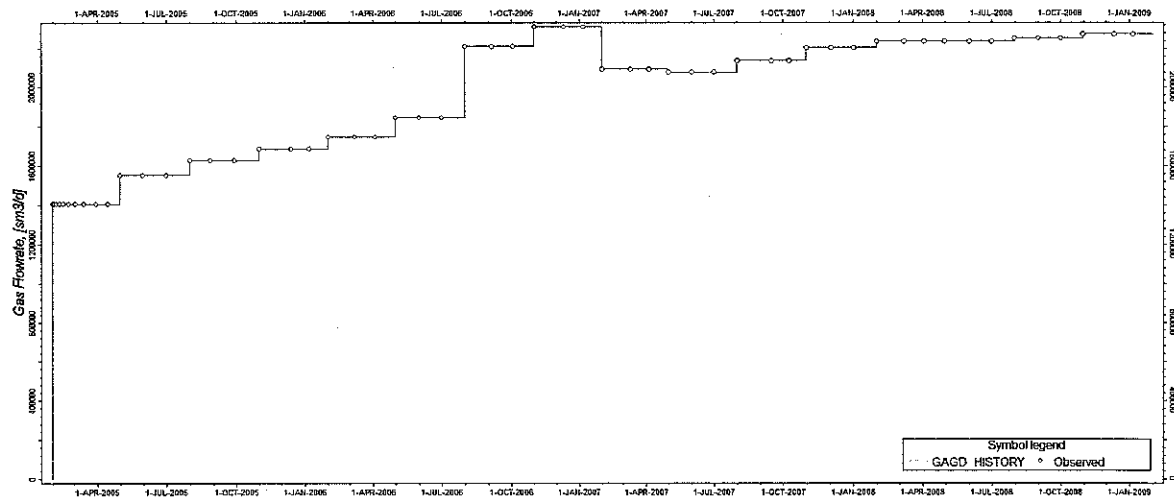


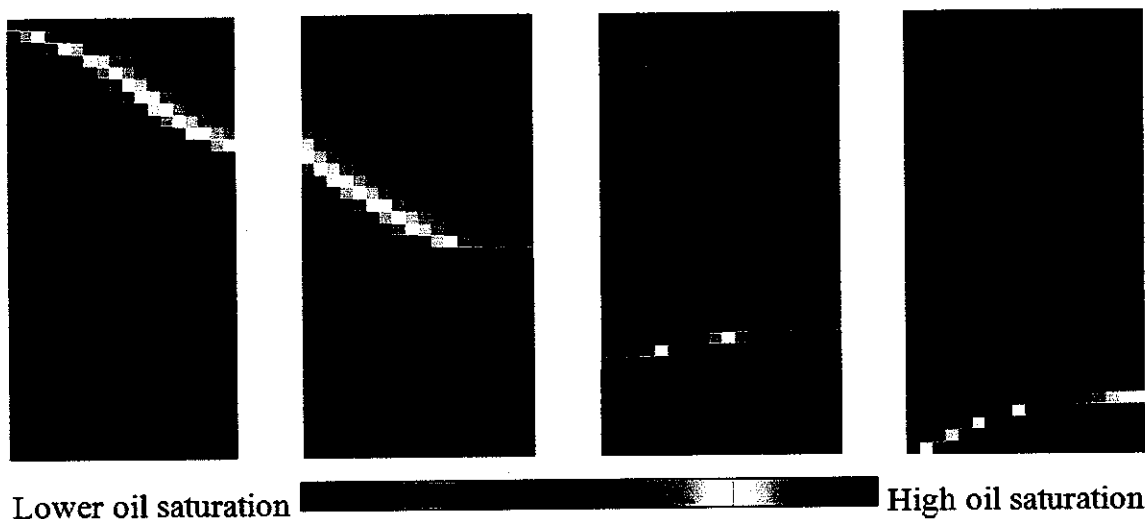
Figure 4.20: Matched Gas Production Rate for Well P01

#### 4.6 Development Strategy Optimization

Based on the best case in laboratory investigation, optimization on development strategy was done on the model with  $k_v/k_h=0.8$ , please refer to Section 3.2.2.6 for well orientations detail. For validation purpose, history matching process was done prior to optimization process (refer to Section 4.5 for detail).

Figure 4.21 (a)–(d) show that effect of gravity force can be observed in the heterogeneous reservoir when two vertical wells were used. Non-uniform displacement [Figure 4.21 (a)–(d)], early breakthrough [Figure 4.21 (d)], and late

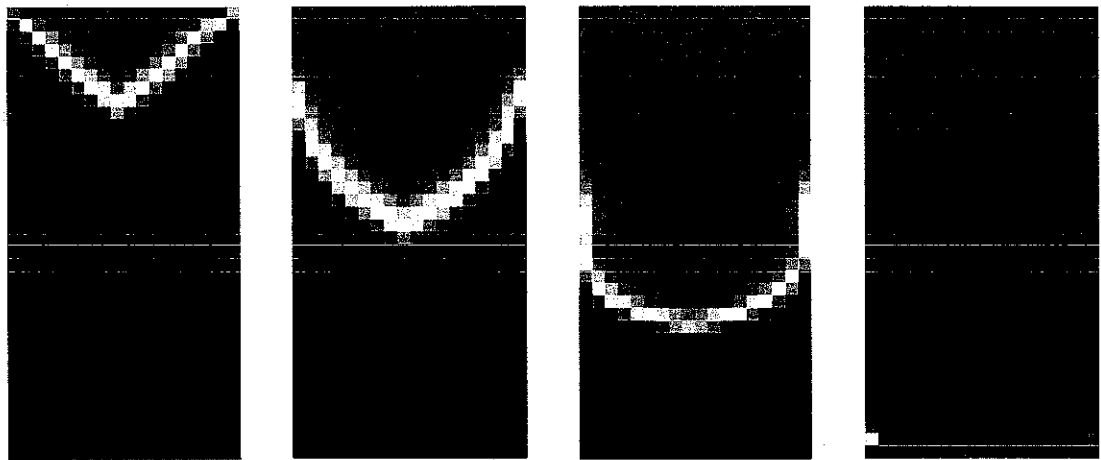
production (Figure 4.27) were some of the weakness as if vertical wells are used in this candidate. However, this kind of well orientation gave the highest ultimate recovery factor (63.89%ROIP) on the applied candidate (Figure 4.27). Figure 4.27 shows that after 0.85 of pore volume injected, a deeper injector will yield a higher and faster recovery. It is suggested that for a candidate with a higher  $k_v$ , the injector can be set at a deeper depth but this is only true when the gas has the time and opportunity to migrate upward.



(a) Across 1<sup>st</sup> Layer (b) Across 2<sup>nd</sup> Layer (c) Across 3<sup>rd</sup> Layer (d) Across 4<sup>th</sup> Layer

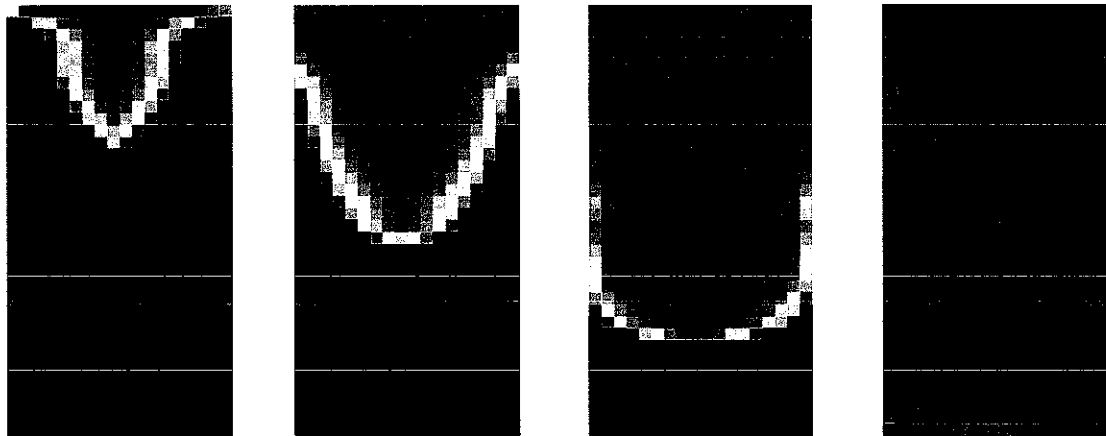
Figure 4.21: Fluid Front Displacement for Two Vertical Wells

For vertical injector with horizontal producer combination, a tongue-like displacement can be observed as the gas expands downward as shown in Figure 4.22 and 4.23. The gas has moved to the next layer before actually fill up the current layer. The gas has a higher tendency to move downward than horizontally. When the vertical permeability is more dominant, the well control is very crucial to avoid early gas breakthrough or water coning. For field application, the industry will try to avoid or delay the early break though by implement some inflow control valves or inflow control devices. These devices are aimed to increase the resistivity of the phases to flow and thus, create a more consistent front. However, it is impossible to have these devices to implement in the laboratory investigation. The effect of implement the inflow control devices were further discussed in the next sessions where simulations were run in Gulfaks model.



Lower oil saturation  High oil saturation  
 (a) Across 1<sup>st</sup> Layer (b) Across 2<sup>nd</sup> Layer (c) Across 3<sup>rd</sup> Layer (d) Across 4<sup>th</sup> Layer

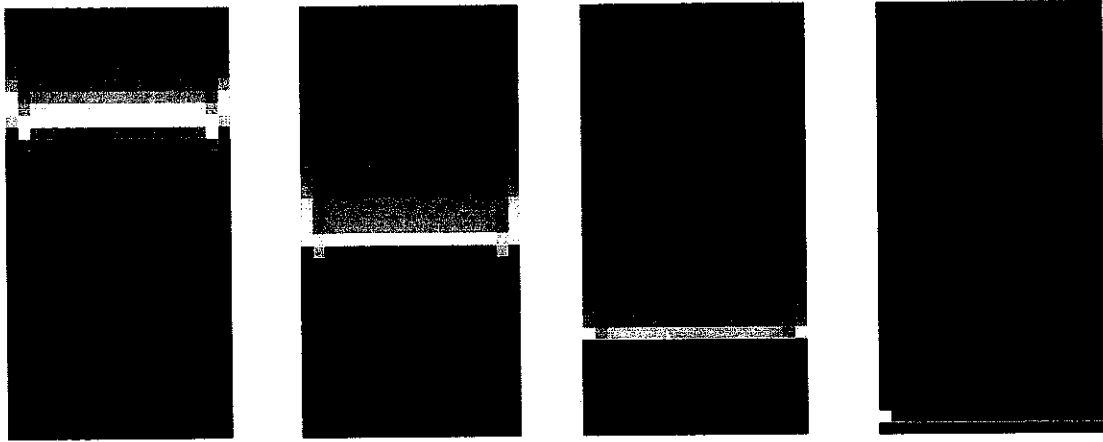
Figure 4.22: Fluid Front Displacement for Shallow Vertical Injector



Lower oil saturation  High oil saturation  
 (a) Across 1<sup>st</sup> layer (b) Across 2<sup>nd</sup> Layer (c) Across 3<sup>rd</sup> Layer (d) Across 4<sup>th</sup> Layer

Figure 4.23: Fluid Front Displacement for Deep Vertical Injector

Figure 4.24 (a)-(d) show that two horizontal wells combination yields the most stable displacement front compared with the previous three types. However, this Toe to Heel in GAGD oil recovery did not perform as expected. Mahmoud (2006) also encountered the same problem, the reason given was CO<sub>2</sub> gas did not rise to the top of the pay zone; instead, it found a path of least resistance to the horizontal well. Although the design of well seem fine in ECLIPSE, the dog leg severity number might be exceed and need to pay more attention when design the real well (Wang, 2011). Whereby it is the measurements on the degree of changes for a specific well in every 100ft.



Lower oil saturation  High oil saturation

(a) Across 1<sup>st</sup> layer (b) Across 2<sup>nd</sup> Layer (c) Across 3<sup>rd</sup> Layer (d) Across 4<sup>th</sup> Layer

Figure 4.24: Fluid Front Displacement for Horizontal Injector and Horizontal Producer

Front displacements during field implementation are shown in Figure 4.25 and 4.26. Refer to Figure 4.25, due to fractional pressure along the horizontal well and a more dominant vertical permeability, water coning can be observed (red line). To minimize the water coning effect, research another run has been done to investigate the effectiveness of an inflow control valve on the GAGD process. Extra effort in the investigation on the effectiveness of the inflow control valve since extra money needs to be invested and there will be an increase in difficulty on well completion on a real field application level. The specification and function of the inflow control valve used in this research is described in Section 2.5 of the thesis.

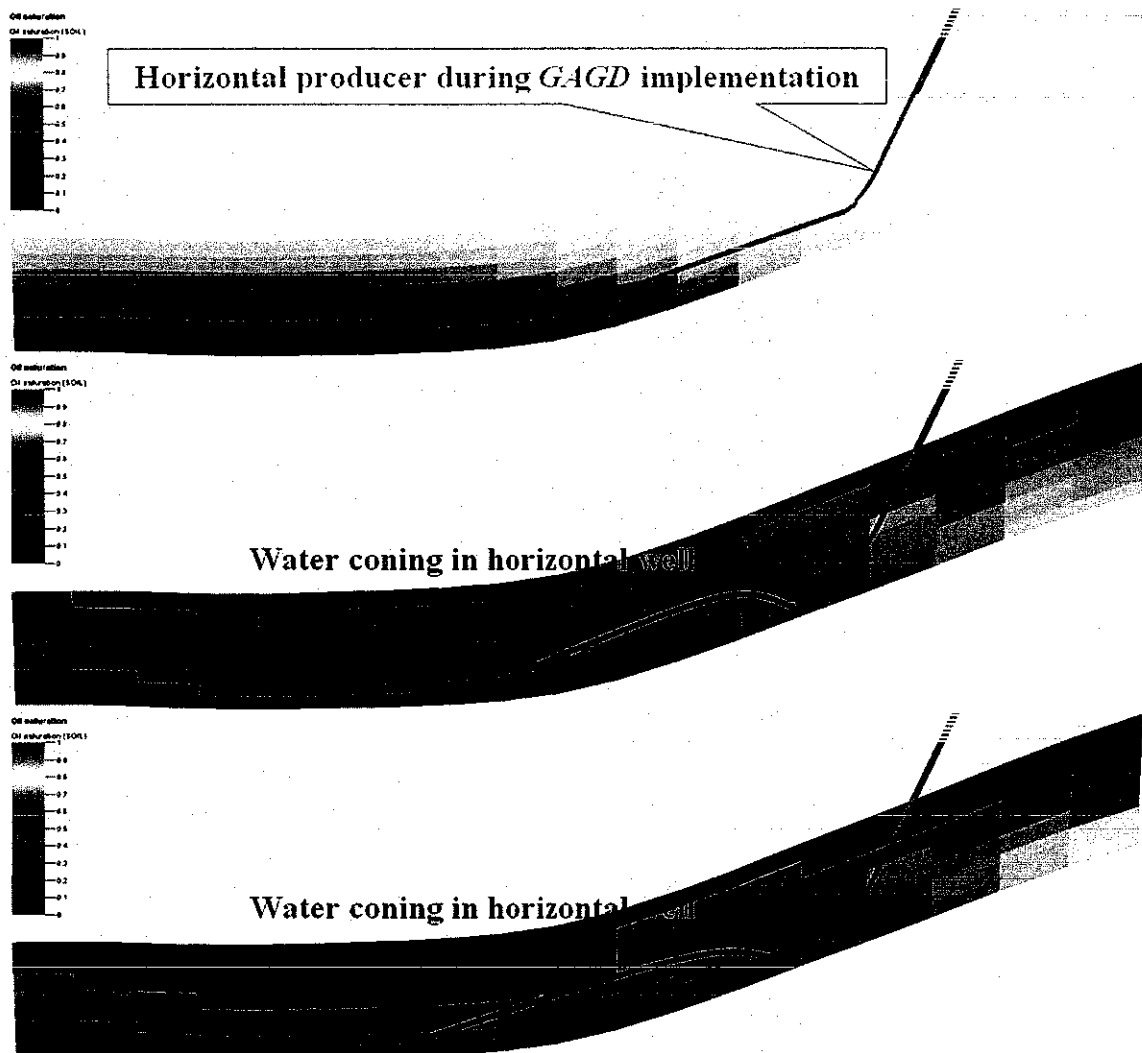


Figure 4.25: Oil Saturation Change along Horizontal Producer

Refer to Figure 4.26, there is a better front displacement in the horizontal producer with the inflow control valve compare to the horizontal well without any inflow control valve. In this research, inflow control valves were placed at the high permeability grid to balance up the permeability different along the horizontal well. From the fluid front displacement, it can be observed that there is a better from displacement for horizontal well with inflow control valve, further investigation were also done to investigate the different in recovery factor with and without in flow control valve in horizontal well.

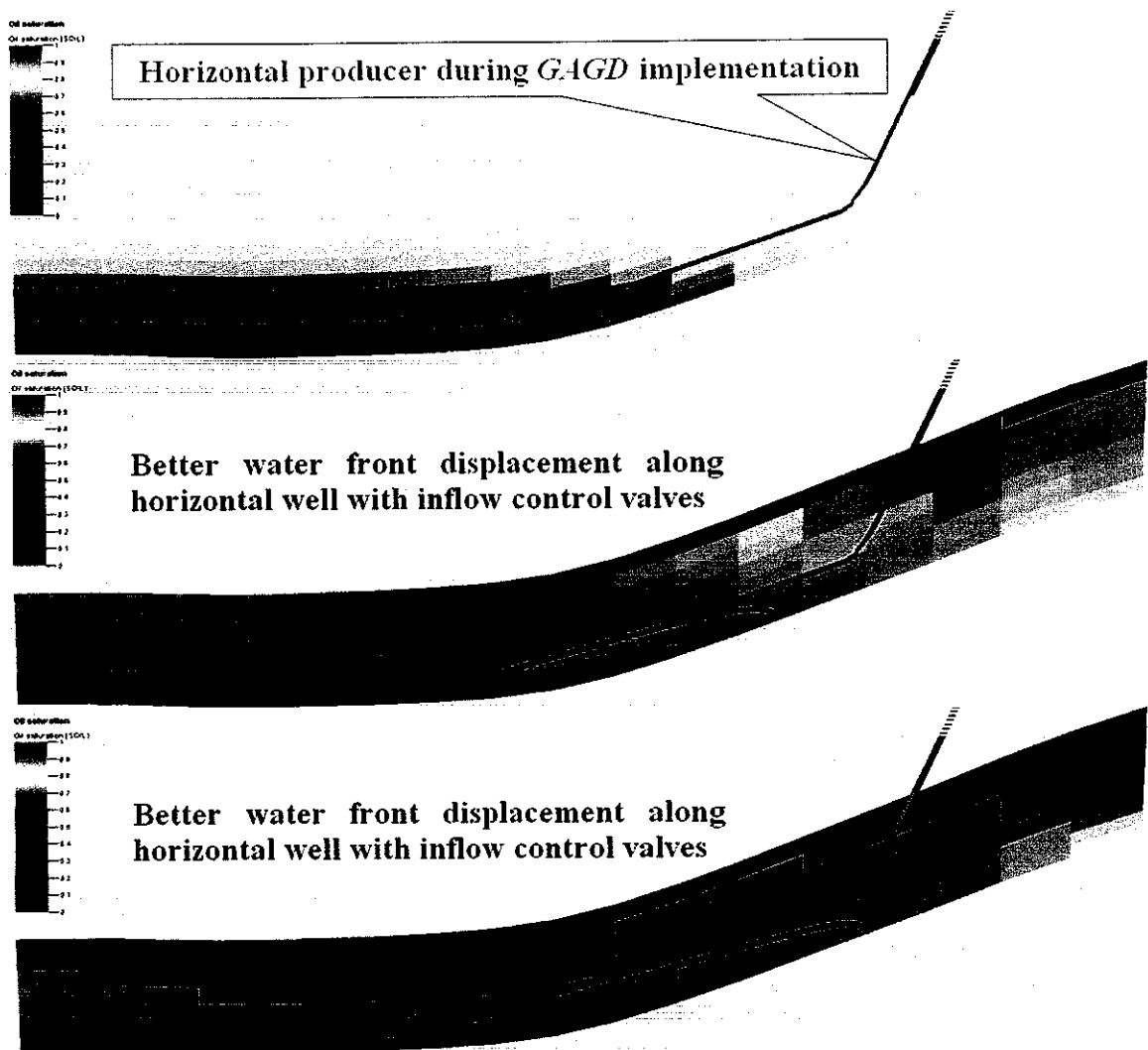


Figure 4.26: Oil Saturation Change along Horizontal Producer with Inflow Control Valves

Figure 4.27 shows the recovery factor for different well arrangements over every pore volume injected. The results can be explained in three phase:

- i. Phase I, a deep vertical injector with horizontal producer give the highest recovery. The gas was injected nearer to the producer, due to the lower density, gas will then migrate to the top part of the reservoir.
- ii. Phase II, two vertical wells start to show an increase in recovery. However, a deep vertical injector with horizontal producer still shows a higher recovery. The design with two horizontal wells shows that gas sweep the reservoir more stable front (refer to the color different between Figure 4.21-4.24).
- iii. Phase III, two vertical well combination shows the highest ultimate recovery (63.89%ROIP).

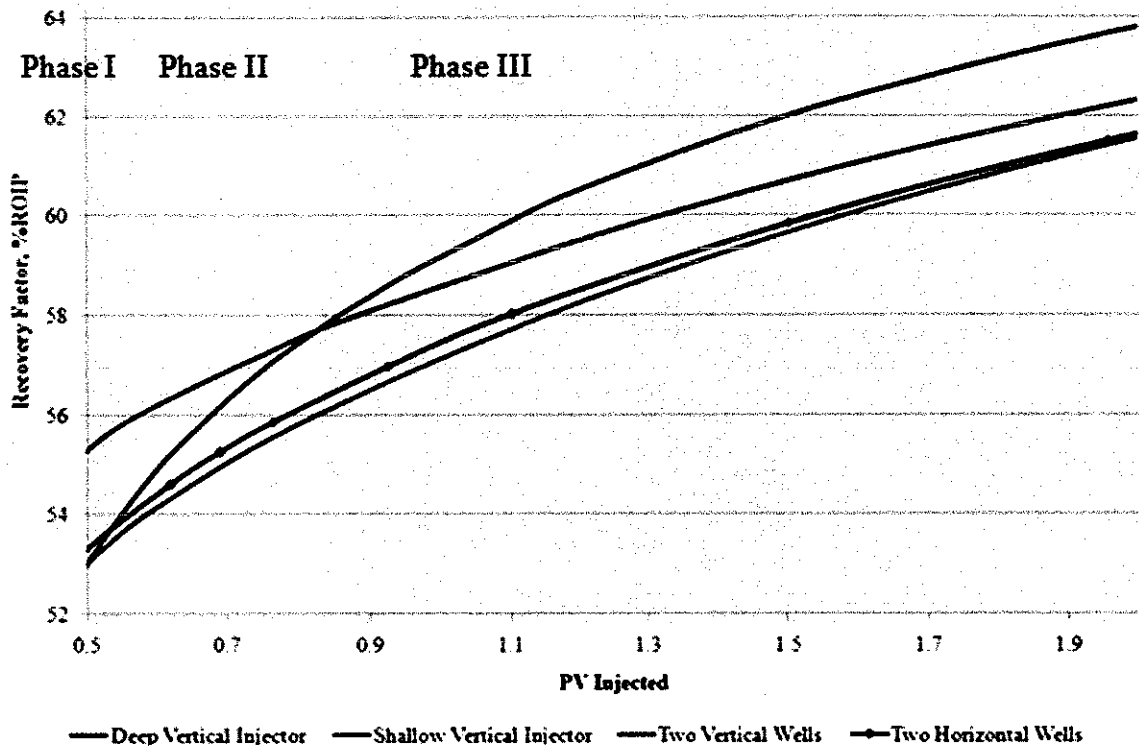


Figure 4.27: Recovery Factor for Different Well Arrangement over Pore Volume Injected

Recovery factor for different development strategies (refer to section 3.2.2.6) applied on Gulfaks field is shown in Figure 4.28. The case for continue the production by introducing GAGD process with inflow control valve shows the highest recovery (26.7%IOIP), followed by continue the production by introducing GAGD process (26.4%IOIP), continue the production by introducing WAG process (23.8%IOIP), and lastly continue the production with existing producer well (23.5%IOIP). Results show that GAGD process is a better choice to be implemented in Gulfaks field which tends to agree with investigation from previous researchers. In which the previous researchers (Rao, 2001; Kulkarni and Rao, 2004; Paidin, 2006; Mahmoud, 2006) also found that GAGD process is a better choice compared to WAG process. Refer to Figure 4.28, there is a big difference between the recovery factor by applying WAG (blue line) and GAGD (green and red line). For WAG process, water and gas were alternatively injected into segment four of Gulfaks field where each cycle lasts for four months. For the cases between GAGD process with and without inflow control valves, the recovery trend seems to be identical until the water and gas phase reach the horizontal producer. From 1<sup>st</sup> July 2018 onwards, the difference in recovery factor between these two conditions starts to be very drastic.

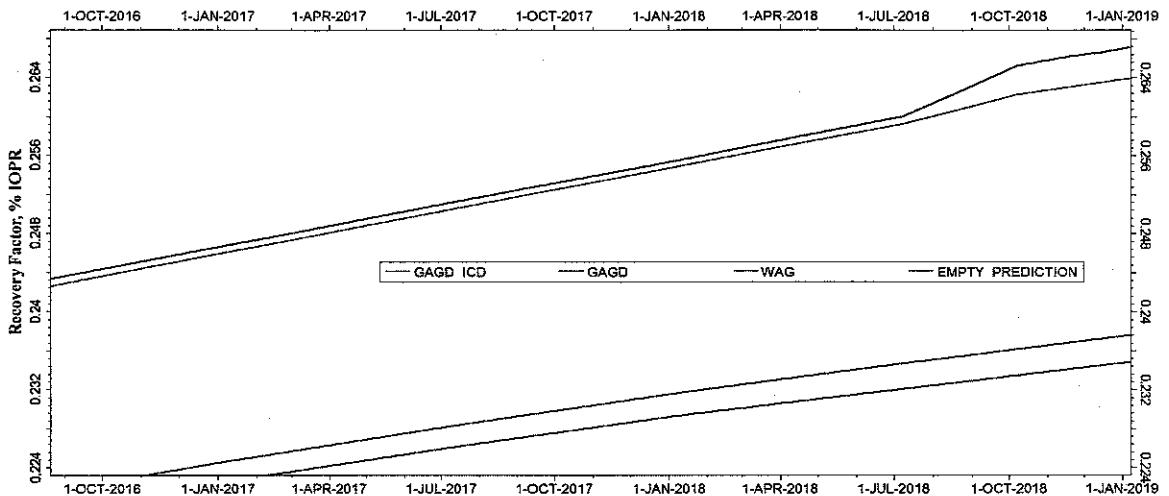


Figure 4.28: Recovery Factor for Different Development Strategy Implemented in Gulfaks Field

For well orientation design, two important points can be highlighted:

- i. Well design was fully depended on the candidate characterization.
- ii. Desired well design will be chosen based on the objective.
- iii. Simulation investigation is a good choice to simulate the effect of different well design on a specific process before real field implementation.

Previous works (Sharma, 2005; Mahmoud, 2006; and Paidin, 2006) used CO<sub>2</sub> as the injection gas due to its miscibility with the oil. Since density difference between all the phases is the key success of GAGD, investigation has been done to investigate the effect of gas density on the recovery factor. The tornado chart in Figure 4.29 shows that oil density is the main influence in GAGD recovery. This result compliances with finding from previous researchers (Mahmoud and Rao, 2007; Koederitz *et al.*, 1989) which found that gravity dominance is easier to achieve when density difference between phase increase.

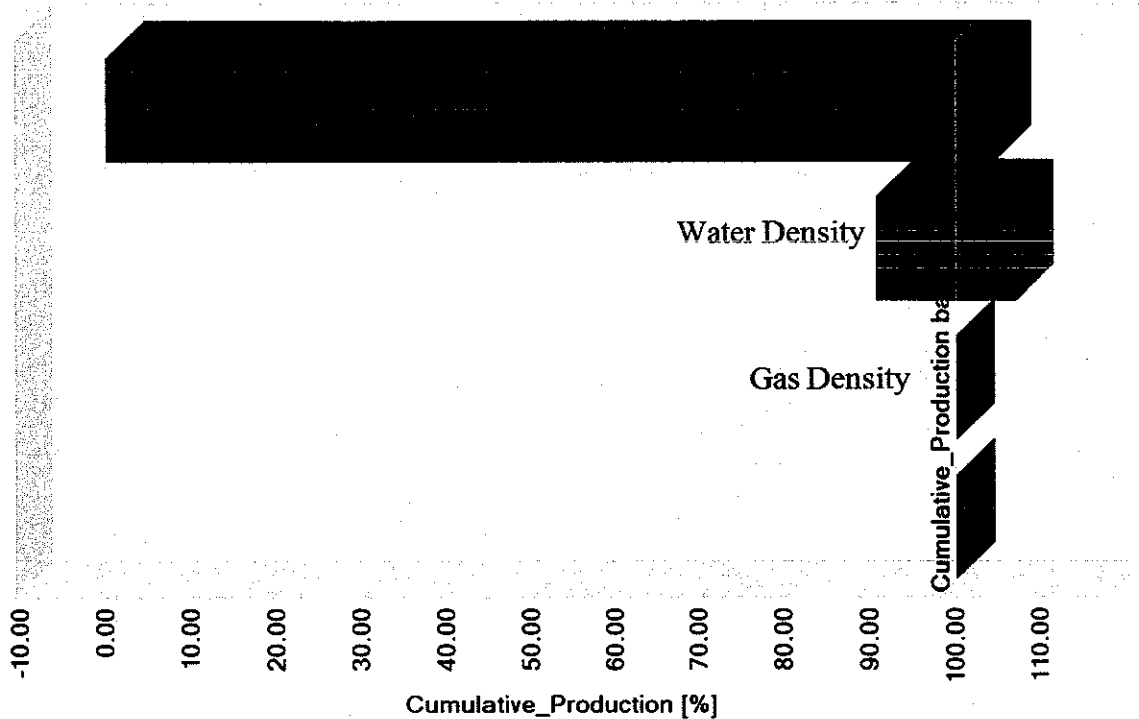


Figure 4.29: Change in Recovery Factor with Different Injected Gas Density

In order to effectively capture the miscibility effect of different injection gas to the reservoir oil, effect of different type of injection gas were investigated using E300 simulator. Figure 4.30 show the effect of choosing different injection gas in GAGD process. Results show that methane gas is the best gas to be use as injection gas in GAGD process but cost might be the draw down during the selection process. CO<sub>2</sub> is the second best gas to be select due to the high recovery during the GAGD process especially in the case where there is a big source of CO<sub>2</sub>. However, in the case where there is a difficulty to search for the source, CO<sub>2</sub> might not be a good selection. Research show that compress air is a good gas candidate for it low cost and high recovery factor. Every reservoir is specific so simulation is a must prior to any decision making.

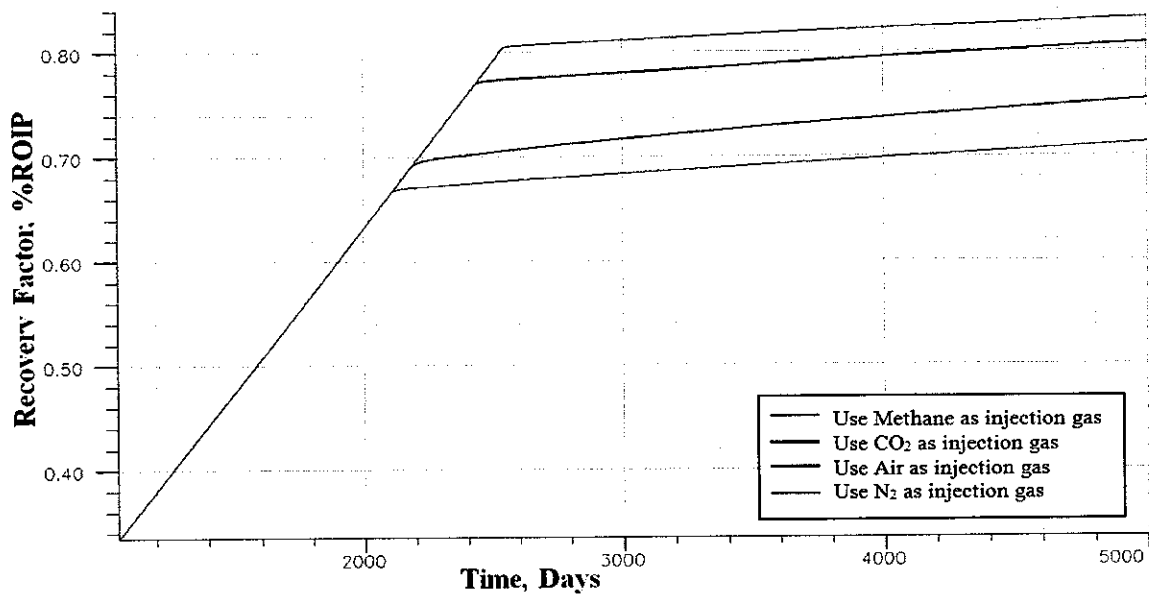


Figure 4.30: Recovery Factor for Different Injection Gas Used

Figure 4.31 shows the fluid displacement during miscible GAGD process. It can be observed that there is a stable displacement during miscible GAGD process with a small transition zone in the front. Compare with Figure 4.24, the reservoir is displaced in a much more effective way. This can be observe from the color in the displaced zone where there is a really low oil saturation compare to Figure 4.24.

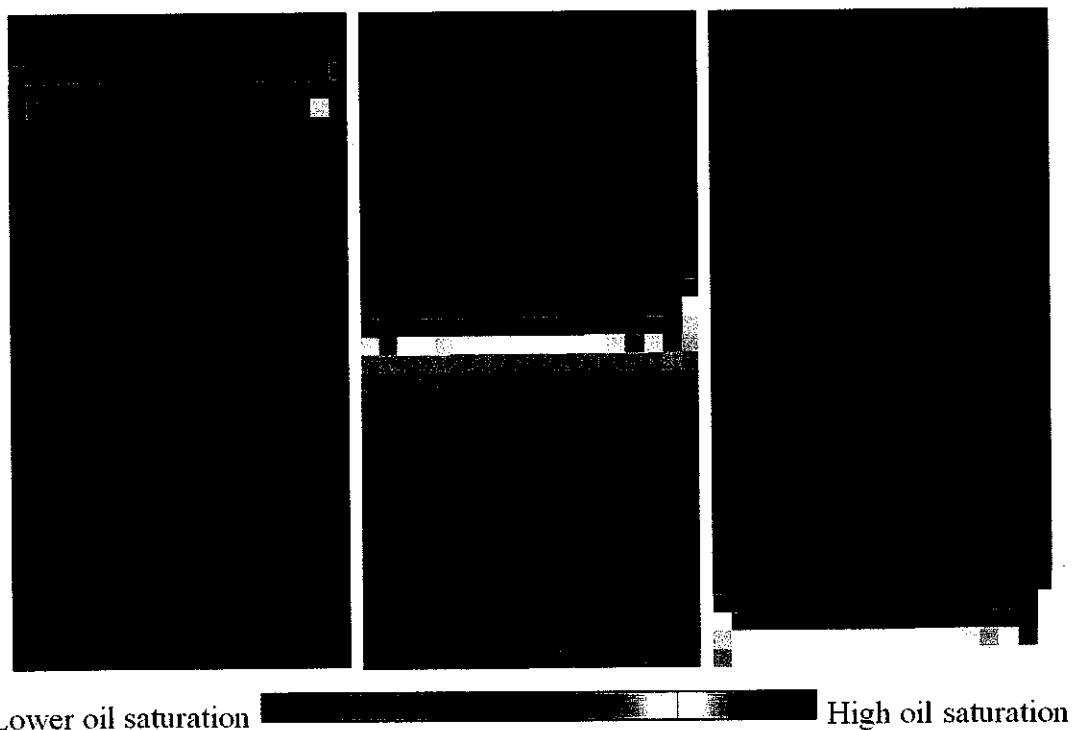


Figure 4.31: Front Displacement during Miscible Displacement

#### **4.7 Scaling of Production Time**

Dimensionless time scaling shows that one second in laboratory will be equivalent to five minutes in Gelama Merah (please refer to Appendix E for detail). For the most optimum case ( $k_v/k_h=0.8$ ), the time required in field to achieve 64.73%ROIP in laboratory was 5.8493hr, which is equivalent to 73days in Gelama Merah. This result was reasonable when compared to the result from Mahmoud (2006) and Sharma (2005) which range from 69-975 days (please refer to Table 2.1 for their experimental conditions).

#### **4.8 Effect of Gravity Number on Recovery Factor**

Base on the Figure 4.32, it is suggested that there is a polynomial relationship between the relationship between the recovery performance and the recovery numbers. This finding indicates that the performance of GAGD process appears to be well characterized by the use of Gravity number. Thus, the visual physical model has been proven in this study to be a very useful tool for analyzing an oil recovery scheme at a laboratory scale. Although the results from visual physical model are more reliable, the laboratory investigation is too time consuming (two months for one run) as mentioned in Section 3.2.2.6. Results from the laboratory visual physical model and the simulated results do converge to each other with a general polynomial equation of whereby the Recovery (%ROIP) =  $4.9307\ln(x)+30.153$ . This also shows the reliability of the simulation model to investigate the effect of gravity number on recovery factor.



## CHAPTER 5

### CONCLUSIONS AND SUGGESTIONS

#### 5.1 Conclusions

Major findings from this research can be summarized as follow:

- i. The history matched runs have validated the usability of the ECLIPSE model to run the prediction case. To get a valid simulation model for prediction run, in laboratory level, the simulation results from ECLIPSE model was history matched over the visual physical model. The simulated well bottom hole pressure and recovery factor must be within 1% difference with the visual physical model results from laboratory investigation. The fluid displacement was also compared with the actual fluid displacement from the visual physical model done in the laboratory. For field level of investigation, gas and oil production rate from ECLIPSE model were matched over the actual production rate from Gulfaks field.
- ii. Results from the simulations and laboratory measurements suggested that GAGD process is more favourable in the reservoir with more dominance in vertical permeability. This is provided that there is a very good well control done that yields a piston like displacement to avoid an early breakthrough in the horizontal producer.
- iii. For a small-scale investigation, the development strategy with two vertical wells yielded the highest recovery for GAGD process with a recovery of 63.89%ROIP. However, this is not true for field application since there are some inflow-control tools that can be inserted in the well. For type of injection gas, simulation results proposed CO<sub>2</sub> to be the better candidate over N<sub>2</sub> methane and air because of the lower minimum miscible pressure and more cost efficient.

- iv. GAGD process with inflow control valves attached to the horizontal producer has been suggested to be the best well design for Gulfaks field. Simulation on Gulfaks field shows that GAGD process is a better selection (26.4%IOIP) over WAG process (23.8%IOIP) and the recovery could be further increased with the usage of inflow control valves (26.7%IOIP).

## 5.2 Suggestions

Further GAGD simulation and visualization is recommended to explore some unanswered questions. The important recommendations are:

- i. Sensitivity test shows that compressed gas may be used to replace CO<sub>2</sub> during GAGD implementation. Thus, it is suggested that laboratory investigation should be conducted using compressed gas.
- ii. A higher strength and thermal resisted glass based visual physical model should be constructed to investigate all parameters in miscible GAGD. Temperature may affect the physical and chemical properties of the fluids and gas in place. Thus, it will be good if the model can be further modified to investigate the effect of temperature change on GAGD process.
- iii. Since fracture might create a high vertical permeability in the reservoir, it is suggested that study should be done to investigate the effect of fractures on the recovery.
- iv. Grid refinement should be applied around the wellbore during the simulation run to give a more detail visualization on the viscous fingering near the wellbore.

## REFERENCES

- [1] Abdullah M. Z., Rasol M. N., and Bandal M., "Gelama Merah-1 Well Test Report," PETRONAS Carigali Sdn. Bhd., Kajang, Selangor, Rep. *SUB-BLOCK 6S-18*, 2003.
- [2] Ahmed T., "Fundamentals of Rock Properties," in *Reservoir Engineering Handbook*, 2nd ed. Houston, Texas: Gulf Professional Publishing, 2001, ch. 4, pp. 184–186.
- [3] Ahmed T., "Relative Permeability Concept," in *Reservoir Engineering Handbook*, 2nd ed. Houston, Texas: Gulf Professional Publishing, 2001, ch. 5, pp. 288–289.
- [4] Amyx J. W., Bass D. M., and Whiting R. L., "Fundamental Properties of Fluid-Permeated Rocks," in *Petroleum Reservoir Engineering Physical Properties*. New York, United State: McGRAW-HILL BOOK COMPANY, 1960, ch. 2, pp. 37.
- [5] Arps J. J., (1964). Engineering Concepts Useful in Oil Finding. *APPG Bull* [Online]. 157-169.  
Available:[http://www.springer.com/cda/content/document/cda\\_downloaddocument/9783540727408-c1.pdf?SGWID=0-0-45-453398-p173759610](http://www.springer.com/cda/content/document/cda_downloaddocument/9783540727408-c1.pdf?SGWID=0-0-45-453398-p173759610)
- [6] Aziz K., (1984, November). Ten Golden Rules for Simulation Engineers. *Journal of Petroleum Engineering* [Online]. 1157.  
Available:[http://www.netl.doe.gov/technologies/oilgas/publications/SWCReports/2001FinalReports/2001PSU\\_Wileyville.pdf](http://www.netl.doe.gov/technologies/oilgas/publications/SWCReports/2001FinalReports/2001PSU_Wileyville.pdf)
- [7] Baviere M., (1991, May-June). Basic Concepts in Enhanced Oil Recovery Process. *Oil and Gas Science and Technology* [Article]. 57(3), 251-258.  
Available: Elsevier Science Publishers LTD/Critical Reports on Applied Chemistry
- [8] Blackwell R. J., Terry J. R., Lindley D. C., and Henderson J. R., (1960). Recovery of Oil by Displacements with Water-Solvent Mixtures. *Petroleum Transactions* [Online]. 219, pp. 293–300.

- Available:<http://www.onepetro.org/mslib/app/pdfpurchase.do?itemChronicleId=09014762800d1cf7&itemSocietyCode=SPE>
- [9] Bobek J. E., (1990). Reservoir Simulation [Monograph]. 13. Available: <http://precise.petronas.com.my/search~S14?/treservoir+simulation/treservoir+simulation/1%2C10%2C21%2CB/frameset&FF=treservoir+simulation&1%2C%2C4/indexsort=->
- [10] Brookfield Engineering Laboratories. (2010, April). Brookfield Digital Viscometer. Brookfield. Massachusetts, United States. [Online]. Available: <http://www.viscometers.org/PDF/Manuals/laboratory/DVE.pdf>
- [11] Carlson M. R., "History Matching," in *Practical Reservoir Simulation*. Tulsa, Oklahoma: PennWell Corporation, 2003, ch. 12, pp. 251.
- [12] Caudle, B.H and Dyes, A.B.: "Improving Miscible Displacement by gas-Water Injection" Transactions of AIME, 213 (1958), 281-284.
- [13] Charles R. S., Tracy G. W., and Farrar R. L., "Properties of Reservoir Rocks," in *Applied Reservoir Engineering, 1st vol.* United States: Oil & Gas Consultants International, INC, 1999, ch. 2, pp. 1-57.
- [14] Christensen J. R., Stenby E. H., and Akauge A., "Review of WAG field experience," presented at the 1998 SPE International petroleum conference and exhibition of Mexico, Villhermosa, Mexico, March 3-5, 1998, SPE 71203, Paper 39883.
- [15] Crichlow H. B., "A Simulation Approach," in *Modern Reservoir Engineering*, Englewood Cliffs, New Jersey: Prentice Hall, 1977.
- [16] Dake L. P., "Darcy's Law and Applications," in *Fundamentals of Reservoir Engineering*, Amsterdam, The Netherlands: ELSEVIER SCIENCE B.V., 1978, ch. 4, sec. 4.4, pp. 100-108.
- [17] Ertekin T., Abou-Kassem J. H., and King G. R., (2001). *Basic Applied Reservoir Simulation* [Book]. 7. Available: Universiti Teknologi PETRONAS Library, item ID: IPB195508.
- [18] Fanchi J. R., "Rock-Fluid Interaction," in *Principles of Applied Reservoir Simulation*, 2nd ed. Houston, Texas: Gulf Professional Publishing, 2001, ch. 14, pp. 120-128.
- [19] Fenghour A., Wakeham W. A., and Vesovic V.. (1998). *The Viscosity of Carbon Dioxide. Journal of Physical Chemistry Reference Data* [Online]. 27, pp. 31-44.

Available:<http://webbook.nist.gov/cgi/fluid.cgi?T=22&PLow=0&PHigh=100&PInc=5&Applet=on&Digits=5&ID=C124389&Action=Load&Type=IsoTherm&TUnit=C&PUnit=psia&DUnit=lbm%2Fft3&HUnit=kJ%2Fmol&WUnit=m%2Fs&VisUnit=cP&STUnit=lb%2Fft&RefState=DEF#Refs>

- [20] Green and Willhite.: "Enhanced Oil Recovery" SPE Text Book Series vol. 6, 1998.
- [21] Harari Z., Wang S. T., and Saner S., (1995, December). Pore-Compressibility Study of Arabian Carbonate Reservoir Rocks. *SPE Formation Evaluation Journal* [Online]. 10(4), 207-214.  
Available:<http://www.onepetro.org/mslib/app/pdfpurchase.do?itemChronicleId=0901476280071e76&itemSocietyCode=SPE>
- [22] Heinemann Z. E., "Wettability," in *Fluid Flow in Porous Media*, 1st vol. Leoben, Austria: MONTANUNIVERSITÄT LEOBEN, 2005, ch. 1, sec. 1.2.2, pp. 14–19.
- [23] Holm L. W. and Josendal V. A., (1982, February). Effect of Oil Composition on Miscible-Type Displacement by Carbon Dioxide. *SPE Journal* [Online]. 22(1), pp. 87–90.  
Available:<http://www.onepetro.org/mslib/app/pdfpurchase.do?itemChronicleId=09014762800639fa&itemSocietyCode=SPE>
- [24] Holmes, J. A., Barkve, T. And Schrenkel, P. J. (1998, October). "Development Application of a Multisegment Well Model to Simulate Flow in Advanced Wells". SPE 50646, SPE European Petroleum Conference, The Hague.  
Available:<http://www.onepetro.org/mslib/app/Preview.do?paperNumber=00050646&societyCode=SPE>
- [25] Honarpour M., Koederitz L., and Harvey A. H., "Determination of Wettability," in *Relative Permeability of Petroleum Reservoir*. Boca Raton, Florida: CRC Press, Inc, 1986, ch. 3, sec 6(A), pp. 58–60.
- [26] Institute of Petroleum Engineering, "Fundamental Properties of Reservoir Rocks," Heriot-Watt University, Edinburgh, Scotland, Reservoir Engineering Teaching Module, 2010.
- [27] Izgec O., Demiral B., Bertin H., and Akin S., (2007, May). CO<sub>2</sub> Injection into Saline Carbonate Aquifer Formations I: Laboratory Investigation. *Transport Porous Media* [Online]. 72, 1-24.

- Available: <http://www.springerlink.com/content/j41163p7r1031517/>
- [28] Jackson, D. D., Andrews, G. L., Claridge, E. L., "Optimum WAG ratio Vs Rock wettability in CO<sub>2</sub> flooding", SPE 14303, presented at 60th Annual technical conference and exhibition of the Society of Petroleum engineers held in Las Vegas, Nevada, Sept 22-25,1985.
- [29] Joshi, S.D.: *Horizontal Well Technology*, Pennwell Publishing Co, OK (1990) 1-21.
- [30] Kasiri N. and Bashiri A., (2011, March). A Gas-assisted Gravity Drainage Process in Naturally Fractured Reservoirs. *Taylor & Francis [Online]. 33(11)*, 1058-1066.  
Available: [www.tandfonline.com/doi/abs/10.1080/15567030903515567](http://www.tandfonline.com/doi/abs/10.1080/15567030903515567)
- [31] Kifni S. M., "Equity Beats," MIDF Research, Malaysia, Rep. PP 10744/06/2011(1), February 2011. Available:  
<http://www.midf.com.my/project/midf/media/2011/02/16/122351-736.pdf>.
- [32] Koederitz L. F., Harvey A. H., and Honarpour M., "Reservoir Rocks," in *Introduction to Petroleum Reservoir Analysis*. Houston, Texas: Gulf Publishing Company, 1989, ch. 2, pp. 24–43.
- [33] Kulkarni M. M., "Multiphase Mechanisms and Fluid Dynamics in Gas Injection Enhanced Oil Recovery Process," Ph.D. dissertation, The Craft and Hawkins Department of Petroleum Engineering, Louisiana State University, Baton Rouge, 2005.
- [34] Kulkarni M. M. and Rao D. N., "Is Gravity Drainage an Effective Alternative to WAG," presented at the 'American Institute of Chemical Engineers' 2004 Annual Meeting, Austin, Texas, Nov, 7-12, 2004.
- [35] Latil M., "Introduction," in *Enhance Oil Recovery*. Paris, France: Institut Francais Petrole Publications, Gulf Publishing Company, 1980, ch. 1, pp. 1-2.
- [36] Lucia F. J., "Petrophysical Rock Properties," in *Carbonate Reservoir Characterization An Integrated Approach*, 2nd ed. Berlin, New York: Springer Berlin Heidelberg, 2007, ch. 1, pp. 10–11.
- [37] Ma S. Z., "Enhanced Heavy Oil Recovery by Dilute Alkaline Flooding," M.S. thesis, Petroleum Systems Engineering, University of Regina, Regina, Saskatchewan, 2005.
- [38] Mackay E., "ECLIPSE Tutorial 1," Heriot-Watt University, Edinburgh,

Scotland, Sample Report, 6 February 2009.

- [39] Mahmoud T. N., "Demonstration and Performance Characterization of the Gas Assisted Gravity Drainage (GAGD) Process Using a Visual Model," M.S. thesis, Petroleum Engineering Department, University of Wisconsin-Madison, Madison., Wisconsin, 2006.
- [40] Mahmoud T. N. and Rao D. N., "Mechanisms and Performance Demonstration of the Gas-Assisted Gravity-Drainage Process Using Visual Models", presented at the 2007 SPE Annual Technical Conference and Exhibition, Anaheim, California, 11-14 November, 2007. Paper 110132.
- [41] Makse H. A., D. L. Johnson, and L. M. Schwartz. (2000, May 1). Packing of Compressible Granular Materials. *Physical Review Letters* [Online]. pp. 4160–4163.  
Available: <http://lisg1.engr.cuny.cuny.edu/~makse/publicationlist/MJS.pdf>
- [42] Mattax C. C. and Dalton R. L., (2002, Feb 27). *Reservoir Simulation* [Book]. 13(ISBN 1555630286).  
Available: <http://www.getcited.org/?PUB=102926212&showStat=Ratings>
- [43] *Model 1100 Pressurized Viscometer Instruction Manual, Ver. 5.8*, OFI Testing Equipment, Inc., Houston, Texas, 2009, pp. 1-45.  
Available: [http://www.ofite.com/instructions/130-81\\_v1.pdf](http://www.ofite.com/instructions/130-81_v1.pdf)
- [44] Musa S. A. E., "Reservoir Engineering Study of Unity Oil Field, Sudan," M.S. thesis, The Department of Petroleum Engineering of University of Petroleum, University of Petroleum, Beijing, Dec 2004.
- [45] Naami A. M., Catania P., and Islam M. R., "Numerical and Experimental Modeling of Viscous Fingering in Two-Dimensional Consolidated Porous Media," presented at the Technical Meeting/Petroleum Conference of the South Saskatchewan Section, South Saskatchewan, Canada, 18-21 October 1999.  
Available: <http://www.onepetro.org/mslib/servlet/onepetropreview?id=PETSOC-99-118&soc=PETSOC>
- [46] Owens W. W. and Archer D. L., (1971, July). The Effect of Rock Wettability on Oil-water Relative Permeability Relationships. *Journal of Petroleum Technology* [Online]. 23(7), 873–878.  
Available: <http://www.onepetro.org/mslib/app/Preview.do?paperNumber=00003034&societyCode=SPE>

- [47] Paidin W. R., "Physical Model Study of the Effects of Wettability and Fractures on Gas-Assisted Gravity Drainage (GAGD) Performance," M.S. thesis, Petroleum Engineering Department, Louisiana State University, Baton Rouge, 2006.
- [48] Paidin W. R., Mwangi P., and Rao D. N., "Economic Evaluation within the Scope of the Field Development and Application of the Gas-Assisted Gravity Drainage (GAGD) Process in an Actual Northern Louisiana Field", presented at the 2010 Hydrocarbon Economics and Evaluation Symposium, Dallas, Texas, 8-9 March, 2010. Paper 1929723.
- [49] Pauzi N., Low F. N., Abas A., Juwaini A. R., and Maksari H., "Revitalizing The West Lutong," presented at the 1999 SPE Asia Pacific Improved Oil Recovery Conference, Kuala Lumpur, Malaysia, October 25-26, 1999, SPE 57266.
- [50] PETRONAS GARIGALI SDN. BHD., "Final Well Report, Gelama Merah-1 & Gelama Merah-1 ST1, Malaysia," PETRONAS CARIGALI SDN. BHD., Kuala Lumpur, Malaysia, Rep. *Final*, December 2002–2003.
- [51] Quek C. J. and Chang K., "Advance Rock Properties Report for PETRONAS CARIGALI SDN. BHD.," PETRONAS CARIGALI SDN. BHD., Kajang, Selangor, Rep. *SCM 02045*, 2004.
- [52] Rao, D. N., "Gas Injection EOR - A New Meaning in the New Millennium", *Journal of Canadian Petroleum Technology*, 41 (2), 11-19, 2001.
- [53] Rao D. N., Ayirala S. C., Kulkarni M. M., and Sharma A. P., "Development of Gas Assisted Gravity Drainage (GAGD) Process for Improved Light Oil Recovery," presented at the SPE/DOE Symposium on Improved Oil Recovery, Tulsa, Oklahoma April 17-21, 2004, Paper SPE 89357- MS.
- [54] Richard M. F. and Ronald W. R., "Process and Process Variables," in *Elementary Principles of Chemical Processes*, 3rd ed. United States of America: John Wiley & Sons, Inc, 1999, ch. 5, sec. 3.3, pp. 50–51.
- [55] Richard F. M. and Wallace D. W. JR., "Definition and World Resources of Natural Bitumens," in *U.S. Geological Survey Bulletin 1944*, United States Government Printing Office, 1990, ch. 1, pp. 8.  
Available: <http://pubs.usgs.gov/bul/1944/report.pdf>
- [56] Saleri N. G., Toronyi R. M., and Synder D. E. (1992, December). Data and Data

- Hierarchy. *Journal of Petroleum Technology* [Online]. 44(12), 1286-1293.  
Available:<http://www.onepetro.org/mslib/app/pdfpurchase.do?itemChronicleId=0901476280068cf0&itemSocietyCode=SPE>
- [57] Schlumberger Information Solutions. (2009, May) ECLIPSE Blackoil Reservoir Simulation. Schlumberger. [Training Manual].
- [58] Schlumberger Information Solutions. (2010, May) Petrel for Reservoir Engineering. Schlumberger. [Training Manual].
- [59] Shafi'i M. R. M. D., Salleh I. K., Daud W. A. W., and Anwar M. L., "Reservoir Fluid Study (DST#1)," PETRONAS Carigali Sdn. Bhd., Kajang, Selangor, Rep. *PRSS-LS-03-32*, 2003.
- [60] Sharma A. P., "Physical Model Experiments of Gas Assisted Gravity Drainage," M.S. thesis, The Craft and Hawkins Department of Petroleum Engineering, Louisiana State University, Baton Rouge, Louisiana, 2005.
- [61] Span R. and Wagner W., (1996). A New Equation of State for Carbon Dioxide Covering the Fluid Region from the Triple-Point Temperature to 1100K at Pressures up to 800MPa. *Journal of Physical Chemistry Reference Data* [Online]. 25(6), pp. 1509–1596.  
Available:<http://webbook.nist.gov/cgi/fluid.cgi?T=22&PLow=0&PHigh=100&PInc=5&Applet=on&Digits=5&ID=C124389&Action=Load&Type=IsoTherm&TUnit=C&PUnit=psia&DUnit=lbm%2Fft3&HUnit=kJ%2Fmol&WUnit=m%2Fs&VisUnit=cP&STUnit=lb%2Fft&RefState=DEF#Refs>
- [62] Teknica Petroleum Services Ltd, "Reservoir Simulation," Teknica Petroleum Services Ltd, Calgary, Alberta, Tech. Rep., April 2001.  
Available:[http://www.4shared.com/account/document/emqVVhn6/Teknica\\_Petroleum\\_Services\\_-\\_H.html](http://www.4shared.com/account/document/emqVVhn6/Teknica_Petroleum_Services_-_H.html)
- [63] Thomas G. W., "History Matching," in *Principles of Hydrocarbon Reservoir Simulation*, Boston: International Human Resources Development Corporation, 1982.
- [64] Torsaeter O. and Abtahi M., "Experimental Reservoir Engineering Laboratory Workbook," Department of Petroleum Engineering and Applied Geophysics, Norwegian University of Science and Technology, Trondheim, Norway, Lab Rep. *Jan*, 2003.
- [65] Turta A. T., Singhal A. K., Goldman J., and Zhao L., "Toe-to-Heel

- Waterflooding. Part II: 3D Laboratory-Test Results,” presented at the 2003 SPE Annual Technical Conference and Exhibition, Denver, United State March 16, 2006, Paper SPE 84077.
- [66] Ursin J. R. and Zolotukhin A. B., “Wettability and Capillary Pressure,” in *Introduction to Reservoir Engineering*. Stavanger, 1997, ch. 6, pp. 83–105.
- [67] Vesovic V., Wakeham W. A., Olchowy G. A., Sengers J. V., Watson J. T. R., and Millat J., (1990). The transport properties of carbon dioxide. *Journal of Physical Chemistry Reference Data* [Online]. 19, pp. 763–808.  
Available:<http://webbook.nist.gov/cgi/cbook.cgi?Source=1990VES%2FWAK763-808>
- [68] Vinci Technologies, “HePorosimeter Production Series for Grain Volume Measurement Operating Manual,” VINCI Technologies, Nanterre, France, Rep. *API21v3*, July 2007.
- [69] Wang D., “Fundamentals, Formulations and Solution Process,” Schlumberger, Houston, Texas, 2011.
- [70] Wood D. J., Lake L. W., Johns R. T., and Nunez V., “A Screening Model for CO<sub>2</sub> Flooding and Storage in Gulf Coast Reservoir Based on Dimensionless Groups,” presented at the 2006 SPE/DOE Symposium on Improved Oil Recovery, Tulsa, Oklahoma, 22-26 April, 2006. Paper 100021.
- [71] Zainul A. J., Misman R., and Ali A. J., “Overview of Petroleum Resources of Malaysia,” in *The Petroleum Geology and Resources of Malaysia*, Kuala Lumpur, Malaysia: Petroliaam Nasional Berhad, 1999, ch. 3, pp. 35–49.
- [72] Zhang L. and Dusseault M. B., (1994, March). Are Horizontal Wells Always Better Producers than Vertical Wells? *Petroleum Society of Canada* [Online]. pp. 1–9.
- [73] Available:<http://www.onepetro.org/mslib/app/pdfpurchase.do?itemChronocleId=0901476280209b3e&itemSocietyCode=PETSOC>

## APPENDIX

### Appendix A Fluid Viscosity Calculation

Figure A1 and A2 show the viscometer fluid viscosity (cP) for brine and mineral oil at 600 RPM from OFITE Pressurized Viscometer Model 1100. The results are reported in Table 4.2 and later use in ECLIPSE simulator.

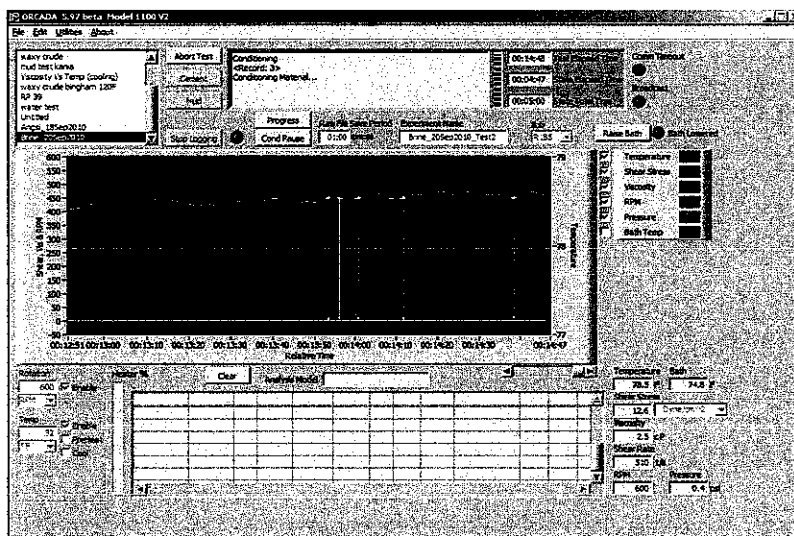


Figure A1: Brine viscosity at 600 RPM

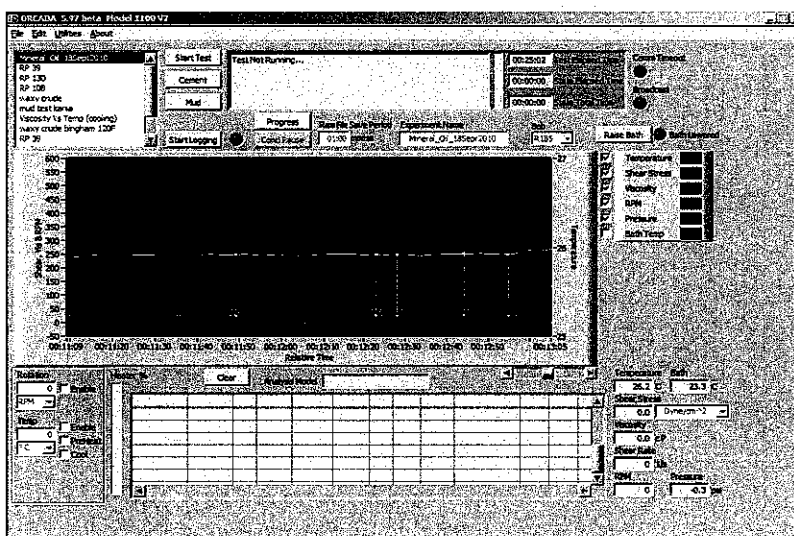


Figure A2: Mineral Oil Viscosity at 600 RPM

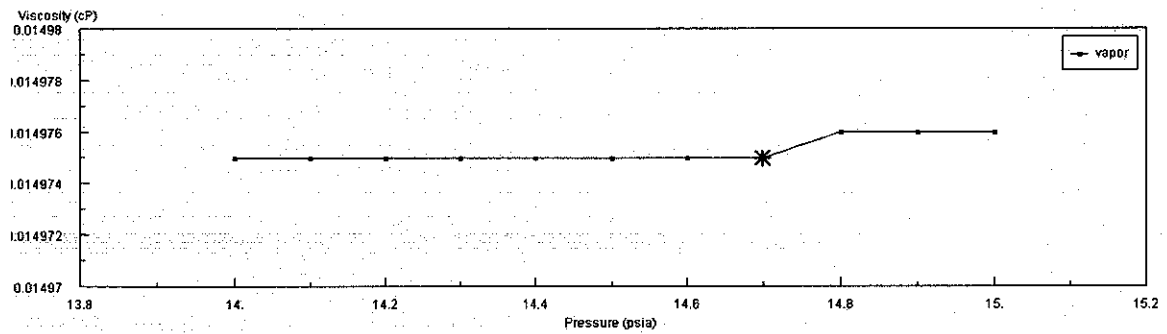


Figure A3: Carbon Dioxide Viscosity at 25.9 °C and 14.7 psia (Vesovic *et al.*, 1990; Span and Wagner, 1996; Fenghour *et al.*, 1998)

Table A1 shows the summary for laboratory measurement and papers referred for all the phase used during visual physical model measurements. These values were then used in ECLIPSE as a reference viscosity which is then scaled to the reservoir condition.

Table A1: Viscosity Test Result

Viscosity test report				Date: 20 September 2010	
				By: Tham Boon Keat	
Sample	Spindle	RPM	Temperature, °C	Viscosity, cP	Average Viscosity, cP
Brine	R1B5	600	25.9	2.4	2.5
Brine	R1B5	600	25.9	2.6	
Brine	R1B5	600	25.9	2.6	
Brine	R1B5	600	25.9	2.4	
Brine	R1B5	600	25.9	2.5	
Mineral Oil	R1B5	600	25.9	25.0	25.0
Mineral Oil	R1B5	600	25.9	25.0	
Mineral Oil	R1B5	600	25.9	25.0	
Mineral Oil	R1B5	600	25.9	25.0	
Mineral Oil	R1B5	600	25.9	25.0	
CO <sub>2</sub>			25.9	0.01	0.01

## Appendix B Relative Permeability Calculation

All the relative permeability calculation was done by using Microsoft Excel according to Wyllie-Garner Correlation for unconsolidated sand (Ahmed, 2001). The connate water saturation for the visual physical model was recorded and using Wyllie-Garner Correlation for unconsolidated sand,  $k_{ro}$  and  $k_{rw}$  were calculated. All the formulas were pre-set in Excel and but input the connate water saturation, the Excel will compute the relative permeability for each phase. Figure D1 shows the relative permeability value for the model with  $k_v/k_h$  of 0.8, 0.9, and 1.0, respectively.

	A	B	C	D	E	F	G	H	I	J
1	<b>Wyllie-Garner Correlation</b>									
2	Key in Swc	0.12								
3	Key in Sgc									
4	Key in Soc									
5										
6	Sw	Sw*	Kro	Krw	Sg	So	So*	Kro	Krg	
7	0.25	0.1477	0.6191	0.0032		0.05	0.83	0.9432	0.8390	0.0002
8	0.30	0.2045	0.5033	0.0086		0.10	0.78	0.8864	0.6964	0.0015
9	0.35	0.2614	0.4030	0.0179		0.20	0.68	0.7727	0.4614	0.0117
10	0.40	0.3182	0.3170	0.0322		0.30	0.58	0.6591	0.2863	0.0396
11	0.45	0.3750	0.2441	0.0527		0.40	0.48	0.5455	0.1623	0.0939
12	0.50	0.4318	0.1834	0.0805		0.50	0.38	0.4318	0.0805	0.1834
13	0.60	0.5455	0.0939	0.1623		0.60	0.28	0.3182	0.0322	0.3170
14	0.70	0.6591	0.0396	0.2863		0.70	0.18	0.2045	0.0086	0.5033
15										

Figure B1: Relative Permeability Calculation for  $k_v/k_h=0.8, 0.9, \text{ and } 1.0$  from Excel Application

## **Appendix C Porosity and Permeability Measurements**

### **Porosity and Permeability Measurement Procedure**

1. The equipments were prepared according to the set-up in Section 3.2.2.5.
2. The measurement model was first packed with desired glass beads.
3. The dry weight of the measurement model was recorded.
4. The measurement model was set vertically with the inlet at the bottom.
5. The Jasco Pump was set to 5 cm<sup>3</sup>/min.
6. The Jasco Pump was started.
7. The outlet valve of measurement model was closed to desired opening for pressure to build up.
8. The inlet pressure was monitored to be less than 90 psig (maximum allowable pressure).
9. The inlet and outlet pressure were recorded once the inlet and outlet flow rate were stable.
10. The porosity was calculated accordingly.
11. The result was validated with Helium Porosimeter Test.

### **Flooding Test Procedure**

1. The equipments were prepared according to the set-up in Section 3.2.2.1.
2. The fluid properties measurement, porous media characterization, and leaking test were done prior to flooding test.
3. The brine was injected into the visual physical model until the pressure and flow rate in inlet and outlet were constant.
4. The fluid container from the pump was replaced by mineral oil.
5. The webcam was initiated to record the fluid front displacement.
6. The mineral oil was injected into the visual physical model until no more brine was displaced.
7. The total mineral oil injected and brine produced were recorded for further calculation.
8. The CO<sub>2</sub> gas was injected vertically downward for GAGD displacement.
9. The total CO<sub>2</sub> injected and fluids produced were recorded for further calculation.
10. The video recording and gas injection were stopped.
11. The visual physical model was unpacked and cleaned.

### **Packing, Cleaning, and Repacking Procedure**

1. The visual physical model was connected to a vacuum pump for leaking test.
2. Epoxy and silicon were applied to seal the leaking parts.
3. The upper part of visual physical model was open for glass beads packing if the model was not leak.
4. The visual physical model was packed by sieve shaker while measurement model was packed by shaker table.
5. The packing step was repeated until the glass beads level was constant.
6. All desired tests were done on all the models.
7. The results were recorded.
8. The models were unpacked.
9. The used glass beads were washed with soap.
10. The used glass beads were then rinsed with acetone for 1 hour.
11. The used glass beads were placed in oven at 90°C for 24 hours to dehumidify.
12. The used glass beads were then sieved out according to glass beads size.

### **Porosity and Permeability Calculation**

Mass of measurement model filled with water,  $m_{m+w}$  was calculated by:

$$m_{m+w} = m_m + PV * \rho_w \quad (A1)$$

PV of the system was calculated by:

$$PV = \frac{m_{m+w} - m}{(\rho_w)} \quad (A4)$$

Since the BV has be known,  $\phi$  was calculated by:

$$\phi = \frac{PV}{BV} \quad (A5)$$

k was calculated by (Torsaeter and Abtahi, 2003 and Dake) where  $k_v$  and  $k_h$  are assumed to be the same (Turta et al., 2006):

$$k(Darcy) = \frac{q(cm^3/min) * \mu(cP) * L(cm)}{15 * \pi * D^2(cm^2) * \Delta P(atm)} \quad (A6)$$

Table C1: Porosity, and Permeability for Homogeneous Model

Size, $\mu\text{m}$	$M_{me}$ , g	$M_{me, w}$ , g	$D_V$	$B_V$	$\phi$	$Q$ , $\text{cm}^3/\text{min}$	$P_{me}$ , atm	$P_{me, w}$ , atm	$\Delta P$ , atm	$k$ , Darcy
30-60	713	777.47	63.21	147	0.43	5	0.3130	0.2722	0.0408	12.48274
90-150	722	784.70	61.47	147	0.42	5	0.6124	0.5784	0.0340	14.97929
212-400	733	793.00	58.80	147	0.40	5	0.8710	0.8506	0.0204	24.96548
425-600	735	709.46	54.39	147	0.37	5	0.8778	0.8642	0.0136	37.44822

Table C2: Porosity Results from Helium Porosimeter

Active Sample: 20 Tank Size: 1.5" Last Calibration: 14/06/06 11:39 AM

No	Sample ID	Core Dia (mm)	Core Length (mm)	Bulk Vol (cc)	Grain density (g/cc)	Effective Core Porosity (%)	Data Time of Test	Pref (psi)	Pexp (psi)	Porosity
1	36-60	40.00	78.00	98.02	3.40	0.43	20/08/2010 21:06:08	97.59	51.33	0.43
2	36-60	40.00	78.00	98.02	3.38	0.43	20/08/2010 21:11:22	97.64	51.82	
3	36-60	40.00	78.00	98.02	3.39	0.43	20/08/2010 21:15:47	97.71	51.86	
4	36-60	40.00	78.00	98.02	3.38	0.42	20/08/2010 21:20:23	97.81	51.51	
5	36-60	40.00	78.00	98.02	3.40	0.44	20/08/2010 21:25:35	97.85	52.89	
6	90-150	40.00	78.00	98.02	3.36	0.42	20/08/2010 21:49:08	97.79	52.73	0.42
7	90-150	40.00	78.00	98.02	3.39	0.43	20/08/2010 21:53:34	97.61	52.73	
8	90-150	40.00	78.00	98.02	3.41	0.42	20/08/2010 21:58:05	97.59	52.72	
9	90-150	40.00	78.00	98.02	3.47	0.42	20/08/2010 21:02:35	97.61	52.74	
10	90-150	40.00	78.00	98.02	3.31	0.42	20/08/2010 21:07:12	97.61	54.28	
11	212-400	40.00	78.00	98.02	3.47	0.40	20/08/2010 21:28:46	98.20	54.33	0.40
12	212-400	40.00	78.00	98.02	3.51	0.40	20/08/2010 21:33:09	98.25	54.39	
13	212-400	40.00	78.00	98.02	3.50	0.40	20/08/2010 21:37:33	98.35	54.38	
14	212-400	40.00	78.00	98.02	3.49	0.40	20/08/2010 21:44:15	98.43	54.41	
15	212-400	40.00	78.00	98.02	3.54	0.39	20/08/2010 21:48:43	98.49	51.84	
16	425-600	40.00	78.00	98.02	3.14	0.36	20/08/2010 21:02:34	97.86	51.85	0.36
17	425-600	40.00	78.00	98.02	3.15	0.36	20/08/2010 21:07:18	97.94	51.88	
18	425-600	40.00	78.00	98.02	3.12	0.36	20/08/2010 21:11:42	98.01	51.89	
19	425-600	40.00	78.00	98.02	3.12	0.36	20/08/2010 21:16:04	98.07	51.91	
20	425-600	40.00	78.00	98.02	3.13	0.38	20/08/2010 21:20:25	98.15	52.67	

Table C3: Porosity Measurement from Measurement Model and Helium Porosimeter

Size, $\mu\text{m}$	Porosity		
	Measurement model	Helium Porosimeter	% Different
30-60	0.43	0.43	0.0
90-150	0.42	0.42	0.0
212-400	0.40	0.40	0.0
425-600	0.37	0.36	2.8

### Average Porosity Calculation

From Ahmed, 2001, volumetric-weighted average porosity was calculated from A7,

$$\phi = \frac{\sum \phi_i \times A_i \times h_i}{\sum A_i h_i} \quad (\text{A7})$$

Average porosity for  $k_v/k_h=0.8$ ;

$$\begin{aligned} \phi_{kv/kh=0.8} &= \frac{(0.43 + 0.42 + 0.40 + 0.37) \times (55 \times 25.75)}{55 \times 25.75 \times 4} \\ &= 0.41 \end{aligned}$$

Average porosity for  $k_v/k_h=0.9$ ;

$$\begin{aligned} \phi_{kv/kh=0.9} &= \frac{(0.43 + 0.40) \times (55 \times 51.5)}{55 \times 51.5 \times 2} \\ &= 0.42 \end{aligned}$$

Average porosity for  $k_v/k_h=1.0$ ;

$$\phi_{kv/kh=1.00} = 0.43$$

### $k_v/k_h$ Calculation

$k_v$  and  $k_h$  were calculated by using Equation A8 and A9, respectively (Koederitz *et al.*, 1989). Figure A1 shows a print-screen on how Excel was applied to calculate the  $k_v/k_h$  for different models. Table A4 shows the summary of porosity and permeability for three different heterogeneous models that have been used in laboratory investigations.

$$k_{recip} = \frac{\sum_{i=1}^n L_i}{\sum_{i=1}^n (L_i/k_i)} \quad (\text{A8})$$

$$k_{arith} = \frac{\sum_{i=1}^n (k_i h)}{\sum_{i=1}^n h_i} \quad (\text{A9})$$

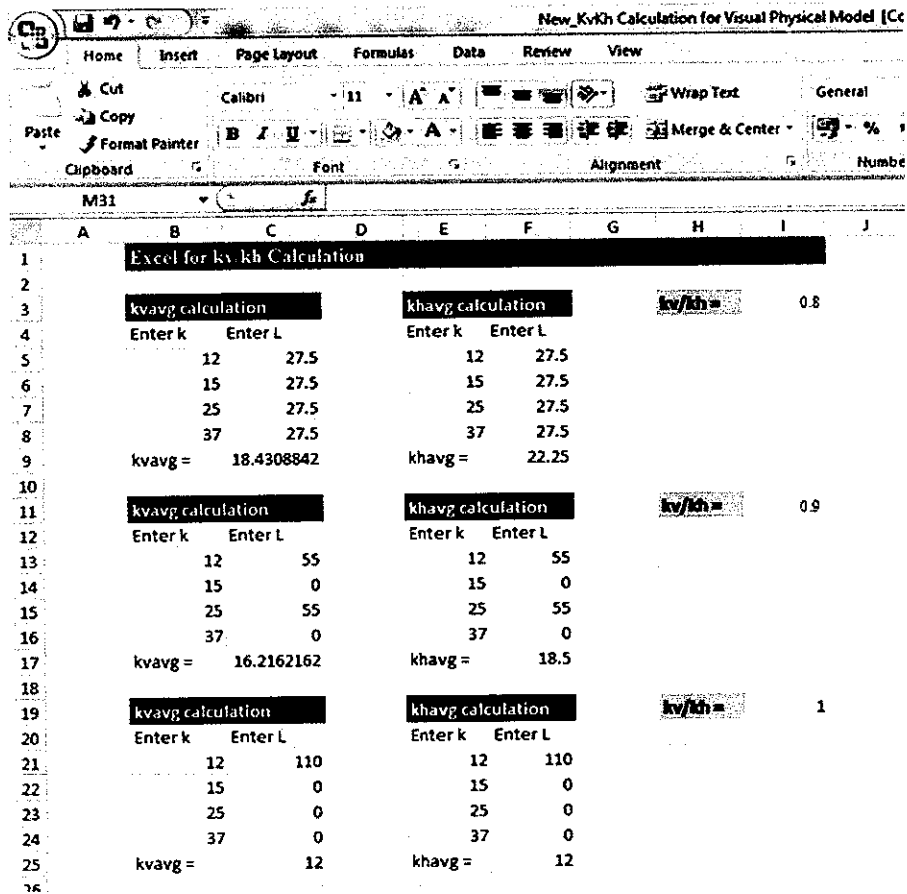


Figure C1:  $k_v/k_h$  Calculation from Excel Application

Table C4: Porosity, and Permeability for Heterogeneous Model

$k_v/k_h$	Porosity for each layer	Average Porosity %	Permeability for each layer, Darcy
0.8	0.43	0.41	12
	0.42		15
	0.44		25
	0.37		37
0.9	0.43	0.42	12
	0.40		25
1.0	0.43	0.43	12

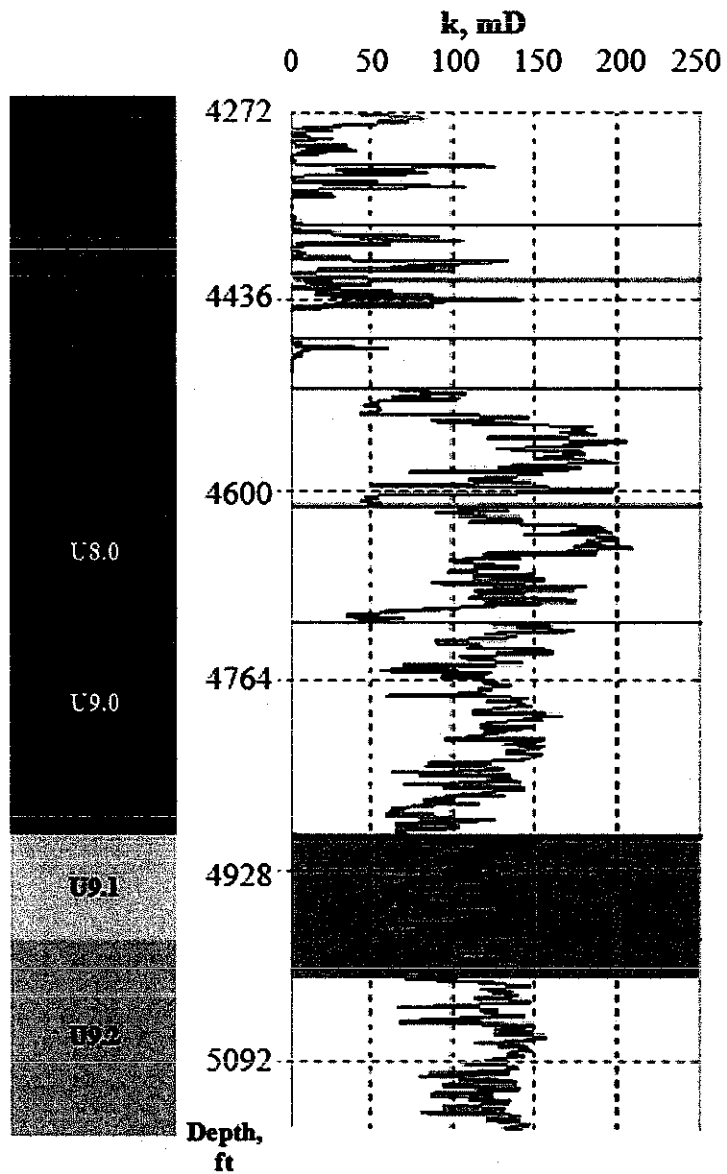


Figure C2: Permeability Distribution for Gelama Merah 1 (PETRONAS CARIGALI, 2002-2003)

## Appendix D Time Scaling

### Laboratory Investigation

$$k_v/k_h=0.8$$

$$k = 2.196 \times 10^{-11} \text{ m}^2$$

$$kr_o^0 = 0.62$$

$$g_c = 1$$

$$g = 9.81 \text{ m/s}^2$$

$$\Delta\rho = (840-1.8035) \text{ kg/m}^3 \\ = 838.1965 \text{ kg/m}^3$$

$$S_{wi} = 0.3$$

$$S_{or} = 0.29$$

$$\phi = 0.5801$$

$$\mu_{oil} = 0.025 \text{ Pa.s}$$

$$h = 1.1 \text{ m}$$

$$t = 1 \text{ s}$$

$$t_{dVPM} = \frac{2.196 \times 10^{-11} \text{ m}^2 * 0.62 * 838.1965 \text{ kg/m}^3 * 9.81 \text{ m/s}^2 * 1 \text{ s}}{1.1 \text{ m} * 0.5801 * 0.025 \text{ Pa.s} * 1 * (1 - 0.3 - 0.29)} = 1.71167 \times 10^{-5}$$

### Gelama Merah

$$k = 9.869233 \times 10^{-14} \text{ m}^2$$

$$kr_o^0 = 0.48$$

$$g_c = 1$$

$$g = 9.81 \text{ m/s}^2$$

$$\Delta\rho = (51.69-8.73) \text{ lb/ft}^3 \times 16.0184 \text{ (kg/m}^3\text{)/(lb/ft}^3\text{)} \\ = (827.9914-139.8407) \text{ kg/m}^3 \\ = 688.1507 \text{ kg/m}^3$$

$$S_{wi} = 0.36$$

$$S_{or} = 0.2$$

$$\phi = 0.27$$

$$\mu_{oil} = 1.36 \text{ cP} \times 0.001 \text{ Pa.s/cP} \\ = 0.00136 \text{ Pa.s}$$

$$h = 115 \text{ ft} \times 0.3048 \text{ m/ft}$$

$$= 35.052 \text{ m}$$

$$t = 1 \text{ s}$$

$$t_{dGM} = \frac{9.869233 \times 10^{-14} \text{ m}^2 * 0.48 * 688.1507 \text{ kg/m}^3 * 9.81 \text{ m/s}^2 * 1 \text{ s}}{35.052 \text{ m} * 0.27 * 0.00136 \text{ Pa.s} * 1 * (1 - 0.2 - 0.36)} = 5.64689 \times 10^{-8}$$

### **Dimensionless Time Scaling**

$$\frac{t_{dVPM}}{t_{dGM}} = \frac{1.71167 \times 10^{-5}}{5.64689 \times 10^{-8}} = 303.1173$$

**Thus, one second in lab is equal to five minutes in Gelama Merah**

## Appendix E Gravity Number Calculation

Length of Model	: 0.55m
Thickness of Model	: 1.1m
Absolute Permeability	: $2.942 \times 10^{-13} \text{m}^2$
$\Delta\mu$ between Mineral Oil and CO <sub>2</sub>	: 0.02499Pa.s
$\Delta\rho$ between Mineral Oil and CO <sub>2</sub>	: $838.1965 \text{kg.m}^{-3}$
Injection Rate	: $2 \times 10^{-5} \text{m}^3 \text{min}^{-1}$

$$\text{Darcy Velocity, } vd = \frac{q, \text{m}^3 \text{s}^{-1}}{A \times \phi} \quad (\text{E1})$$

$$vd_{kv/kh=0.8} = \frac{2 \times 10^{-5}}{0.605 \times 58.01}$$

$$= 5.6986 \times 10^{-7} \text{m.s}^{-1}$$

$$vd_{kv/kh=0.9} = \frac{2 \times 10^{-5}}{0.605 \times 58.75}$$

$$= 5.6269 \times 10^{-7} \text{m.s}^{-1}$$

$$vd_{kv/kh=1.0} = \frac{2 \times 10^{-5}}{0.605 \times 10^{-3} \times 60.5}$$

$$= 5.4641 \times 10^{-7} \text{m.s}^{-1}$$

$$N_G = \frac{\Delta\rho g K}{\Delta\mu v_d} \quad (\text{E2})$$

$$N_{G_{kv/kh=0.8}} = \frac{838.1965 \text{kg.m}^{-3} \times 9.81 \text{m.s}^{-2} \times 2.942 \times 10^{-13} \text{m}^2}{0.02499 \text{Pa.s} \times 5.6986 \times 10^{-7} \text{ms}^{-1}}$$

$$= 0.1699$$

$$N_{G_{kv/kh=0.9}} = \frac{838.1965 \text{ kg} \cdot \text{m}^{-3} \times 9.81 \text{ m} \cdot \text{s}^{-2} \times 2.942 \times 10^{-13} \text{ m}^2}{0.02499 \text{ Pa} \cdot \text{s} \times 5.6269 \times 10^{-7} \text{ m} \cdot \text{s}^{-1}}$$

$$= 0.1720$$

$$N_{G_{kv/kh=1.0}} = \frac{838.1965 \text{ kg} \cdot \text{m}^{-3} \times 9.81 \text{ m} \cdot \text{s}^{-2} \times 2.942 \times 10^{-13} \text{ m}^2}{0.02499 \text{ Pa} \cdot \text{s} \times 5.4641 \times 10^{-7} \text{ m} \cdot \text{s}^{-1}}$$

$$= 0.1771$$

## **Appendix F Detail of Materials and Equipments Used**

### **Visual Physical Model**

Model : VPM-G-02

Maximum Pressure : 40Psig

Description is available at: B. K. Tham, "Visual Physical Model and Measurement Model Operating Manual," Universiti Teknologi PETRONAS, Tronoh, Perak, December, 2010.

### **Measurement Model**

Model : MM-G-01

Maximum Pressure : 90Psig

Description is available at: B. K. Tham, "Visual Physical Model and Measurement Model Operating Manual," Universiti Teknologi PETRONAS, Tronoh, Perak, December, 2010.

### **Ballotini Impact Beads**

Manufacture : Potters Industries Inc.

Size range : 30-60, 90-150, 212-400, 425-600 $\mu$ m

MSDS is available at:

<http://ntruddockcompany.thomasnet.com/Asset/BallotiniImpactBeads.pdf>

### **Light Mineral Oil (330779)**

Manufacture : Sigma-Aldrich

Density : 0.840g/ml (25.9°C)

Viscosity : 25cP (25.9°C)

MSDS is available at:

<http://nanomechanics.pratt.duke.edu/MSDS/Mineral%20oil%20light.pdf>

### **Brine**

Manufacture : Customized

Density : 1.02g/ml (25.9°C)

Viscosity : 2.5cP (25.9°C)

### **HPLC Pump (PU-2080)**

Manufacture : JASCO

Flow rate range : 1  $\mu$ m/min-10mL/min

Maximum Pressure : 50MPa

Description is available at:

[http://www.jasco.com.br/imagem/catalogo/PU2080\\_072.pdf](http://www.jasco.com.br/imagem/catalogo/PU2080_072.pdf)

### **Portable Density Meter (DMA 35N)**

Manufacturer : Anton Paar GmbH

Density measuring range : 0-1.999  $\pm$ 0.001 g/cm<sup>3</sup>

Temperature measuring range : 0-40  $\pm$ 0.2°C

Description is available at: <http://i.b5z.net/i/u/1643541/f/DMA35N.pdf>

### **Moisture Removal Trap (MT200-2-S)**

Manufacture : Agilent Technologies

Removal capacity : 52.5g

Maximum effluent concentration : 39ppb

Description is available at:

[http://www.semlab.com.tr/tr/hafun/download/Agilent\\_GC\\_accessories.pdf](http://www.semlab.com.tr/tr/hafun/download/Agilent_GC_accessories.pdf)

### **Digital Pressure Gages**

Manufacture : Dwyer

Model : DPGA-08 and DPGW-08

Pressure range : 0-100psi

Description is available at:

[http://www.dwyer-inst.com/PDF\\_files/Priced/DPGA&DPGW\\_cat.pdf](http://www.dwyer-inst.com/PDF_files/Priced/DPGA&DPGW_cat.pdf)

### **Gas Mass Flow Controller**

Manufacture : Dwyer

Model : GFC-2100-02-CO2

Flow range : 0-20sccm

Description is available at: [http://www.dwyer-inst.com/PDF\\_files/GFC\\_cat.pdf](http://www.dwyer-inst.com/PDF_files/GFC_cat.pdf)

### **Pressure Transmitter**

Manufacture : Dwyer

Model : 626-10-GH-P8-E1-S2

Pressure range : 0-100 psi

Description is available at :

[http://www.dwyer-inst.com/PDF\\_files/Priced/626&628\\_cat.pdf](http://www.dwyer-inst.com/PDF_files/Priced/626&628_cat.pdf)

### Process Indicator

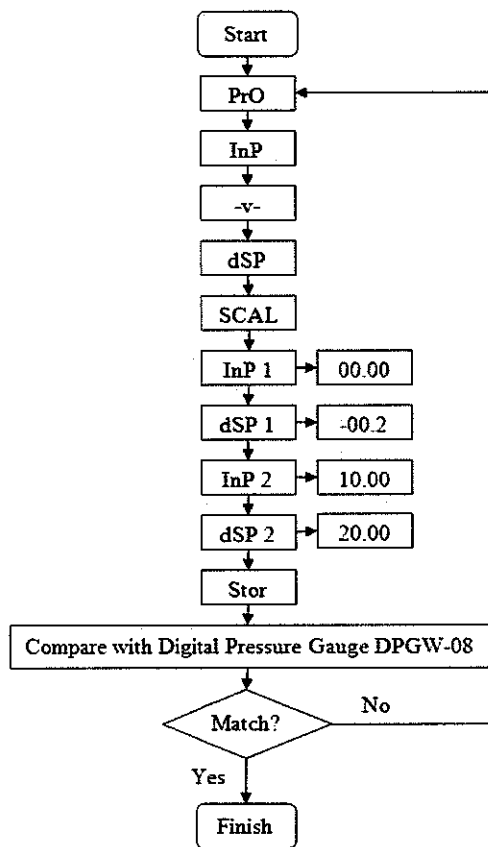
Manufacture : Dwyer

Model : LCI132-00-240VAC

Pressure range :  $\pm 100$  VDC;  $\pm 20$  VDC

Description is available at: [http://www.dwyer-inst.com/PDF\\_files/Priced/LCI132\\_cat.pdf](http://www.dwyer-inst.com/PDF_files/Priced/LCI132_cat.pdf)

Calibration steps :



### Sieve Shaker

Manufacture : CSC Scientific Company, Inc.

Model : EFL 2000

Sieve Capacity : 200mm or 8"

Description is available at: [http://www.qclabequipment.com/END\\_MINOR\\_QC.pdf](http://www.qclabequipment.com/END_MINOR_QC.pdf)

### Viscometer

Manufacture : OFITE

Model : 1100

Description is available at: : [http://www.ofite.com/instructions/130-81\\_v1.pdf](http://www.ofite.com/instructions/130-81_v1.pdf)

**Webcam**

Manufacture : Logitech

Model : C500

Description is available at:

<http://www.logitech.com/en-us/webcam-communications/webcams/devices>

## Appendix G List of Publications

The following is a complete list of the publications written during the preliminary work or the work contained in this thesis. This includes accepted and published works.

1. Tham Boon Keat, Mehmet Raif Birol Demiral, and Ismail Bin Mohd Saaid, "Effect of Reservoir Heterogeneity on Gas Assisted Gravity Drainage Project," presented at the International Conference on Integrated Petroleum Engineering and Geoscience, Kuala Lumpur, Malaysia, 15-17 June 2010.  
Available: [www.utp.edu.my/estcon2010/images/docs/icipeg2010-final-approved.pdf](http://www.utp.edu.my/estcon2010/images/docs/icipeg2010-final-approved.pdf)
2. Akmal Aulia, Tham Boon Keat, Muhammad Sanif Bin Maulut, Noaman El-Khatib, and Mazuin Jasamai, "Mining Data from Reservoir Simulation Results," presented at the International Conference on Integrated Petroleum Engineering and Geoscience, Kuala Lumpur, Malaysia, 15-17 June 2010.  
Available: [www.utp.edu.my/estcon2010/images/docs/icipeg2010-final-approved.pdf](http://www.utp.edu.my/estcon2010/images/docs/icipeg2010-final-approved.pdf)
3. Akmal Aulia, Tham Boon Keat, Muhammad Sanif Bin Maulut, Noaman El-Khatib, and Mazuin Jasamai. (2010, November). Smart Oilfield for Data Mining for Reservoir Analysis. *International Journal of Engineering and Technology IJET-IJENS*. [Online]. 10(6).  
Available: [www.ijens.org/103606-8787%20IJET-IJENS.pdf](http://www.ijens.org/103606-8787%20IJET-IJENS.pdf)
4. Tham Boon Keat, Mehmet Raif Birol Demiral, Ismail Bin Mohd Saaid, and Elias Abllah (2011, July). The Effects of  $k_v/k_h$  on Gas Assisted Gravity Drainage Process. *International Journal of Engineering & Technology IJET-IJENS*. [Online]. 11(3).  
Available: [www.ijens.org/vol%2011%20I%2003/1111303-5858%20IJET-IJENS.pdf](http://www.ijens.org/vol%2011%20I%2003/1111303-5858%20IJET-IJENS.pdf)

## Appendix H ECLIPSE Data Overview

Table H1 gives an overview on all the sections in ECLIPSE simulator. ECLIPSE is designed to use an ASCII text file, usually specified as: \*.DATA, in which all model informations is identified. The \*.DATA file, commonly called a 'data file' or 'data deck,' is subdivided into sections: RUNSPEC, GRID, EDIT, PROPS, REGIONS, SOLUTION, SUMMARY, SCHEDULE. Within these sections, you can use keywords to identify input data, request output data (to various media), and specify conditions. The basic function of each section is shown in Table H1.

Table H1: Minimal ECLIPSE Data for Simulation Run

	ECLIPSE Object	Purpose in Simulation	Minimum Required Data	Additional Data
Basic Simulation	RUNSPEC	General model characteristic.		
	GRID	Grid geometry and basic rock properties.	Porosity, permeability, grid sizes.	Seismic data, surface, location map, polygon
	EDIT	Modification of the processed GRID data.	Multiplier, transmissibility, grid.	
	PROPS	PVT and SCAL properties	PVT, relative permeability, saturation function, capillary pressure, rock compaction, fluid properties (density, compressibility)	Reports (PVT, SCAL)
	REGIONS	Subdivision of the reservoir	Equilibration region, saturation region, facies	
	SOLUTION	Initialization	Contacts, reference pressure, aquifers	Volume In Place (Hydrocarbon and non-hydrocarbon)
	SUMMARY	Request output for line plots	Pressure, rates, saturations	
	SCHEDULE	Well, completions, rate data, flow correlations, surface facilities, simulator advance, control and termination	Development strategy, well controls, group control, completion data, surface facilities, surface network, EOR, water/gas injection, well data (*trajectory, location, diameters)	Well Deviation survey, Well logs data (perforation, reservoir properties), vertical lift performance table, completion / equipment, OFM data (history and forecast), Decline curve analysis

## Simulation Script for Gulfaks Field

RUNSPEC

```
TITLE -- Generated : Petrel
GAGD_ICD

WELLDIMS -- Generated : Petrel
 3 8 2 3 /

START -- Generated : Petrel
 1 FEB 2005 /

DISGAS -- Generated : Petrel

WATER -- Generated : Petrel

OIL -- Generated : Petrel

GAS -- Generated : Petrel

PETOPTS -- Generated : Petrel
INITNNC /

MONITOR -- Generated : Petrel

MULTOUT -- Generated : Petrel

METRIC -- Generated : Petrel

DIMENS -- Generated : Petrel
 28 7 8 /

TABDIMS -- Generated : Petrel
 1* 1* 22 9* 1 /

GRID

INCLUDE -- Generated : Petrel
'GAGD_ICD_GRID.INC' /

NOECHO -- Generated : Petrel

INCLUDE -- Generated : Petrel
'GAGD_ICD_GRID.GRDECL' /

INCLUDE -- Generated : Petrel
'GAGD_ICD_PROP_PERMX.GRDECL' /

INCLUDE -- Generated : Petrel
```

```

'GAGD_ICD_PROP_PERMY.GRDECL' /

INCLUDE -- Generated : Petrel
'GAGD_ICD_PROP_PERMZ.GRDECL' /

INCLUDE -- Generated : Petrel
'GAGD_ICD_PROP_PORO.GRDECL' /

ECHO -- Generated : Petrel

EDIT

PROPS

INCLUDE -- Generated : Petrel
'GAGD_ICD_PROPS.INC' /

REGIONS

NOECHO -- Generated : Petrel

INCLUDE -- Generated : Petrel
'GAGD_ICD_PROP_SATNUM.GRDECL' /

INCLUDE -- Generated : Petrel
'GAGD_ICD_PROP_PVTNUM.GRDECL' /

INCLUDE -- Generated : Petrel
'GAGD_ICD_PROP_ROCKNUM.GRDECL' /

INCLUDE -- Generated : Petrel
'GAGD_ICD_PROP_EQLNUM.GRDECL' /

ECHO -- Generated : Petrel

SOLUTION

INCLUDE -- Generated : Petrel
'GAGD_ICD_SOL.INC' /

SUMMARY

INCLUDE -- Generated : Petrel
'GAGD_ICD_SUM.INC' /

SCHEDULE
INCLUDE -- Generated : Petrel
'GAGD_ICD_SCH.INC' /

```

## Example of ECLIPSE Blackoil Data Script

-----  
-->This is the first SPE comparison problem, reported by Odeh  
-----

RUNSPEC

TITLE

ODEH PROBLEM - IMPES OPTION - 1200 DAYS

DIMENS

10 10 3 /

NONNC

OIL

WATER

GAS

DISGAS

FIELD

EQLDIMS

1 100 10 1 1 /

TABDIMS

1 1 16 12 1 12 /

WELLDIMS

2 1 1 2 /

NUPCOL

4 /

START

19 'OCT' 1982 /

NSTACK

24 /

FMTOUT

FMTIN

UNIFOUT

UNIFIN

## GRID

-- IN THIS SECTION , THE GEOMETRY OF THE SIMULATION GRID AND THE ROCK PERMEABILITIES AND POROSITIES ARE DEFINED.

-- THE X AND Y DIRECTION CELL SIZES ( DX, DY ) AND THE POROSITIES ARE CONSTANT THROUGHOUT THE GRID. THESE ARE SET IN THE FIRST 3 LINES

-- AFTER THE EQUALS KEYWORD. THE CELL THICKNESSES ( DZ ) AND PERMEABILITES ARE THEN SET FOR EACH LAYER. THE CELL TOP DEPTHS ( TOPS ) ARE NEEDED ONLY IN THE TOP LAYER ( THOUGH THEY COULD BE SET THROUGHOUT THE GRID ). THE SPECIFIED MULTZ VALUES ACT AS MULTIPLIERS ON THE TRANSMISSIBILITIES BETWEEN THE CURRENT LAYER AND THE LAYER BELOW.

-- ARRAY VALUE ----- BOX -----

EQUALS

'DX' 1000 /

'DY' 1000 /

'PORO' 0.3 /

'DZ' 20 1 10 1 10 1 1 /

'PERMX' 500 /

'MULTZ' 0.64 /

'TOPS' 8325 /

'DZ' 30 1 10 1 10 2 2 /

'PERMX' 50 /

'MULTZ' 0.265625 /

'DZ' 50 1 10 1 10 3 3 /

'PERMX' 200 /

/ EQUALS IS TERMINATED BY A NULL RECORD

-- THE Y AND Z DIRECTION PERMEABILITIES ARE COPIED FROM PERMX

-- SOURCE DESTINATION ----- BOX -----

COPY

'PERMX' 'PERMY' 1 10 1 10 1 3 /

'PERMX' 'PERMZ' /

-- OUTPUT OF DX, DY, DZ, PERMX, PERMY, PERMZ, MULTZ, PORO AND TOPS DATAIS REQUESTED, AND OF THE CALCULATED PORE VOLUMES AND X, Y AND Z

-- TRANSMISSIBILITIES

RPTGRID

-- Report Levels for Grid Section Data

--

'DX'

'DY'

'DZ'  
 'PERMX'  
 'PERMY'  
 'PERMZ'  
 'MULTZ'  
 'PORO'  
 'TOPS'  
 'PORV'  
 'TRANX'  
 'TRANY'  
 'TRANZ'

/

PROPS

-----  
 -- THE PROPS SECTION DEFINES THE REL. PERMEABILITIES, CAPILLARY PRESSURES, AND THE PVT PROPERTIES OF THE RESERVOIR FLUIDS  
 -----

-- WATER RELATIVE PERMEABILITY AND CAPILLARY PRESSURE ARE TABULATED AS A FUNCTION OF WATER SATURATION.

-- SWAT KRW PCOW  
 SWFN

0.12	0	0
1.0	0.00001	0 /

-- SIMILARLY FOR GAS

--  
 -- SGAS KRG PCOG  
 SGFN

0	0	0
0.02	0	0
0.05	0.005	0
0.12	0.025	0
0.2	0.075	0
0.25	0.125	0
0.3	0.19	0
0.4	0.41	0
0.45	0.6	0
0.5	0.72	0
0.6	0.87	0
0.7	0.94	0
0.85	0.98	0
1.0	1.0	0 /

-- OIL RELATIVE PERMEABILITY IS TABULATED AGAINST OIL SATURATION FOR OIL-WATER AND OIL-GAS-CONNATE WATER CASES

-- SOIL KROW KROG  
 SOF3

0	0	0
0.18	0	0

0.28	0.0001	0.0001
0.38	0.001	0.001
0.43	0.01	0.01
0.48	0.021	0.021
0.58	0.09	0.09
0.63	0.2	0.2
0.68	0.35	0.35
0.76	0.7	0.7
0.83	0.98	0.98
0.86	0.997	0.997
0.879	1	1
0.88	1	1 /

-- PVT PROPERTIES OF WATER

-- REF. PRES. REF. FVF COMPRESSIBILITY REF VISCOSITY  
 VISCOSIBILITY

PVTW

4014.7	1.029	3.13D-6	0.31	0 /
--------	-------	---------	------	-----

-- ROCK COMPRESSIBILITY

-- REF. PRES COMPRESSIBILITY

ROCK

14.7	3.0D-6	/
------	--------	---

-- SURFACE DENSITIES OF RESERVOIR FLUIDS

-- OIL WATER GAS

DENSITY

49.1	64.79	0.06054 /
------	-------	-----------

-- PVT PROPERTIES OF DRY GAS (NO VAPOURISED OIL)

-- WE WOULD USE PVTG TO SPECIFY THE PROPERTIES OF WET GAS

-- PGAS BGAS VISGAS

PVDG

14.7	166.666	0.008
264.7	12.093	0.0096
514.7	6.274	0.0112
1014.7	3.197	0.014
2014.7	1.614	0.0189
2514.7	1.294	0.0208
3014.7	1.080	0.0228
4014.7	0.811	0.0268
5014.7	0.649	0.0309
9014.7	0.386	0.047 /

-- PVT PROPERTIES OF LIVE OIL (WITH DISSOLVED GAS)

-- WE WOULD USE PVDO TO SPECIFY THE PROPERTIES OF DEAD OIL

-- FOR EACH VALUE OF RS THE SATURATION PRESSURE, FVF AND VISCOSITY ARE SPECIFIED. FOR RS=1.27 AND 1.618, THE FVF AND

VISCOSITY OF UNDERSATURATED OIL ARE DEFINED AS A FUNCTION OF PRESSURE. DATA

-- FOR UNDERSATURATED OIL MAY BE SUPPLIED FOR ANY RS, BUT MUST BE SUPPLIED FOR THE HIGHEST RS (1.618).

-- RS POIL FVFO VISO

PVTO

0.001 14.7 1.062 1.04 /  
0.0905 264.7 1.15 0.975 /  
0.18 514.7 1.207 0.91 /  
0.371 1014.7 1.295 0.83 /  
0.636 2014.7 1.435 0.695 /  
0.775 2514.7 1.5 0.641 /  
0.93 3014.7 1.565 0.594 /  
1.270 4014.7 1.695 0.51  
5014.7 1.671 0.549  
9014.7 1.579 0.74 /  
1.618 5014.7 1.827 0.449  
9014.7 1.726 0.605 /

/

-- OUTPUT CONTROLS FOR PROPS DATA

-- ACTIVATED FOR SOF3, SWFN, SGFN, PVTW, PVDG, DENSITY AND ROCK KEYWORDS

RPTPROPS

-- PROPS Reporting Options

'PVTW' 'PVTG' 'PVDG' 'DENSITY' 'GRAVITY' 'SDENSITY' 'ROCK' 'ROCKTAB'

/

SOLUTION

----- THE SOLUTION SECTION DEFINES THE INITIAL STATE OF THE SOLUTION

----- VARIABLES (PHASE PRESSURES, SATURATIONS AND GAS-OIL RATIOS)

-----  
-- DATA FOR INITIALISING FLUIDS TO POTENTIAL EQUILIBRIUM

-- DATUM DATUM OWC OWC GOC GOC RSVD RVVD SOLN

-- DEPTH PRESS DEPTH PCOW DEPTH PCOG TABLE TABLE METH EQUIL

8400 4800 8500 0 8200 0 1 0 0 /

-- VARIATION OF INITIAL RS WITH DEPTH

-- DEPTH RS

RSVD

8200 1.270

8500 1.270 /

-- OUTPUT CONTROLS (SWITCH ON OUTPUT OF INITIAL GRID BLOCK PRESSURES)

RPTSOL  
-- Initialisation Print Output  
'PRES' /

## SUMMARY

----- THIS SECTION SPECIFIES DATA TO BE WRITTEN TO THE  
SUMMARY FILES AND WHICH MAY LATER BE USED WITH THE ECLIPSE  
GRAPHICS PACKAGE

-----  
--REQUEST PRINTED OUTPUT OF SUMMARY FILE DATA

## RUNSUM

-- FIELD OIL PRODUCTION  
FOPR

-- WELL GAS-OIL RATIO FOR PRODUCER  
WGOR  
'PRODUCER'  
/

-- WELL BOTTOM-HOLE PRESSURE  
WBHP  
'PRODUCER'  
/

-- GAS AND OIL SATURATIONS IN INJECTION AND PRODUCTION CELL  
BGSAT  
10 10 3  
1 1 1  
/  
BOSAT  
10 10 3  
1 1 1  
/

-- PRESSURE IN INJECTION AND PRODUCTION CELL  
BPR  
10 10 3  
1 1 1 /  
SCHEDULE

----- THE SCHEDULE SECTION DEFINES THE OPERATIONS TO BE  
SIMULATED

-----  
-- CONTROLS ON OUTPUT AT EACH REPORT TIME  
RPTSCHED  
'CPU=2' 'NEWTON=2' /

IMPES

1.0 1.0 10000.0 /

-- SET 'NO RESOLUTION' OPTION

DRSDT

0 /

-- SET INITIAL TIME STEP TO 1 DAY AND MAXIMUM TO 6 MONTHS

TUNING

1 182.5 /

1.0 0.5 1.0E-6 /

/

-- WELL SPECIFICATION DATA

-- WELL GROUP LOCATION BHP PI

-- NAME NAME I J DEPTH DEFN

WELSPPCS

'PRODUCER' 'G' 10 10 8400 'OIL' /

'INJECTOR' 'G' 1 1 8335 'GAS' /

/

-- COMPLETION SPECIFICATION DATA

-- WELL -LOCATION- OPEN/ SAT CONN WELL

-- NAME I J K1 K2 SHUT TAB FACT DIAM

COMPDAT

'PRODUCER' 10 10 3 3 'OPEN' 0 -1 0.5 /

'INJECTOR' 1 1 1 1 'OPEN' 1 -1 0.5 /

/

-- PRODUCTION WELL CONTROLS

-- WELL OPEN/ CNTL OIL WATER GAS LIQU RES BHP

-- NAME SHUT MODE RATE RATE RATE RATE RATE

WCONPROD

'PRODUCER' 'OPEN' 'ORAT' 20000 4\* 1000 /

/

-- INJECTION WELL CONTROLS

-- WELL INJ OPEN/ CNTL FLOW

-- NAME TYPE SHUT MODE RATE

WCONINJE

'INJECTOR' 'GAS' 'OPEN' 'RATE' 100000 /

/

TSTEP

1.0 14.0 13\*25.0

/

RPTSCHED

'PRES' 'SOIL' 'SWAT' 'SGAS' 'RS' 'RESTART=2' 'FIP=1' 'WELLS=2'

'SUMMARY=2'

'CPU=2' 'NEWTON=2' /

TSTEP

25.0

/

RPTSCHED

'SUMMARY=2' 'CPU=2' 'NEWTON=2' /

TSTEP

13\*20.0 7\*13.0

/

RPTSCHED

'PRES' 'SOIL' 'SWAT' 'SGAS' 'RS' 'RESTART=2' 'FIP=1' 'WELLS=2'

'SUMMARY=2'

'CPU=2' 'NEWTON=2' /

TSTEP

14 /

-- YEAR 3

RPTSCHED

'SUMMARY=2' 'CPU=2' 'NEWTON=2' /

TSTEP

17\*10.0

/

RPTSCHED

'PRES' 'SOIL' 'SWAT' 'SGAS' 'RS' 'RESTART=2' 'FIP=1' 'WELLS=2'

'SUMMARY=2'

'CPU=2' 'NEWTON=2' /

TSTEP

12.5

/

RPTSCHED

'SUMMARY=2' 'CPU=2' 'NEWTON=2' /

TSTEP

8.5 16\*5.0

/

RPTSCHED

'PRES' 'SOIL' 'SWAT' 'SGAS' 'RS' 'RESTART=2' 'FIP=1' 'WELLS=2'

'SUMMARY=2'

'CPU=2' 'NEWTON=2' /

TSTEP

5.0

/

RPTSCHED

'SUMMARY=2' 'CPU=2' 'NEWTON=2' /

TSTEP

19\*5.0

/

RPTSCHED

'PRES' 'SOIL' 'SWAT' 'SGAS' 'RS' 'RESTART=2' 'FIP=1' 'WELLS=2'  
'SUMMARY=2'  
'CPU=2' 'NEWTON=2' /

TSTEP

5.0

/

RPTSCHED

'SUMMARY=2' 'CPU=2' 'NEWTON=2' /

TSTEP

19\*5.0

/

RPTSCHED

'PRES' 'SOIL' 'SWAT' 'SGAS' 'RS' 'RESTART=2' 'FIP=1' 'WELLS=2'  
'SUMMARY=2'  
'CPU=2' 'NEWTON=2' /

TSTEP

5.0

/

IMPLICIT

TUNING

10 /

/

/

TSTEP

10.0 /

END

---

**Example of ECLIPSE Compositional Data Script**

---

-- SPE 9723  
-- "Comparison of Solutions to a Three-Dimensional Black-Oil Reservoir Simulation Problem"  
-- Aziz S. Odeh  
-- Eclipse 100 is also available  
-- Keyword RPTGRIDL to control the output of local grid properties to the PRT file  
-- Keyword COMPKRIL to set relative permeabilities for injector completions in LGRs  
-- Keyword COMPAGHL to set completion gravity head in LGRs  
-- Keyword COMPMBIL to set voidage mobility for injector completions in LGRs

-----  
RUNSPEC

TITLE

ODEH PROBLEM - IMPLICIT OPTION

START

19 'OCT' 1982 /

FIELD

FMTIN

FMTOUT

GAS

OIL

WATER

DISGAS

--UNIFOOTS

NSTACK

35 /

MONITOR

NUPCOL

4 /

RSSPEC

LGR

1 400 0 0 0 10 'NOINTERP' 0 /

DIMENS

10 10 3 /

EQLDIMS  
1 100 10 1 1 /

REGDIMS  
1 1 0 0 /

TABDIMS  
1 1 16 20 1 20 20 1 /

WELLDIMS  
3 5 2 3 /

--UNIFOUT

GRID

---

---

GRIDFILE  
2 /

----- IN THIS SECTION , THE GEOMETRY OF THE SIMULATION GRID  
AND THE ROCK PERMEABILITIES AND POROSITIES ARE DEFINED.

---

-- THE X AND Y DIRECTION CELL SIZES ( DX, DY ) AND THE POROSITIES  
ARE CONSTANT THROUGHOUT THE GRID. THESE ARE SET IN THE FIRST  
3 LINES AFTER THE EQUALS KEYWORD. THE CELL THICKNESSES ( DZ )  
AND PERMEABILITES ARE THEN SET FOR EACH LAYER. THE CELL TOP  
DEPTHS ( TOPS ) ARE NEEDED ONLY IN THE TOP LAYER ( THOUGH  
THEY COULD BE.

-- SET THROUGHOUT THE GRID ). THE SPECIFIED MULTZ VALUES ACT  
AS MULTIPLIERS ON THE TRANSMISSIBILITIES BETWEEN THE  
CURRENT LAYER AND THE LAYER BELOW.

-- ARRAY VALUE ----- BOX -----

EQUALS

'DX' 1000 /  
'DY' 1000 /  
'PORO' 0.3 /

'TOPS' 8325 4\* 1 1 /

'DZ' 20 4\* 1 1 /  
'PERMX' 500 4\* 1 1 /

'DZ' 30 4\* 2 2 /  
'PERMX' 50 4\* 2 2 /

'DZ' 50 4\* 3 3 /  
'PERMX' 200 4\* 3 3 /

/

-- THE Y AND Z DIRECTION PERMEABILITIES ARE COPIED FROM PERMX  
-- SOURCE DESTINATION ----- BOX -----  
COPY

'PERMX' 'PERMY' /  
'PERMX' 'PERMZ' /

/

RPTGRID

1 1 1 1 1 1 1 1 1 1 1 1 1 1 1 /

RPTGRIDL

1 1 1 1 1 1 1 1 1 1 1 1 1 1 1 /

CARFIN

A 2 2 2 2 1 1 4 4 4 /

ENDFIN

PROPS

-----  
-- THE PROPS SECTION DEFINES THE REL. PERMEABILITIES, CAPILLARY  
PRESSURES, AND THE PVT PROPERTIES OF THE RESERVOIR FLUIDS  
-----

-- WATER RELATIVE PERMEABILITY AND CAPILLARY PRESSURE ARE  
TABULATED AS A FUNCTION OF WATER SATURATION.

-- SWAT KRW PCOW

SWFN

0.12 0 0  
1.0 0.00001 0 /

-- SIMILARLY FOR GAS

-- SGAS KRG PCOG

SGFN

0 0 0  
0.02 0 0  
0.05 0.005 0  
0.12 0.025 0  
0.2 0.075 0  
0.25 0.125 0  
0.3 0.19 0  
0.4 0.41 0  
0.45 0.6 0  
0.5 0.72 0  
0.6 0.87 0  
0.7 0.94 0  
0.85 0.98 0  
1.0 1.0 0

/

-- OIL RELATIVE PERMEABILITY IS TABULATED AGAINST OIL SATURATION

-- FOR OIL-WATER AND OIL-GAS-CONNATE WATER CASES

-- SOIL KROW KROG

SOF3

0	0	0
0.18	0	0
0.28	0.0001	0.0001
0.38	0.001	0.001
0.43	0.01	0.01
0.48	0.021	0.021
0.58	0.09	0.09
0.63	0.2	0.2
0.68	0.35	0.35
0.76	0.7	0.7
0.83	0.98	0.98
0.86	0.997	0.997
0.879	1	1
0.88	1	1 /

-- PVT PROPERTIES OF WATER

-- REF. PRES. REF. FVF COMPRESSIBILITY REF VISCOSITY  
VISCOSIBILITY

PVTW

4014.7	1.029	3.13D-6	0.31	0 /
--------	-------	---------	------	-----

-- ROCK COMPRESSIBILITY

-- REF. PRES COMPRESSIBILITY

ROCK

14.7	3.0D-6	/
------	--------	---

-- SURFACE DENSITIES OF RESERVOIR FLUIDS

-- OIL WATER GAS

DENSITY

49.1	64.79	0.06054 /
------	-------	-----------

-- PVT PROPERTIES OF DRY GAS (NO VAPOURISED OIL)

-- WE WOULD USE PVTG TO SPECIFY THE PROPERTIES OF WET GAS

-- PGAS BGAS VISGAS

PVDG

14.7	166.666	0.008
264.7	12.093	0.0096
514.7	6.274	0.0112
1014.7	3.197	0.014
2014.7	1.614	0.0189
2514.7	1.294	0.0208
3014.7	1.080	0.0228
4014.7	0.811	0.0268

5014.7 0.649 0.0309  
9014.7 0.386 0.047 /

-- PVT PROPERTIES OF LIVE OIL (WITH DISSOLVED GAS)  
-- WE WOULD USE PVDO TO SPECIFY THE PROPERTIES OF DEAD OIL  
-- FOR EACH VALUE OF RS THE SATURATION PRESSURE, FVF AND  
VISCOSITY ARE SPECIFIED. FOR RS=1.27 AND 1.618, THE FVF AND  
VISCOSITY OF UNDERSATURATED OIL ARE DEFINED AS A FUNCTION  
OF PRESSURE. DATA  
-- FOR UNDERSATURATED OIL MAY BE SUPPLIED FOR ANY RS, BUT  
MUST BE SUPPLIED FOR THE HIGHEST RS (1.618).

-- RS POIL FVFO VISO  
PVTO  
0.001 14.7 1.062 1.04 /  
0.0905 264.7 1.15 0.975 /  
0.18 514.7 1.207 0.91 /  
0.371 1014.7 1.295 0.83 /  
0.636 2014.7 1.435 0.695 /  
0.775 2514.7 1.5 0.641 /  
0.93 3014.7 1.565 0.594 /  
1.270 4014.7 1.695 0.51  
5014.7 1.671 0.549  
9014.7 1.579 0.74 /  
1.618 5014.7 1.827 0.449  
9014.7 1.726 0.605 /

-- OUTPUT CONTROLS FOR PROPS DATA  
-- ACTIVATED FOR SOF3, SWFN, SGFN, PVTW, PVDG, DENSITY AND  
ROCK KEYWORDS

RPTPROPS  
1 1 1 0 1 1 1 1 /

## SOLUTION

----- THE SOLUTION SECTION DEFINES THE INITIAL STATE OF THE  
SOLUTION VARIABLES (PHASE PRESSURES, SATURATIONS AND GAS-  
OIL RATIOS)

-----  
-- DATA FOR INITIALISING FLUIDS TO POTENTIAL EQUILIBRIUM  
-- DATUM DATUM OWC OWC GOC GOC RSVD RVVD SOLN  
-- DEPTH PRESS DEPTH PCOW DEPTH PCOG TABLE TABLE METH  
EQUIL

8200 4800 8500 0 8200 0 1 0 0 /

-- VARIATION OF INITIAL RS WITH DEPTH

-- DEPTH RS  
RSVD  
8200 1.270

8500 1.270 /

-- OUTPUT CONTROLS (SWITCH ON OUTPUT OF INITIAL GRID BLOCK PRESSURES)

RPTSOL  
1 11\*2 /

## SUMMARY

----- THIS SECTION SPECIFIES DATA TO BE WRITTEN TO THE SUMMARY FILES AND WHICH MAY LATER BE USED WITH THE ECLIPSE GRAPHICS PACKAGE  
-----

--REQUEST PRINTED OUTPUT OF SUMMARY FILE DATA

RUNSUM

-- FIELD OIL PRODUCTION  
FOPR

-- WELL GAS-OIL RATIO FOR PRODUCER  
WGOR  
'PRODUCER'  
/

-- WELL BOTTOM-HOLE PRESSURE

WBHP  
'PRODUCER'  
/

-- GAS AND OIL SATURATIONS IN INJECTION AND PRODUCTION CELL  
BGSAT  
10 10 3  
1 1 1  
/

BOSAT  
10 10 3  
1 1 1  
/

-- PRESSURE IN INJECTION AND PRODUCTION CELL  
BPR  
10 10 3  
1 1 1  
/

SCHEDULE

----- THE SCHEDULE SECTION DEFINES THE OPERATIONS TO BE  
SIMULATED

-----  
-- CONTROLS ON OUTPUT AT EACH REPORT TIME  
--RPTSCHED FIELD 10:29 13 JUN 85  
--KRG KRO KRW /

RPTRST  
BASIC=4 FREQ=2 PRESSURE PRES SWAT SGAS SOIL KRG KRO KRW  
PCOG /

-- SET 'NO RESOLUTION' OPTION  
DRSDT  
0.001 /  
-- SET INITIAL TIME STEP TO 1 DAY AND MAXIMUM TO 6 MONTHS  
TUNING  
/  
/  
2\* 50 /

-- WELL SPECIFICATION DATA  
-- WELL GROUP LOCATION BHP PI  
-- NAME NAME I J DEPTH DEFN  
WELSPECS  
'PRODUCER' 'G' 10 10 8250 'OIL' /  
/

WELSPECL  
'INJECTOR' 'G' A 1 1 8255 'GAS' /  
/

COMPDAT  
'PRODUCER' 10 10 3 3 'OPEN' 0 -1 0.5 /  
-- 'INJECTOR' 2 2 1 1 'OPEN' 1 -1 0.5 /  
/

COMPDATL  
'INJECTOR' A 1 1 3 3 'OPEN' 0 -1 0.5 /  
/

-- PRODUCTION WELL CONTROLS  
-- WELL OPEN/ CNTL OIL WATER GAS LIQU RES BHP  
-- NAME SHUT MODE RATE RATE RATE RATE RATE  
WCONPROD  
'PRODUCER' 'OPEN' 'ORAT' 20000 4\* 1000 /  
/

```
-- INJECTION WELL CONTROLS
-- WELL INJ OPEN/ CNTL FLOW
-- NAME TYPE SHUT MODE RATE
WCONINJE
  'INJECTOR' 'GAS' 'OPEN' 'RATE' 100000 /
/
```

```
TSTEP
10*365 /
```

```
END
```

---

## Appendix I Summary of Previous Research on GAGD Projects

Table II summarizes the GAGD performance in field application based on nine of the selected candidate. Refer to Table II, GAGD performance very well on the field level with the minimum recovery of 60%OOIP compare to WAG which is only in an average of 5-10%OOIP.

Table II: Summary of GAGD Performance Based of Nine Fields (Kulkarni and Rao, 2004)

Property	West Hackberry	Hawkins Dexter Sand	Weeks Island S R B - Pilot	Bay St. Elaine	Wizard Lake D3A	Westpem Nisku D	Wolfcamp Reef	Intisar D	Handil Main Zone
Starting Date	Jul 1996	Jan 1975	Oct 1978	May 1982	Oct 1983	Jan 1981	Mid-1983	Dec 1969	Nov 1995
Approximate Size (Acres)	90	N/A	90	0.4 (Pilot)	3725	320	1306	3325	2965
State / Country	Louisiana / USA	Texas / USA	Louisiana / USA	Louisiana / USA	Alberta / Canada	Alberta / Canada	Texas / USA	Libya	Borneo
Rock Type	Sandstone	Sandstone	Sandstone	Shaly-Sand	Dolomite	Carbonate	Limestone	Biomicroite / Dolomite	Sandstone
Porosity (%)	27.6 - 23.9	27	26	32.9	10.94	12	8.5	22	25
Permeability (mD)	300 - 1000	3400	1200	1480	1375	1050	110	200	Oct-00
Connate Water Sat. (%)	19 - 23	13	10	15	5.64	11	20	16 - 38	22
WF Residual Oil Sat. (%)	26	35	22	20	35	Sec. GF	35	20 - 30	28
GI Residual Oil Sat. (%)	8	12	1.9	N/A	24.5	5	10	N/A	N/A
Reservoir Temperature (°F)	205 - 195	168	225	164	167	218	151	226	N/A
Bed Dip Angle (Degrees)	23 - 35	8	26	36	Reef	Reef	Reef	Reef	5 - 12
Pay Thickness (ft)	31 - 30	230	186	35	648	292	824	950	50 - 82
Oil API Gravity	33	25	32.7	36	38	45	43.5	40	31 - 34
Oil Viscosity (cP)	0.9	3.7	0.45	0.667	N/A	0.19	0.43	0.46	0.6 - 1.0
Bubble Pt Pressure (psi)	3295	1985	6013	N/A	2154	3966	1375	2224	2800 - 3200
GOR (SCF/STB)	500	900	1386	584	567	1800	450	509	2000
Oil FVF at Bubble Pt	1.285	1.225	1.62	1.283	1.313	2.45	1.284	1.315	1.1 - 1.4
Injection Gas	Air	N <sub>2</sub>	CO <sub>2</sub>	CO <sub>2</sub>	HC	HC	CO <sub>2</sub>	HC	HC
Reservoir Pressure at end of WF (psi)	3484	1985	5000	3334	2370	4060	970	4100	1000
Minimum Miscibility Pressure (psi)	-	-	N/A	3334	2131	4640	1900	4257	-
WF Recovery (%OOIP)	60	60	60 - 70	76.5*	62.9*	N/A	56.3*	N/A	58
Gas Flood Recovery (%OOIP)	90	> 80.0	60	85	95.5	84	74.8	67.5	N/A

Table I2 shows the research outcome from previous researches. Refer to Table I2, there are some conflict in the research outcome and some parameters that were overlook by the previous researchers. For example, the sensitivity of  $k_v$  on GAGD projects. This research has confirm that  $k_v$  is one of the important parameter to look at during GAGD process in which it the domination of  $k_v$  will increase the recovery as long as the gravity force is keep dominant than viscosity force. Table I2 also shows that there is yet any reported investigation on the effect of  $k_v/k_h$  on GAGD process, which is one of the objectives of this research. It is hope that by gathering all the research outcomes, it will helps to increase the understanding on GAGD process and thus, increase the oil recovery from GAGD projects.

Table I2: Effect of Controlling Parameters on GAGD Projects (Sharma, 2005; Mahmoud, 2006; and Paidin, 2006)

	Controlling parameter	Previous investigation results				Remarks
		Sharma, 2005	Mahmoud, 2006	Paidin, 2006	Mahmoud and Rab, 2007	
1	<b>Dimension of visual model (length × thickness × height)</b>	Latitudinal (250.825mm × 25.4mm × 457.2mm)	Longitudinal (558.8mm × 25.4mm × 254mm)	Latitudinal (25.4mm × 12.7mm × 352.425mm)	Longitudinal (558.8mm × 25.4mm × 254mm)	A latitudinal model is preferred in GAGD investigation
2	<b>Laboratory model</b>	2-D Hele-Shaw type physical model	Visual glass model	Visual glass model	Modified Li and Horne Model	
3	<b>Gas injection rate</b>	-	Higher injection rate increase oil recovery	-	Higher injection rate increase oil recovery	Gravity domination is the key success
4	<b>Grain size</b>	0.065 – 0.5 mm	0.04 – 0.6 mm	0.15 – 0.5 mm	N/A	
5	<b>Phases involved</b>	Gas, oil, water	Gas, oil, water	Gas, oil, water	Gas, oil, water	Black oil model should be use in ECLIPSE simulator
6	<b>Porosity</b>	8.5-32.9 %	45.7 %	32.9-41.0 %	8.5-32.9 %	The porosity can go very high (45.7 %)
7	<b>Injected gas composition</b>	Did not affect the oil recovery in immiscible mode	-	Increment of (10.9 % OOIP)	-	Replacement with ambient gas will save a lot of cost
8	<b>Gas injected</b>	Nitrogen	Carbon dioxide	Nitrogen	Nitrogen and Carbon dioxide	
9	<b>Gravity number, <math>N_G</math></b>	Logarithmic relationship between gravity number and recovery	-	-	Field: 1-30; visual model: 0.2-1.1	An important parameter since GAGD make use of gravity
10	<b>Injection depth</b>	-	Did not affect oil recovery	-	Did not affect oil recovery	Provided with vertical communication between layers

11	Vertical fracture	Higher recovery	Did not show detrimental effects on oil recovery	Average increment of (7.8 %OOIP)	-	Conflicts between the researchers
12	Grain size	-	-	Increase in grain size will increase the $\phi$ , $k$ , and oil recovery	-	Unrealistic implementation in field
13	Vertical permeability, $k_v$	Most important parameter	Not an important parameter	-	-	The conflict may due to the differences in flow rate used
14	<i>As/ks</i>					No research has been reported yet
15	Wettability	-	Recovery was higher in oil-wet than water-wet porous media	-	-	No study on the mixed wettability
16	Constant pressure gas injection compared with constant rate gas injection	Constant pressure gas injection give a higher cumulative oil recovery	-	Constant pressure gas injection give a higher cumulative oil recovery	-	Pressure different between injector and producer is important for recovery
17	Recovery in primary free gravity drainage	-	-	-	43% IOIP	57% residual left for recover
18	Recovery in immiscible, secondary mode	80% of IOIP	83% IOIP	-	83% IOIP	The recovery is numerous
19	Recovery in immiscible, tertiary mode	-	54% ROIP	-	54% ROIP	
20	Recovery in miscible, secondary mode	-	Close to 100%	-	Close to 100%	
21	Recovery in fractured, porous media secondary mode	-	76% IOIP	-	76% IOIP	
22	Recovery in homogeneous porous media, secondary mode	-	73% IOIP	-	73% IOIP	
23	Scale up to field condition	Yes	Yes	-	-	More practicable if scale to field condition
24	Scale from model to field	1 minute in lab is equivalent to 9936 until 29376 minute in field	1 minute in lab is equivalent to 101 until 19710 minute in field	-	-	
25	Material of physical model	Steel core holder	Glass model	Plastic plate and steel frame		Transparent core holder is better for visualization
26	Oil viscosity	0.84-65 cP	0.97-2.93 cP	200-10000 cP	0.84-65 cP	Previous research showed that higher viscosity will result in higher recovery
27	Investigated on fractured reservoir	Yes	Yes	Yes	Yes	There are already lots of study on the effect of fracture reservoir on GAGD project
28	Well design	Horizontal well	Horizontal well	Horizontal well	Horizontal well	Previous research concentrate on horizontal well

29	<p><b>Recommendations of the study</b></p>	<p>1. Effect of <math>k_v/k_h</math> should be conducted.</p> <p>2. Experiment to capture film flow behaviour of oil should be design to capture the effect of spreading coefficient.</p> <p>3. Experiment should be done on oil-wet media.</p> <p>4. Experiment should be done to compare <i>GAGD</i> with other production scheme.</p> <p>5. Experiment should be done on well configuration and reservoir thickness on <i>GAGD</i> oil recovery.</p>	<p>1. Higher strength glass based visual model should be constructed to handle real reservoir pressure and temperature.</p> <p>2. Investigate the optimum injection while keep the gravity force dominant.</p> <p>3. Study should be done on optimum injection method and configuration.</p> <p>4. Study should be done on carbonate porous medium (with and without fracture).</p> <p>5. Study should be done on layered reservoir.</p>	<p>1. Investigation should be done on the productivity of horizontal well.</p> <p>2. Investigation should be done on different well configuration.</p>	<p>1. Investigation on the contribution of: extraction, molecular diffusion, non-linear film flow, solvent (<math>CO_2</math>) dissolution, viscous displacement, capillary retention etc. Should be done on <i>GAGD</i> process.</p>	
----	--	---	--	--	---	--

